Copolymers of Vinylidene fluoride with Functional comonomers and Applications therefrom: Recent Developments, Challenges and Future Trends

Bruno Ameduri

Copolymers of Vinylidene fluoride with Functional comonomers and Applications therefrom: Recent Developments, Challenges and Future Trends

Bruno Ameduri

ICGM, University Montpellier, CNRS, ENSCM,

34095 Montpellier, France.

Abstract

The radical copolymerization of VDF with M monomer, their properties and applications are presented. First, after listing a non-exhaustive series of comonomers and macromonomers, and their reactivity towards VDF deduced from the kinetics of copolymerizations to suggest a reactivity order. This review proposes non-exhaustive examples of conventional and controlled (RDRP) radical copolymerization. Other parameters to control these reactions were exposed, such as initiators including specific radicals (e.g., $^{\circ}CF_3$, $^{\circ}OCF_3$ and borane radicals), as well as various reaction media (aqueous, solution and supercritical CO_2). Crosslinking of these VDF-based copolymers bearing peculiar functions is also useful to enhance the properties of such fluorinated materials. In addition, environmental concerns on such copolymers regarding their persistency are established but more recent studies claim that these macromolecules are polymers of low concern because of the high molar masses and thermal, chemical, photochemical, hydrolytic, inertness and biological stability to satisfy the regulatory assessment criteria. In that way, more recent studies on the mineralization of poly(VDF-*co*-M) copolymers under subcritical water led to fluoride anions which could react onto Calcium to yield CaF_2 to close the loop of these fluorinated copolymers. Finally, several applications are supplied showing that these copolymers are key actors in our daily life (functional coatings, elastomers, thermoplastic elastomers, distillation

membranes, and materials for Energy such as electrolytes for Lithium ion batteries, fuel cell membranes, sensors, actuators, dye sensitized solar cells and photovoltaics).

Keywords: crosslinking; degradation; electrolyte; energy; functional fluoromonomers; kinetics of copolymerization; membrane; radical copolymerization; terpolymerization; vinylidene fluoride.

Table of Contents

Nomenclature

1234yf	2,3,3,3-tetrafluoroprop-1-ene
1234ze	trans-1,3,3,3-tetrafluoroprop-1-ene
AA	acrylic acid
APFO	ammonium perfluorooctanoate
ATRP	atom transfer radical polymerization
BCP	block copolymer
BDE	bond dissociation energy
BDFO	8-bromo-1H,1H,2H-perfluorooct-1-ene
CEM	cation exchange membrane
CMC	critical micellar concentrations
CMRP	cobalt mediated radical polymerization
CNT	carbon nanotube
CRP (RDRP)	controlled radical polymerization (reversible deactivation radical polymerization)
CTA	chain transfer agent
CTFE	chlorotrifluoroethylene
CuAAC	copper(I)-catalyzed azide-alkyne cycloaddition
CSM	cure site monomer
DFT	density functional theory
DMAc	dimethyl acetamide
DMC	dimethyl carbonate
DMF	dimethylformamide
DMSO	dimethyl sulfoxide
DPn	average degree of polymerization

DSC	differential scanning calorimeter
EAPs	Electroactive polymers
EB	electron beam
FE	ferroelectric
GO	graphene oxide
GPE	gel polymer electrolyte
HFP	hexafluoropropylene
IL	Ionic liquid
ITP	iodine transfer polymerization
LIB	lithium ion battery
MADIX	macromolecular design through interchange of xanthate
MAF	2-trifluoromethacrylic acid
MAF-TBE	*tert*-butyl-2-trifluoromethyl acrylate
MALDI-TOF	matrix-assisted laser desorption/ionization time-of-flight
Mn	molar mass
NMP	nitroxide mediated polymerization
NMR	nuclear magnetic resonance
NPs	nanoparticles
OMRP	organometallic mediated radical polymerization
PAVE	perfluoroalkyl vinyl ethers
PE	paraelectric
PEO	poly(ethylene oxide)
PEG	poly(ethylene glycol)

PFPEs	perfluoropolyethers
PFOA	perfluorooctanoic acid
PFOS	perfluorooctane sulfonic acid
PILs	polymer Ionic Liquids
PLC	polymer of low concern
PMMA	poly(methyl methacrylate)
PMVE	perfluoromethyl vinyl ether
PPFR	perfluoro-3-ethyl-2,4-dimethyl-3-pentyl persistent radical
PSt	poly(styrene)
PtBA	poly(*tert*-butyl acrylate)
PTFE	poly(tetrafluoroethylene)
PVDF	poly(vinylidene fluoride)
PVOH	poly(vinyl alcohol)
RAFT	reversible addition-fragmentation chain-transfer
RFE	relaxor-ferroelectric
RT	room temperature
$scCO_2$	supercritical carbon dioxide
SEC	size exclusion chromatography
St	styrene
TBPPi	*tert*-butylperoxypivalate
TFE	tetrafluoroethylene
TFP	3,3,3-trifluoropropene
Tg	glass transition temperature

Tm	melting temperature
TPE	thermoplastic elastomer
TrFE	trifluoroethylene
VAc	vinyl acetate
VDF	vinylidene fluoride
VMD	vacuum membrane distillation
VOH	vinyl alcohol
WCA	water contact angle
XA	xanthate

1. Introduction

Poly(vinylidene fluoride), PVDF, is the second largest fluoropolymer produced after poly(tetrafluoroethylene), PTFE [1]. This specialty materials is usually synthesized by radical polymerization of VDF and is endowed with outstanding properties (electroactive [2,3] and gas barrier-properties as well as solvent, UV and ageing resistance [3,4] and biomedical applications [5,6]). It is involved in many High Tech applications such as water purification [7], paints and coatings [4], Energy (separators and electrolytes for Lithium ion batteries (LIBs)[8], polymer exchange fuel cell membranes [9], backsheets for PV panels [10], and piezoelectric devices [2,11-13]. However, its high crystallinity-rate induces some limitations for both solubility and Li conductivity in LIBs while PVDF is difficult to crosslink [14]. One relevant feature that enables to overcome such problems deals with the copolymerization of VDF with (an)other monomer(s).

In the last five decades, poly(VDF-*co*-coM) copolymers have been of growing interest and manufactured in industrial scale, especially for copolymers based on non-functional comonomers (as TFE, HFP, CTFE, and perfluoroalkyl vinyl ether (PAVE) Fig. 1), but quite a few reviews [15-16] or book chapters [17-18] have summarized their preparations and uses.

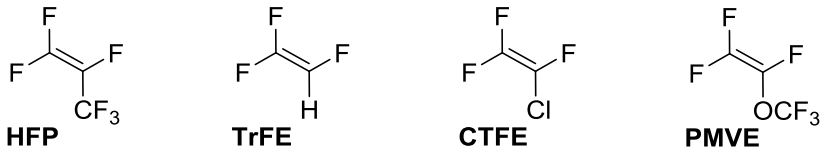

Fig. 1: Structures of fluorinated alkenes frequently used in copolymerization with VDF [15].

Though HFP, CTFE and PMVE were initially used in the copolymerization with VDF in the 60ies, an extensive academic and industrial research has still been developed in the last 30 years on the synthesis, properties and applications of fluorinated copolymers based on VDF [15-23].

The goal of this review aims at presenting non-exhaustive strategies of syntheses of functional monomers as those produced from 2-trifluoromethacrylic acid, ω-trifluorovinyl and or macromonomers and their potentiality to react with VDF (including kinetics of copolymerization), the properties of the resulting copolymers and their applications. Another section described macromolecular engineering structures *via* conventional and controlled (or RDRP) copolymerizations, in various media (aqueous processes, solution or supercritical CO_2), in presence of commercially available or original initiators. A reactivity series of these comonomers (hydrocarbon and halogenated) about that of VDF is proposed. Then, the review discloses the crosslinking of such copolymers followed by regulations, potential risk assessment and Environment concerns. Finally, relevant applications of these VDF-containing copolymers such as functiuonal coatings, elastomers, thermoplastic elastomers, composites, membranes for distillation and water purification, fuel cell membranes, separators and binders for LIBs, electroactive polymers (e.g., piezoelectric/ferroelectric/dielectric devices and actuators), and dye-sensitizors solar cells (DSSCs) will be highlighted and discussed.

2. **Functional monomers able to react with VDF**

This section aims at describing non-exhaustive (functional) M comonomers of VDF and to feature how the function borne by the comonomers induces specific properties and thus the desired applications.

Aliphatic comonomers are first summarized (including peculiar alkyl 2-trifluoromethacrylates and macromonomers) then aromatic ones.

2.1 Aliphatic Functional Comonomers

Synthesizing functional fluoromonomers such as XYC=CZ-*Sp*-**G** (where X,Y and Z designate F, H, Cl atoms or a CF_3 group, *Sp* is a spacer and **G** a functional group) is still challenging and this section summarizes a few synthetic strategies while their radical copolymerizations with VDF are reported in section 3.1.

2.1.1. Non-Halogenated

Quite a few aliphatic non fluorinated monomers have been reported to react with VDF, probably because of the loss of thermal stability of the resulting copolymers and the possibility of chain transfer (labile protons) brought by such comonomers. One example was claimed in a Kureha patent disclosing allyl glycidyl ether (AGE) as comonomers mainly as electrolytes for Lithium ion batteries (LIBs) [24]. Probably low molar mass oligo(VDF-*co*-AGE) copolymers induced some softness required to favor high Li^+ ion transport.

2.1.2. Halogenated

Scheme 1 describes routes to prepare some functional comonomers able to copolymerize with VDF [18]. The strategy starts from the radical addition of iodine monochloride onto CTFE, followed by various chemical modifications to allow the preparation of α-trifluorovinyl functional [as (thio)acetoxy and triethoxysilane] and non-conjugated diene monomers.

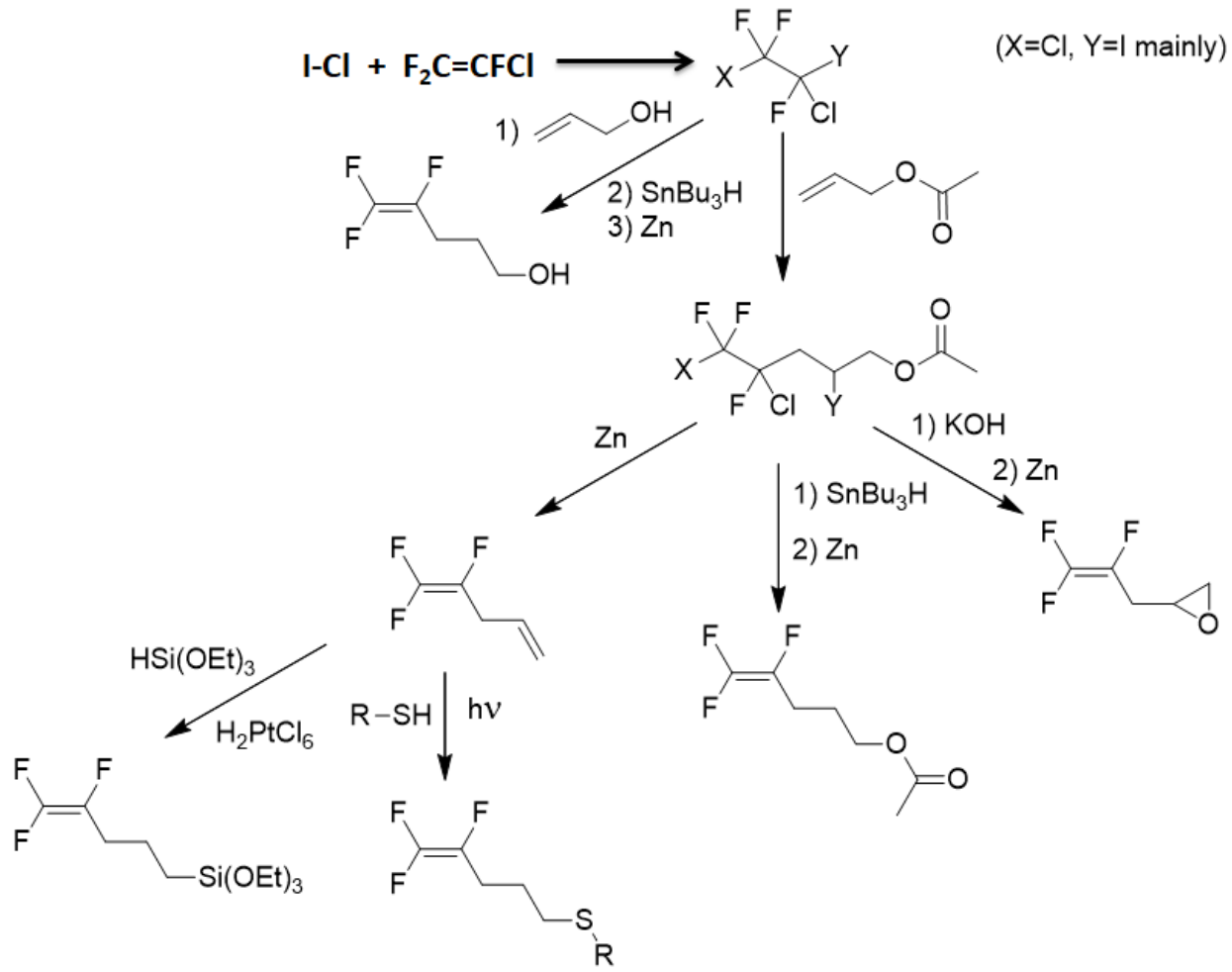

Scheme 1: Various pathways to synthesize trifluorovinyl functional comonomers from CTFE monoadduct [18]. Copyright 2012, Reproduced with permission from Wiley.

2.1.2.1. Fluoroacrylates

Designing novel fluoroacrylates has been challenging to tune their reactivity toward VDF. Acrylates and fluoroacrylates have been peculiar cases in copolymerization with VDF and it is of interest to highlight how the nature of the monomers (and the number of fluorine atoms influence their reactivity). As known, VDF being poorly stabilized by mesomery has a quite low Q value and thus cannot react well with stabilized monomer (as styrene, butadiene, and (meth)acrylate that have high Q values). As an example, Firetto et al. [25] reported the radical copolymerization of VDF with acrylic acid (AA) in supercritical carbon dioxide, initiated by diethylperoxidicarbonate. These authors noted that the resulting poly(VDF-*co*-AA) copolymers were significantly enriched in AA with respect to the initial feed composition where the AA cumulative mole fractions higher 0.60 resulted in completely

soluble copolymer in water. This quite higher reactivity of AA was also evidenced by the assessment of the reactivity ratios: r_{AA} = 305 and r_{VDF} = 0.11 at 50 °C. In contrast and unexpectedly, the Japan Synthetic Rubber [26] claimed a random, linear poly(VDF-*co*-acrylic acid ester) copolymer comprising 5-85 VDF wt%.

In addition, the radical copolymerizations of VDF with acrylic acid (AA) leading to higher VDF content in the copolymers was surprisingly claimed in Solvay Specialty Polymers patents [27-28]. To get such a non-negligible VDF amount in the resulting copolymers, a specific procedure (probably specific suspension process where the organosoluble initiator is soluble in AA phase or a slowly feeding several drops of AA diluted in solvent in the autoclave filled with VDF) was achieved but unfortunately not really detailed. These copolymers were claimed to exhibit excellent heat, ozone and sour (acid gas) gasoline resistances and also excellent resistance to gasoline permeation.

Additionally, α-fluoroacrylates, being even more reactive than hydrocarbon acrylates [29-30], could not lead to poly(VDF-*co*-alkyl α-fluoroacrylate) copolymers containing suitable VDF contents [31]. Thus, inserting one or two fluorine atom(s) in β position enabled to slow down the reactivity of fluoroacrylates in order to produce copolymers with a higher VDF amount (i.e. a functional PVDF bearing statistically dangling functions along the PVDF backbone). Several examples are described hereafter. First, α,β-difluoroacrylate, synthesized in a 3 step-procedure (Scheme 2) from the radical addition of an excess of methanol onto 1,2-difluorodichloroethylene, is less reactive than α-fluoroacrylate [32].

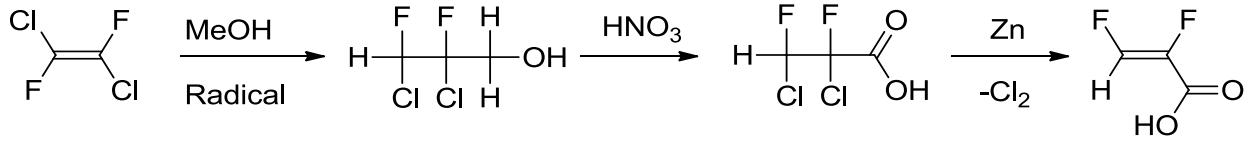

Scheme 2: synthesis of α,β-difluoroacrylic acid from the radical addition of methanol onto 1,2-dichloro-1,2-difluoroethylene (the radicals are generated from 2,5-bis(*tert*-butylperoxy)-2,5-dimethylhexane) initiator [32]

Another difluoroacrylate monomer bearing both fluorine atoms by the same carbon atom [31] was achieved in 3 steps from the radical addition of VDF with highly efficient $BrCCl_3$ chain transfer agent [33] (Scheme 3).

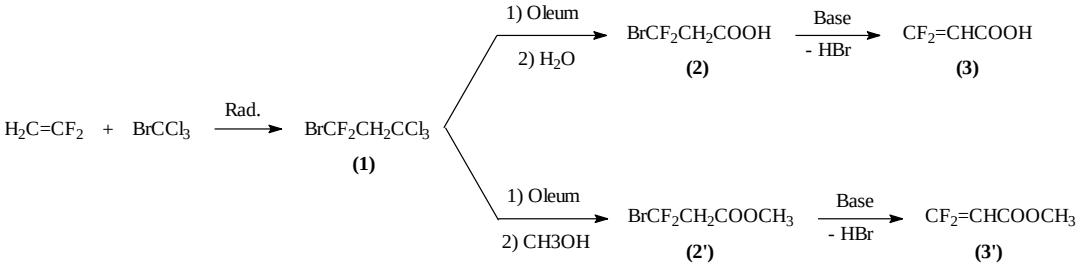

Scheme 3: synthesis of β,β-difluoroacrylate from the radical telomerization of VDF with $BrCCl_3$ [31]

Another fluorinated acrylate monomer, 2-trifluoromethacrylic acid (MAF), discovered in 1984 [34] (Scheme 4) has been currently industrially produced by the Tosoh Company (nowadays Tosoh Finechemical Company) since a few decades [35].

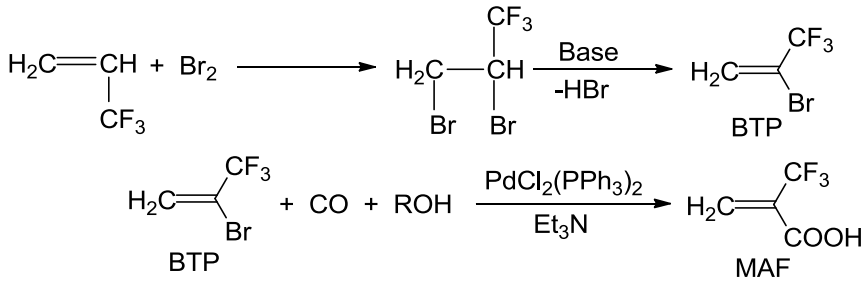

Scheme 4: Synthesis of 2-(trifluoromethyl)acrylic acid (MAF) from 3,3,3-trifluoropropene (TFP). [35] Copyright 2013, Reproduced with permission from Elsevier Science Ltd.

Surprisingly, MAF [35], methyl α,α,β-trifluoroacrylate [36] and HFIB do no homopolymerize under radical initiation but copolymerize with VDF in an alternated fashion [37-38]. Hence, it was of interest to synthesize new functional monomers as suitable VDF partners. Valuable routes consist in modifying MAF that bears specific functions for targeted applications of the resulting copolymers [40]. Hence, the carboxylic acid in MAF could be chemically changed into a wide range of groups (Scheme 5) and various routes have been reviewed in 2013 [35]. However, more recent studies in the last 5 years pushed us to suggest other 2-trifluoromethacrylate bearing specific functions as dimethyl phosphonate

[41], cyclocarbonate [42-43], furane [44], and oligo(perfluoroether)s [45] for coatings, solid polymer electrolytes and self-healing materials.

2.1.2.2. Trifluorovinyloxy monomers

Another series of suitable comonomer of VDF are those bearing a $F_2C=CFO$ end-group (as $F_2C=CFO\text{-}R_F\text{-}G$ where G stands for Br, CN [8,16-17,46-47] (section 5), SO_2F [48-51], though they cannot homopolymerize under radical initiation [52-53] in contrast to $F_2C=CF\text{-}R$ (with R = H [8,16,18,22] or CH_2R'[18,54]). First, as a model, PMVE has shown to be an efficient partner toward VDF as claimed in many patents [14-15,17,21-22].

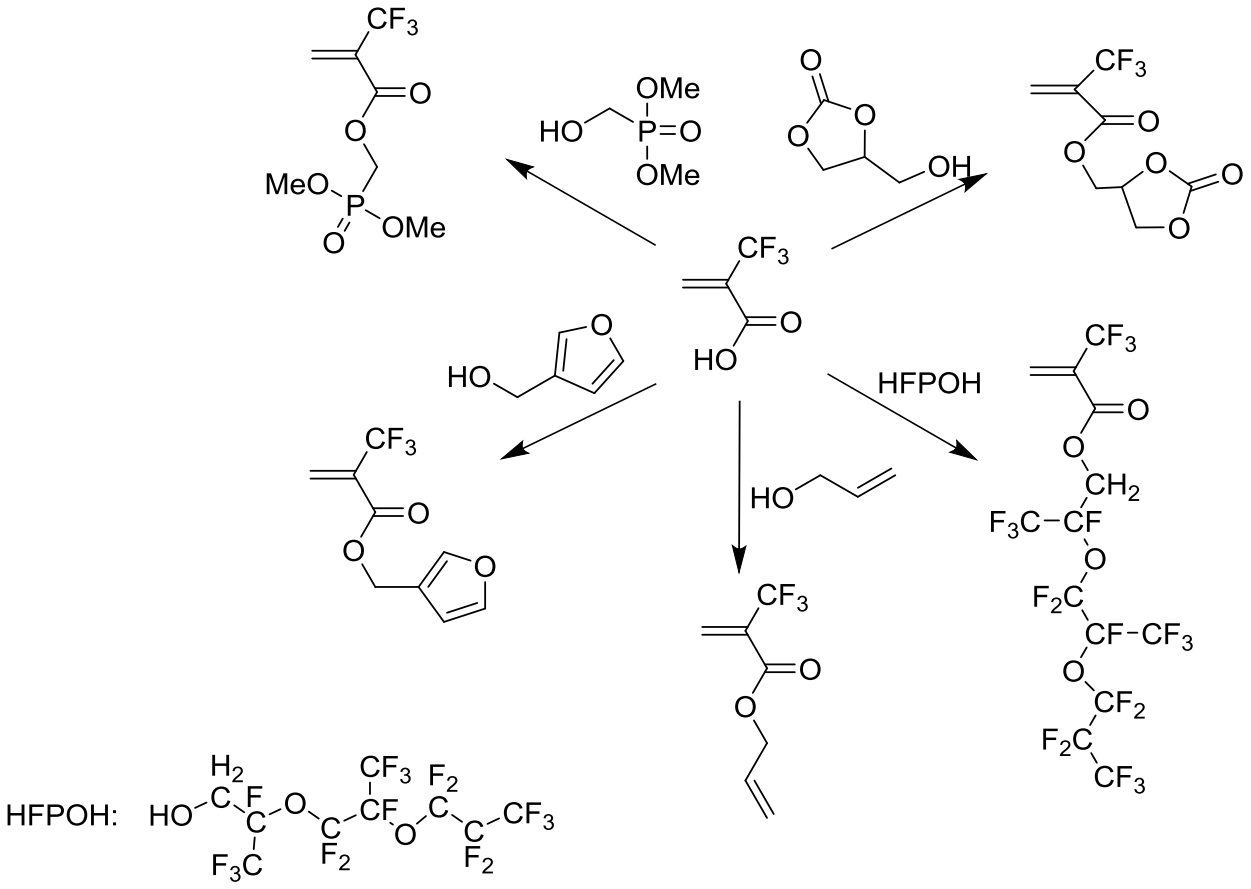

Scheme 5: synthesis of various functional 2-(trifluoromethyl) acrylates from 2-trifluoromethacrylic acid (MAF) [41-45].

2.1.2.3. Fluorinated macromonomers

Oligo(HFPO) can be synthesized by anionic oligomerization of hexafluoropropylene oxide (HFPO) [55]. Two main macromonomers containing oligo(HFPO) moieties are reported below.

Oligo(HFPO)-OCF=CF_2 macromonomers were synthesized in several steps (Scheme 6) [56] after oligomerization of HFPO. Two routes were suggested: i) either the HFPO oligomer was reacted to water to modify the acyl fluoride end-group into a carboxylic acid, followed by reacting NaOH to obtain the corresponding sodium carboxylate extremity. The salt was thermally cracked and then distilled resulting in a perfluorovinyl end-group, ii) the second alternative dealt with the thermal cracking of trimethylsilyl ester at temperature higher than 120 ^{o}C.

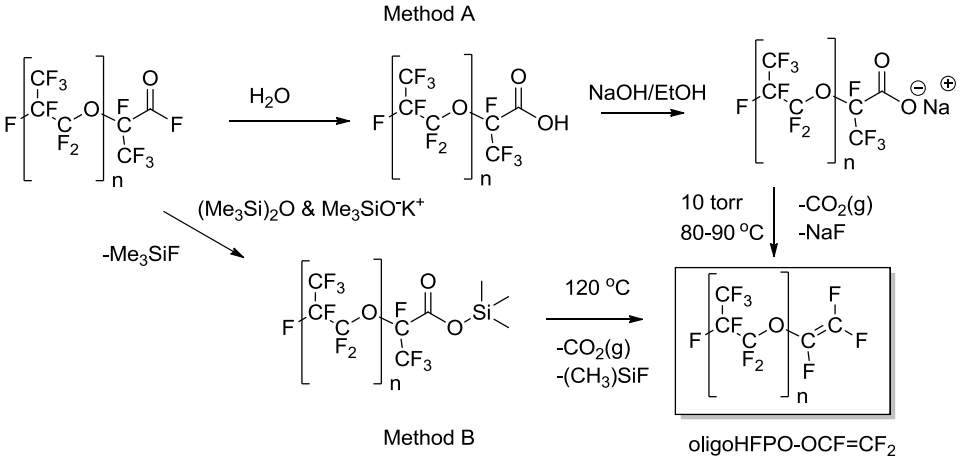

Scheme 6: Strategies in the synthesis of oligo(HFPO)-OCF=CF_2 macromonomer from oligo(hexafluoropropylene oxide) acyl fluoride [56]. Copyright 2015, Reproduced with permission from American Chemical Society.

Another strategy to offer PVDF-*g*-PFPE graft copolymers and in the continuation of this study, the same teams published another ω-unsaturated oligo(HFPO), oligo(HFPO)perfluoroisopropenyl ether (PIPE) macromonomer in 82% yield, obtained from oligo(HFPO) primary iodide (Scheme 7) [57].

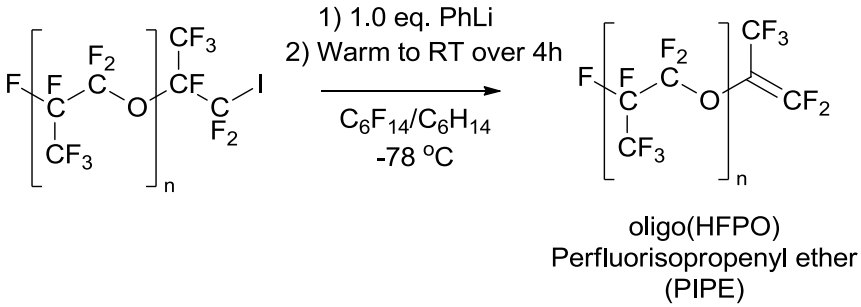

Scheme 7: synthesis of oligo(HFPO)perfluoroisopropenyl ether (PIPE) macromonomer from an oligo(hexafluoropropylene oxide) primary iodide and phenyl lithium in a 50/50 mole ratio of hexane and perfluorohexane [57]. Copyright 2019, Reproduced with permission from RSC.

2.2. Aromatic comonomers

Various aromatic fluorinated monomers have been reported and, as expected, the position of the Fluorine atom(s) or fluorinated group(s) imparts on their reactivity. For example, the reactivity of styrene (St) is similar to that of a styrenic monomer bearing a $(CH_2)_nR_F$ side group in para position to the double bond. Indeed, its high Q value (1.0) compared to that of VDF (0.008) favors rich St-copolymers. α–Fluorostyrene and pentafluorostyrene (PFSt) are more reactive than St as evidenced by their apparent rate coefficients [58,59], the five fluorine atoms in PFSt highly increasing its rate of polymerization. In addition, a para methoxy group (about the double bond) of tetrafluorostyrene (TFMSt) enhances the polymerization-rate even further compared to that of PFSt. The decreasing reactivity series in radical homopolymerization of various styrenes was established as follows: TFMSt > PFSt > 4-trifluoromethyl styrene > St while α-trifluoromethyl styrene does not homopolymerize under radical conditions [60]. Its synthesis, from the palladium-catalyzed coupling reaction of an aromatic organoboron compound **1** with a trifluoromethyl electrophile **2** in the presence of a base (Scheme 8), as well as those of mono- and difluorostyrene were revisited by Walkowiak et al. [61].

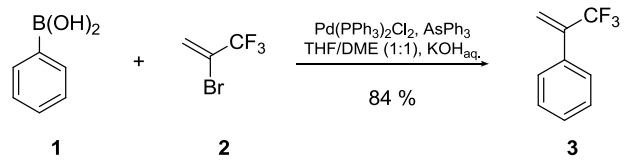

Scheme 8: Suzuki coupling between phenyl boronic acid and 2-bromo-3,3,3-trifluoroprop-1-ene

2.3. Conclusion

Initially, non-functional comonomers were copolymerized with VDF but, in the last 30 years, many efforts have been developed to build a new generation of aliphatic and aromatic functional comonomers to further react with VDF, containing various groups and halogen atoms. Their reactivities in copolymerization with VDF have been reported, as summarized in the following section.

3. Radical copolymerization of VDF with comonomers

This section is divided into three parts, conventional and controlled radical copolymerization of VDF with such above comonomers, including the effect of the choice of initiation system, process and kinetics of copolymerization (section 3.1.6) to establish some comparisons of reactivity between these comonomers versus VDF. A third section concerns the crosslinking of these fluorinated copolymers. Actually, the G function brought by the comonomers enables to bring a property for the desired application (Scheme 9).

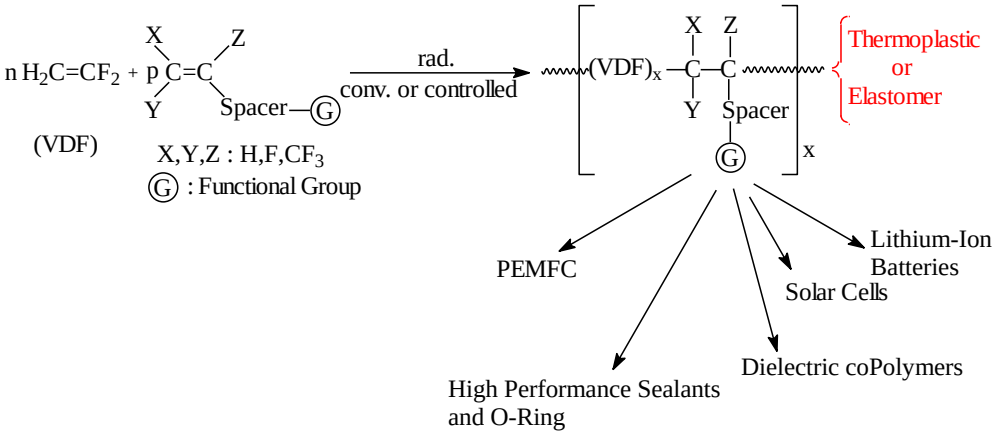

Scheme 9: conventional or controlled radical copolymerization of VDF with functional fluoromonomers (G represents a function as carboxylic, phosphonic or sulfonic acid, trialkoxysilane, furane, oligo(ethylene oxide), oligo(fluoroalkyl ether), etc. and use of the resulting copolymers for diverse applications (PEMFC stands for polymer exchange fuel cell membrane).

3.1 Conventional radical copolymerization

3.1.1. Non-fluorinated comonomers

Inserting phosphorous atoms into fluorinated copolymers is challenging and valuable since the resulting materials should display interesting properties as flame retardancy, adhesion (via phosphonic acid function), complexation and anti-corrosion [62]. One example deals with the copolymerization of vinyl dimethyl phosphonate (VDMP) (that does not propagate under radical conditions) with VDF. First attempts achieved at low temperature failed [63] but more recent success was obtained in presence of 2,5-dimethyl-2,5-di(*tert*-butylperoxy) hexane (DTBPH) initiator (Scheme 10) leading to rich-VDF cooligomers [64].

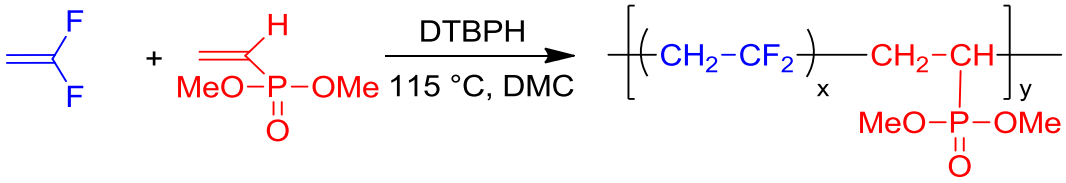

Scheme 10: Conventional radical copolymerization of VDF with vinyl dimethylphosphonate initiated by 2,5-di(*tert*-butylperoxy) hexane (DTBPH) in dimethyl carbonate (DMC) from [64].

These poly(VDF-*co*-VDMP) cooligomers were quite useful for various applications as extraction of precious and noble metals and solid polymer electrolytes (SPEs) for Lithium ion batteries. First, when hydrolyzed into novel fluorinated macromolecules bearing phosphonic acid moieties, were cooligomers could extract Au and rare earths (La, Nd, Dy, Yb and Sc) [65] showing that their selectivity can be tuned according to the polymer nature. Second, when mixed with lithium bis(trifluoromethanesulfonyl)imide) (LiTFSI), SPEs were prepared (with satisfactory Li^+ conductivities and electrochemical stability up to ca. 5 V) and preliminary flammability tests led to encouraging fire-resistance properties (Fig. 2).

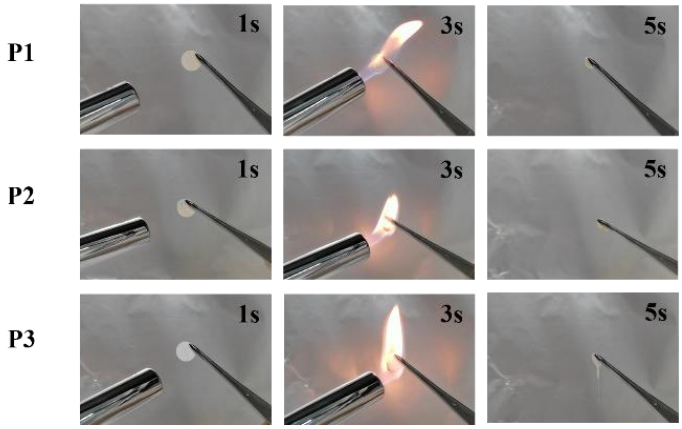

Fig. 2: Flammability tests performed on the SPEs films derived from P1 (90 mol% VDF), P2 (70 mol% VDF), and P3 (ca. 50 mol% VDF) poly(VDF-*co*-VDMP) cooligomers with VDMP/Li+ 2:1 molar ratio versus time [64] (VDMP stands for vinyl dimethylphosphonate). Copyright 2021, Reproduced with permission from Wiley.

3.1.2. Fluorinated comonomers

Poly(VDF-*co*-HFP) copolymers, industrially produced from decades by various companies, are chemically inert and show lower degree of crystallinity than that of PVDF due to the presence of the bulky CF_3 side groups [6,15-17,20-21], even to reach amorphous states from ca. 20 mol.% HFP (Fig. 3 [66]) (called FKM®; section 7.2).

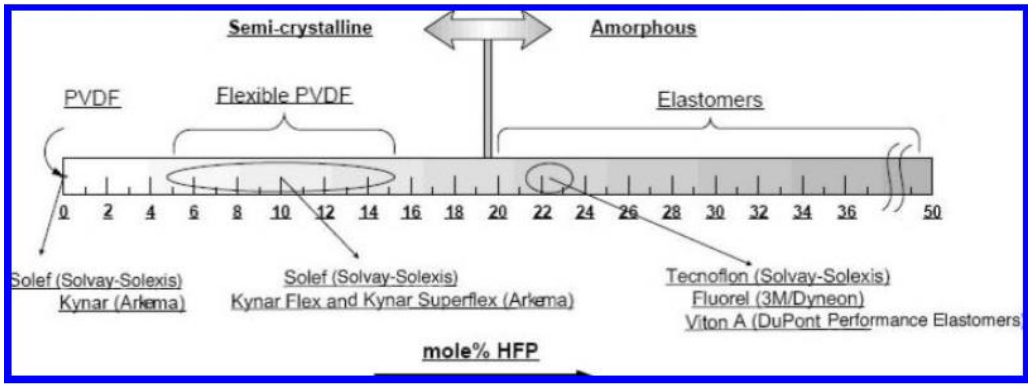

Fig. 3: Semicrystalline or amorphous poly(VDF-*co*-HFP) copolymers according to the HFP content in the copolymer [66]. Copyright 2007. Reproduced with permission from the American Chemical Society.

Similarly, according to the molar composition, poly(VDF-*co*-CTFE) copolymers can also be either semicrystalline or amorphous (Fig. 4) [67].

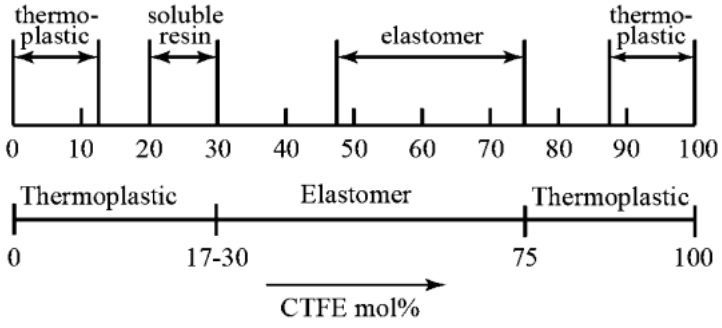

Fig. 4: Relationship between the CTFE content and the thermoplastic or elastomeric behavior of poly(CTFE-*co*-VDF) copolymers. [67] Copyright 2014. Reprinted with permission from the Amer Chem Soc.

8-Bromo-1H, 1H, 2H-perfluorooct-ene (BDFO), synthesized by mono ethylenation of $BrC_6F_{12}Br$ followed by dehydrobromination [68] was copolymerized with VDF in order to prepare original precursors of PVDF-*g*-PS graft copolymers by ATRP of styrene [69].

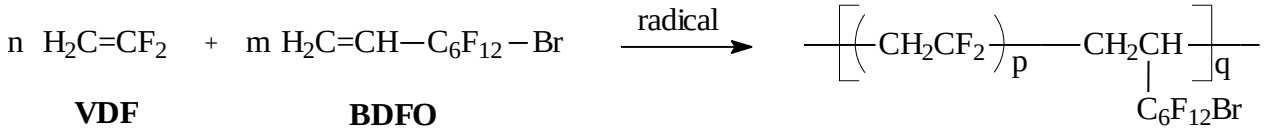

Scheme 11: Radical copolymerization of VDF with 8-bromo-1H,1H,2H-perfluorooct-1-ene (BDFO)[68].

3.1.2.1. Copolymerization of VDF with acrylates and fluorinated acrylates

As mentioned above for styrene, acrylates also are stabilized by resonance and quite reactive about VDF, usually generating acrylate-rich copolymers containing only a few VDF units. Hence, their reactivities can be much reduced by using acrylates bearing fluorine atom or CF_3 groups on unsaturated carbon atoms and several comparable examples of copolymerization of VDF with these fluoroacrylates are supplied hereafter.

In contrast to alkyl α-fluoroacrylates which are even more reactive than acrylates [29-30], the presence of Fluorine atoms in β position reduces its reactivity significantly in homopolymerization while its copolymerization with VDF was successful [32] (Scheme 12).

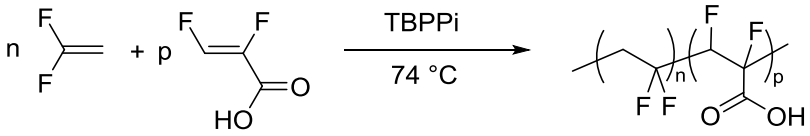

Scheme 12: radical copolymerization of VDF with α,β-difluoroacrylic acid (where TBPPi stands for *tert*-butyl peroxypivalate). [32]

i) Alkyl 2-Trifluoromethacrylate

A peculiar monomer, trifluoromethacrylic acid, MAF, does not homopolymerize under radical initiation [40,60,70-71] but copolymerizes with VDF and, interestingly, in an alternating behavior

(Scheme 13), as evidenced by the kinetics of copolymerization that estimated their reactivity ratios: $r_{VDF} = 0.33 \pm 0.03$ and $r_{MAF} = 0$ at 50 °C [72] while $r_{VDF} = 0.040 \pm 0.03$ and $r_{MAF\text{-}TBE} = 0.036$ at 57 °C [39] (where MAF-TBE stands for *tert*-butyl trifluoromethyl acrylate). Similarly for that involving hexafluoroisobutylene (HFIB), the reaction was very fast, accompanied with a strong exotherm and produced the copolymers in high yields.

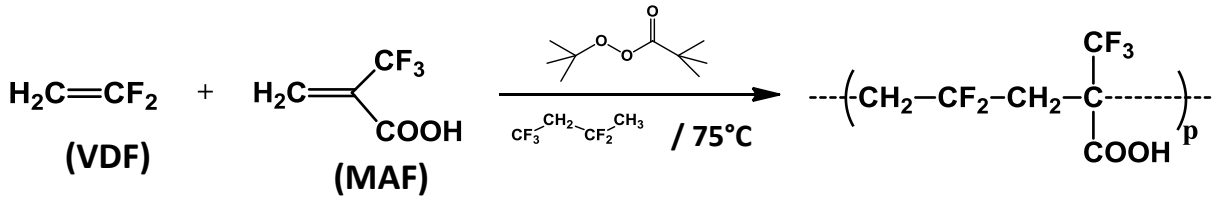

Scheme 13: radical copolymerization of VDF with 2-trifluoromethacrylic acid (MAF) initiated by *tert*-butyl peroxypivalate. [72]

In the same vein, MAF monomer containing C_6F_{13} side group also reacted well with VDF leading to original PVDF bearing C_6F_{13} [73] which could increase both the hydrophobicity (water contact angle worths 114 ° higher than that of PVDF (90 °) and thermal stability of PVDF. Indeed, poly(VDF-*co*-MAF) copolymer undergoes some thermal decomposition from 140 °C (Fig. 5) via a decarboxylation while poly(VDF-*co*-MAF-TBE) is slightly more stable and loses isobutylene first followed by CO_2 (Scheme 14). Indeed, also mentioned in section 2.1.2.1, further modification of MAF led to original monomer bearing triethylene oxide (EO) side group, efficiently copolymerized with VDF [74] yielding poly[VDF-*g*-oligo(EO)] copolymers (Scheme 14) for LIBs applications.

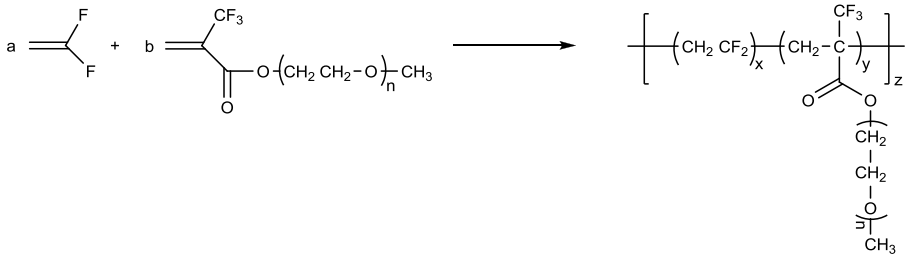

Scheme 14: radical copolymerization of VDF with ω-methyltriethylene oxide 2-trifluoromethyl acrylate [74].

A similar strategy was also used to prepare modified MAF bearing a perfluoroalkylether group which copolymerizes with VDF (Scheme 15) yielding copolymers of molar masses ranging between 35 and 50 $kg.mol^{-1}$.[45] When mixed with lithium bis(trifluoromethanesulfonyl)imide and 1-ethyl-3-methylimidazolium bis(trifluoromethylsulfonyl)imide, homogeneous polymer gel electrolytes (section 7.6.2) were produced with conductivity reaching up to 3×10^{-3} $S \cdot cm^{-1}$ at room temperature.

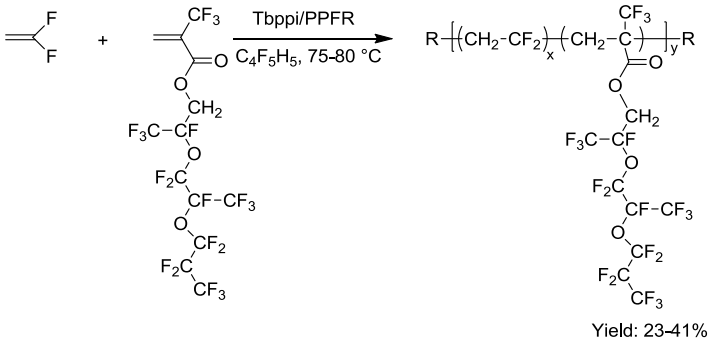

Tbppi: tertiary butyl peroxypivalate
PPFR: perfluoro-3-ethyl-2,4-dimethyl-3-pentyl persistent radical

Scheme 15: Radical copolymerization of VDF with perfluoroalkylether 2-trifluoromethacrylate Initiated by perfluoro-3-ethyl-2,4-dimethyl-3-pentyl persistent radical (PPFR) or *tert*-butyl peroxypivalate (Tbppi) [45].

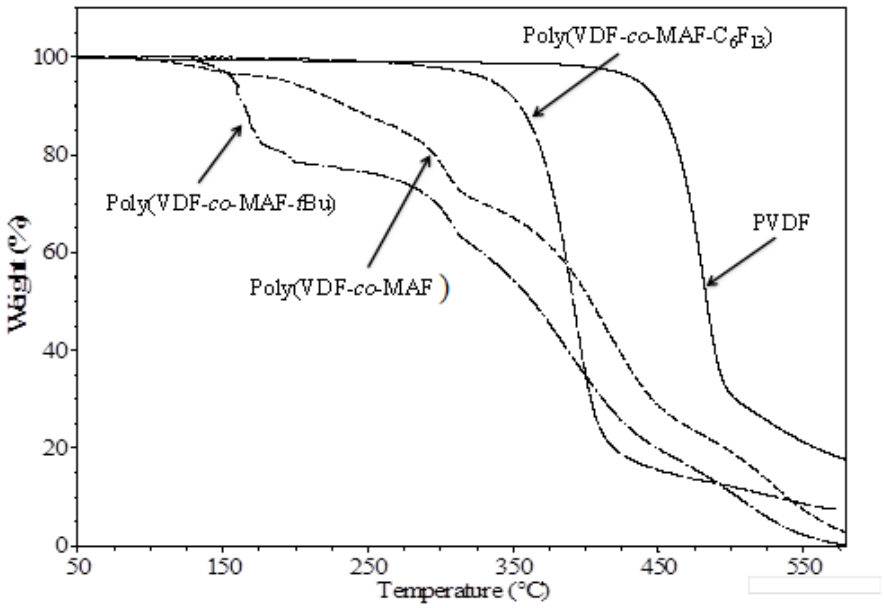

Fig. 5: TGA thermograms of PVDF homopolymer (full curve) and various poly(VDF-co-MAF derivative) copolymers. PVDF homopolymer, Mn >400 000 g mol^{-1}, Td(10%) = 451 °C. Poly(VDF-*co*-MAF-C_6F_{13}), (dashed line; Mn = 17 400 g mol^{-1}, VDF in copolymer 67 mol %, T_{dec}(10%) = 355 °C). Poly(VDF-*co*-MAF), (Mn = 21,000 g mol^{-1}, VDF in copolymer 54 mol %, T_{dec}(10%) = 233 °C). Poly(VDF-*co*-MAF-tBu), (semi-dashed line, Mn = 49 900 g mol^{-1}, VDF in copolymer 49 mol %, T_{dec}(10%) = 176 °C). Heating rate of 20 °C min^{-1} under an air flow [73]. Copyright 2014, Reproduced with permission from the American Chemical Society.

Other commercially available comonomers (F_2C=CHBr [75], F_2C=CHCl [76], H_2C=C(CF_3)Cl [76] and F_2C=CFBr [77] to name a few) have also been copolymerized with VDF.

3.1.2.2. Radical copolymerization of VDF with macromonomers

Quite a few macromonomers have been used in copolymerization with VDF, and, to the best of our knowledge, CTFE (or VDF) telomers and HFPO oligomers are key examples.

CTFE (or VDF) macromonomers obtained by telomerization of CTFE (or VDF, A) with $BrCF_2CFClBr$ followed by dehalogenation (Scheme 16), have been copolymerized with VDF for moisture-barrier coating applications [78]. The resulting copolymers advantageously bear a bromo side group able to be crosslinked in presence of peroxides (section 5).

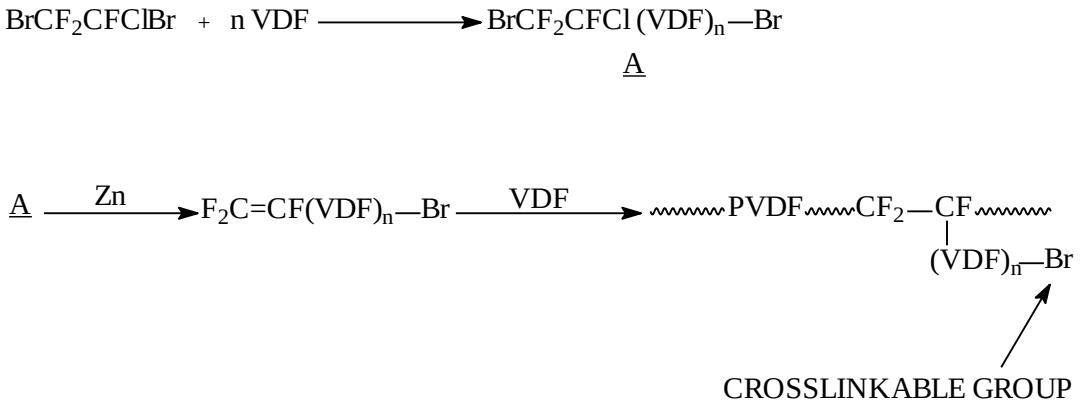

Scheme 16: radical copolymerization of VDF with VDF macromonomers produced by telomerization of VDF in presence of $BrCF_2CFClBr$ followed by dehalogenation [78].

Regarding HFPO macromonomers (their syntheses being depicted in Schemes 6 and 7), two examples are considered hereafter. The first one involved the radical copolymerization of VDF with

this oligo(PFPE) leading to PVDF-*g*-oligo(F-ether), the Tg and $T_{dec5\%}$ of which ranged between -79 and -54 °C and from 410 to 494 °C, respectively (Scheme 17) [56].

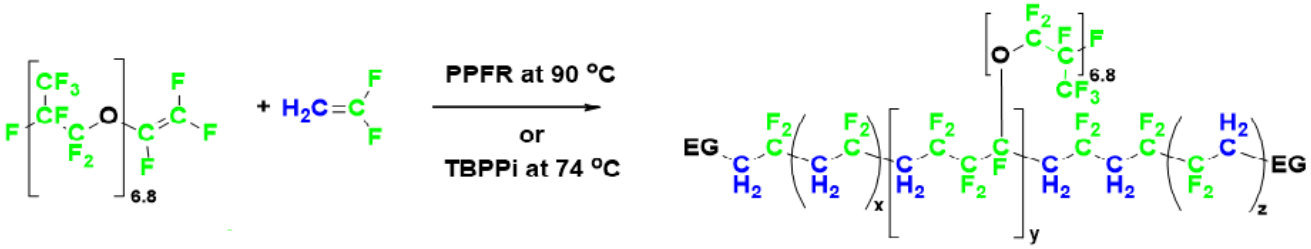

Scheme 17: radical copolymerization of VDF with an ω-trifluorovinyloxy oligoHFPO [where EG, PPFR and TBPPi stand for end-group (e.g. CF_3 or *tert*-Bu(O)), perfluoro-3-ethyl-2,4-dimethyl-3-pentyl persistent radical and *tert*-butyl peroxypivalate, respectively] [56].

Further, the radical copolymerization of such oligo(HFPO)perfluoroisopropenyl ether **(**PIPE) comonomers (Scheme 7) with VDF, initiated by perfluoro-3-ethyl-2,4-dimethyl-3-pentyl persistent radical (PPFR, section 3.1.3.1), led to poly[VDF-*g*-oligo(HFPO)-PIPE] graft copolymers in 76-97 yields (Scheme 18)[57]. Their molar masses ranged between 7,500 and 42,600 $g.mol^{-1}$ while the molar percentages of VDF and oligo(HFPO)-PIPE comonomers reached up to 99% and 20%, respectively.

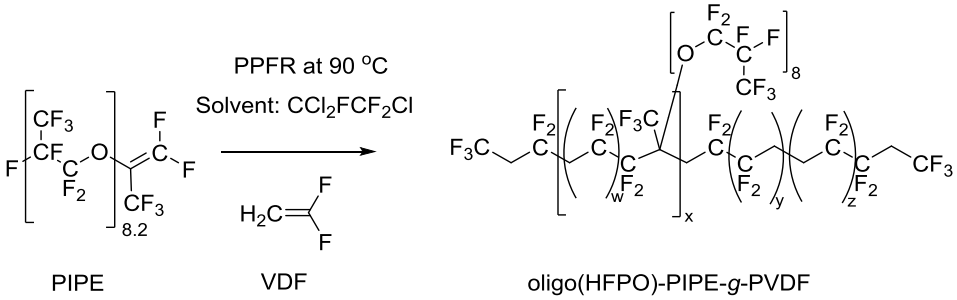

Scheme 18: Radical copolymerization of oligo(HFPO) perfluoroisopropenyl ether (PIPE) macromonomer with VDF initiated by $^{\bullet}CF_3$ radical generated by perfluoro-3-ethyl-2,4-dimethyl-3-pentyl persistent radical (PPFR) at 90 °C yielding PVDF-*g*-PFPE graft copolymers [57].

3.1.2.3. Alternating poly(VDF-*alt*-M) copolymers

Usually, random copolymers based on VDF have been produced but only three M_x peculiar comonomers (hexafluoroacetone, MAF, hexafluoroisobutylene (Fig. 6) and alkyl trifluoroacrylate) were reported to lead to alternating poly(VDF-*alt*- M_x) copolymers.

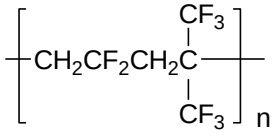

Fig. 6: structure of alternating poly(VDF-*alt*-HFIB) copolymer (HFIB stands for hexafluoroisobutylene) [35-37].

Alternated poly(VDF-*alt*-HFIB) copolymer was produced by emulsion copolymerization [37-38,79]. The alternance was evidenced by the product of the reactivity ratios that is close to zero (r_{VDF} = 0.136 and r_{HFIB} = 0.047 at 65 °C [79], but, as the sense of addition, it is still difficult to explain from known rules of alternance and conventional theories based on the electronic delocalization of fluoromonomers.

Such a copolymer was industrially marketed by the Allied Chemical Corporation (then Honeywell Company) under the CM1® tradename, but its production seems to be stopped because of the severe HFIB toxicity. The comparison of its properties to those of PVDF and PTFE was reported by Minhas and Petrucelli [37]. This thermoplastic (Tg=132 °C while the melting temperature, T_m, depends on the reaction conditions, initiators and media, ranging from 325-7 °C [37] to 350 °C [79] when the reaction was carried out at 0 °C) is poorly soluble in common solvents but can be melt processed [37] in contrast to PTFE. Though this copolymer contains two methylene groups in the VDF-HFIB dyad, its thermal and chemical stabilities are in the same order as those of PTFE as well as its critical surface tension of 19 dyne.cm^{-1} (20 and 31 dyne.cm^{-1} for PTFE and ECTFE, respectively) explained by the presence of both CF_3 side groups bringing some protection.

3.1.3. Beyond initiation and process

Usually the conventional radical copolymerization of VDF with a comonomer is industrially carried out in aqueous process initiated by water soluble persulfates or organosoluble peroxides (including pentafluoropropionyl peroxide). However, peculiar initiators and processes have also been investigated, as summarized below.

3.1.3.1. Specific radcal initiators

Scarce fluorinated initiators have been used in radical copolymerizations of VDF with other comonomers. The goal was both to allow an efficient initiation (as reported by Tedder and Walton in the 70-80ies [80]) and to be able to get "true" molar masses since the fluorinated end-group acts as a label in ^{19}F NMR spectroscopy. Several examples are supplied hereafter.

i) Use of $CF_3O°$ radical

The radical copolymerization of VDF with HFP, initiated by a bis(trifluoromethylperoxy) dicarbonate releasing a $CF_3O°$ radical, (Scheme 19) [81] yielded novel poly(VDF-*co*-HFP) copolymers bearing CF_3O end-groups (Scheme 20).

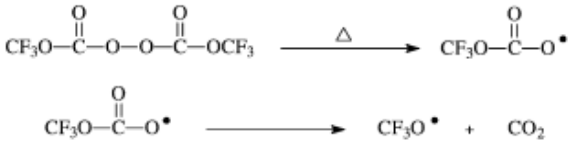

Scheme 19: Decarboxylation reaction of $CF_3C(O)O°$ yielding $CF_3O°$ radical [81].

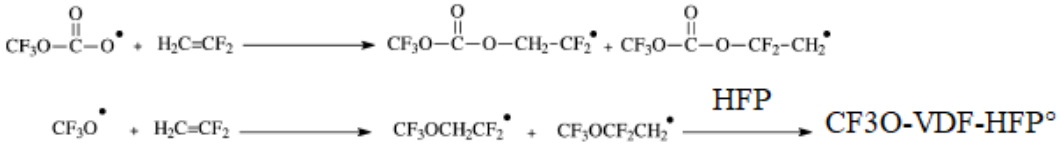

Scheme 20: Four different end-groups radicals generated by two types of initiation from bis(trifluoromethyl peroxy) dicarbonate.

ii) Use of $°CF_3$ radical

Though several strategies have been reported to release $CF_3°$ radical from various organofluorinated synthons [82-87] (Scheme 21), a few have been used in radical (co)polymerization of VDF [83,86, 88].

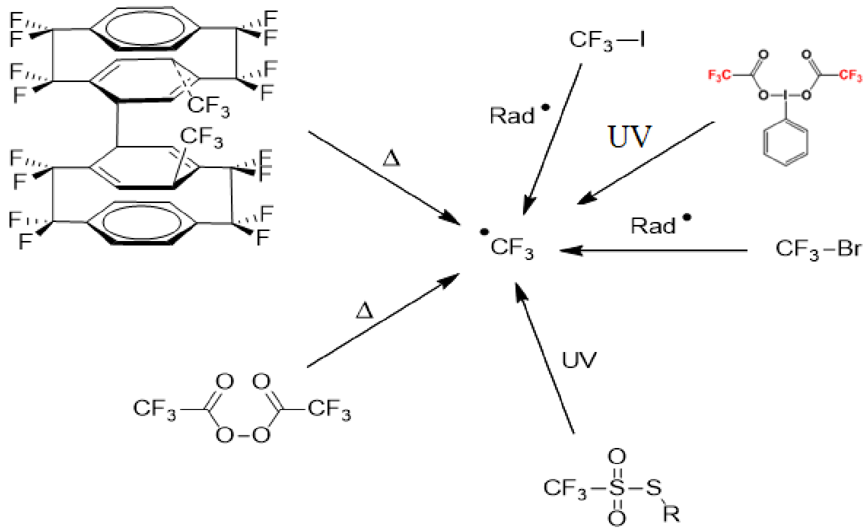

Scheme 21: various strategies to generate a trifluoromethyl radical [82-87]

Among them, perfluoro-3-ethyl-2,4-dimethyl-3-pentyle radical (PPFR), persistent at room temperature, is able to release a CF_3° radical from 90 °C [86, 88] (Scheme 22) and has been successfully used to synthesize various VDF-containing copolymers bearing CF_3 end-groups from seven fluoroalkenes (Scheme 23) [88] and two macromonomers (Schemes 17-18) [55-56].

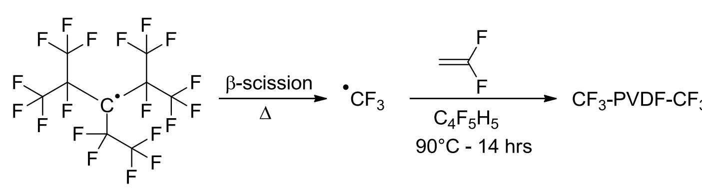

Scheme 22: release of CF_3° radical from perfluoro-3-ethyl-2,4-dimethyl-3-pentyle radical (PPFR) under heat and initiation of the radical polymerization of VDF [86]

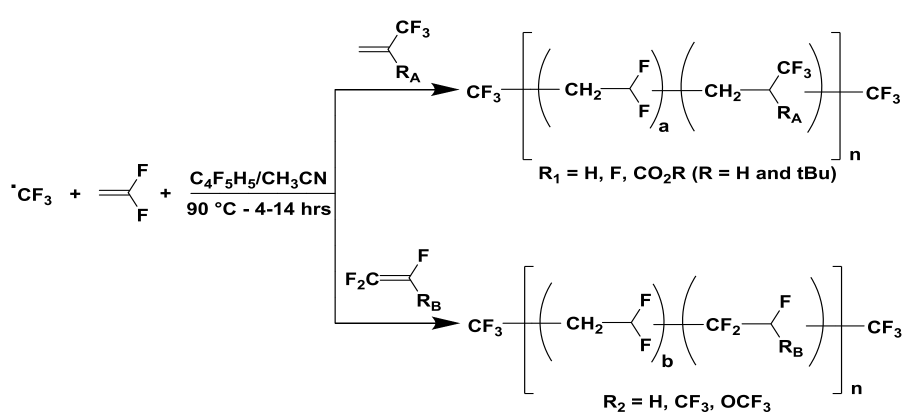

Scheme 23: Radical copolymerization of VDF with various fluorinated comonomers initiated by a trifluoromethyl radical generated from a persistent perfluoro-3-ethyl-2,4-dimethyl-3-pentyle radical [88]. Copyright 2013, Reproduced with permission from the American Chemical Society.

From CF_3SO_2K

More recently, potassium trifluoromethyl sulfonite that also releases a trifluoromethyl radical from 80 °C, (Scheme 24) in the presence of an oxidant (e.g. persulfate) was able to initiate the aqueous copolymerization of VDF with HFP (or PMVE, Scheme 25), as well as the terpolymerization of these three monomers [89-90].

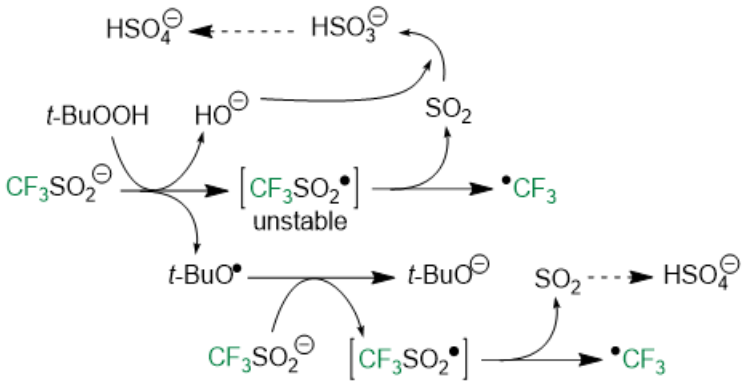

Scheme 24: Mechanism of the oxidation of trifluoromethyl sulfinate, leading to the generation of $•CF_3$ radicals [90]. Copyright 2021, Reproduced with permission from the American Chemical Society.

The interest of such reactions was i) the absence of any (fluoro)surfactant as usually involved in such process and ii) the presence of CF_3 end groups that enhances the thermostability of the resulting copolymers in contrast to commercially available ones which undergo some "unzipping" degradation from sulfonate end-groups.

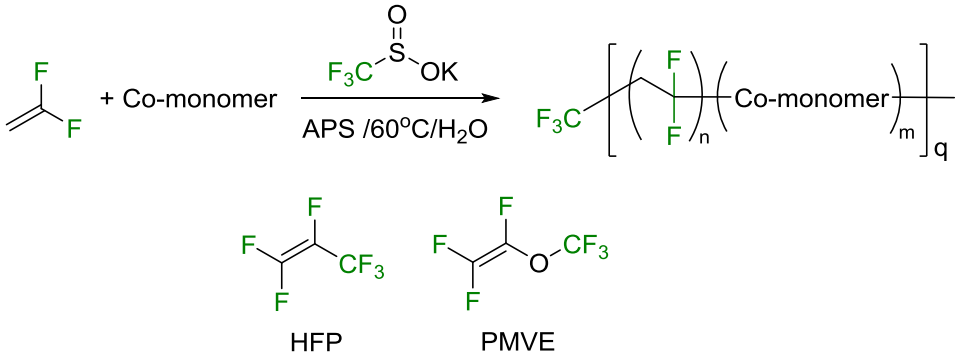

Scheme 25: Radical copolymerization of VDF with HFP (or PMVE), initiated by CF_3SO_2K and ammonium persulfate (APS) [89-90]

iii) Releasing Borane radical

In the presence of oxygen, triakyl boron derivatives are able to generate $RO^{\bullet}$ peroxy radical that initiates the (co)polymerization of fluoroalkenes (Scheme 26) while $^{\bullet}OBR_2$ plays the role of a counter radical stabilized by the back donating effect on the radical from the π orbital. This source of initiator for the borane-mediated polymerization of fluoroalkenes occurs at room temperature as pioneered and comprehensively studied by Chung [91-92] on the co- and terpolymerization of VDF with various comonomers for various applications.

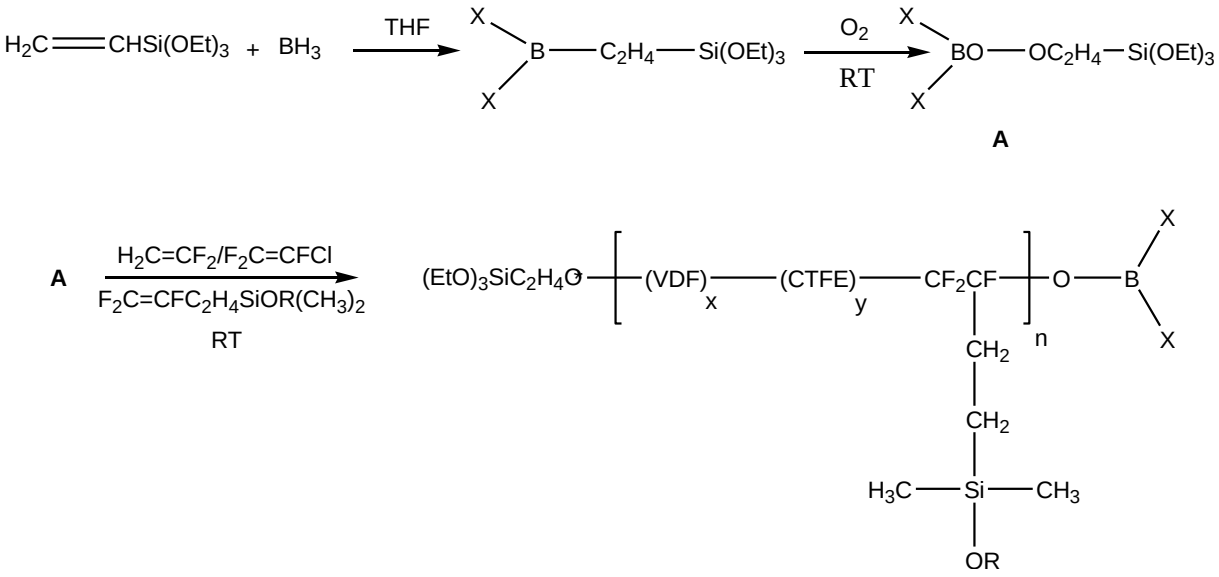

Scheme 26: Synthesis of poly[VDF-*ter*-CTFE-*ter*-$CF_2CFRSi(OR)_3$] terpolymers by borane mediated terpolymerization of VDF, CTFE and a trifluorovinyl silane comonomer (where X can be H or $C_2H_4Si(OEt)_3$) [92]. Copyright 2014, Reproduced with permission from John Wiley & Sons Inc.

3.1.3.2. Various media in radical copolymerization of VDF

i) Aqueous processes

Many patents disclose the aqueous processes (emulsion, suspension or dispersion) copolymerization of VDF with other comonomers, well cited in books [2-4,17,20] or reviews [16, 52].

Prior to 2006, all manufacturers of FPs used perfluorooctanoic acid (PFOA) or perfluorooctane sulfonic acid (PFOS) as efficient surfactants for such processes. But the US Environment Protection Agency (EPA) *via* the 2010-2015 PFOA stewardship program [93-97] aimed to ban these specific perfluoroalkyl substances (PFASs) since 2015. But there is no scientific evidence to justify considering that VDF-containing copolymers have the same level of regulatory concern as PFASs (see section 6). Hence, new innovating (with a shorter fluorinated group) emulsifiers [94,98-100] or hydrocarbon and biobased ones have been used in (co)polymerization of various fluoroolefins including VDF [101-103]. For example, short Adona® surfactant ($CF_3OC_3F_6OCHFCF_2CO_2^-$) [99] or other similar types as APFDO or Gen®X [94] were used in emulsion copolymerization of VDF with HFP.

Another more recent example deals with the emulsion copolymerization of VDF with PMVE [104] in presence of $HOCH_2CH(CF_3)CO_2H$ as the surfactant. This derivative is potentially degradable and was totally mineralized under subcritical water [105]. It was first involved in the homopolymerization of VDF [105] and then in copolymerization of VDF with PMVE (Scheme 27). The resulting copolymer displayed molar masses up to 103 $kg.mol^{-1}$ (showing quite a few transfer-up to 0.33%) and an excellent thermal stability (the decomposition temperature at which 5 wt% was lost, $T_{dec,5\%}$ was 450 °C under air).

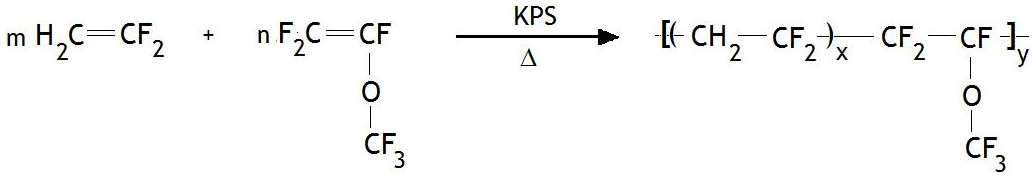

Scheme 27: synthesis of poly(VDF-*co*-PMVE) copolymer initiated by potassium persulfate (KPS). In presence of $HOCH_2CH(CF_3)CO_2H$ surfactant [104].

By cryo-TEM analysis, the resulting latexes displayed particle sizes of ca. 200 nm (Fig. 7).

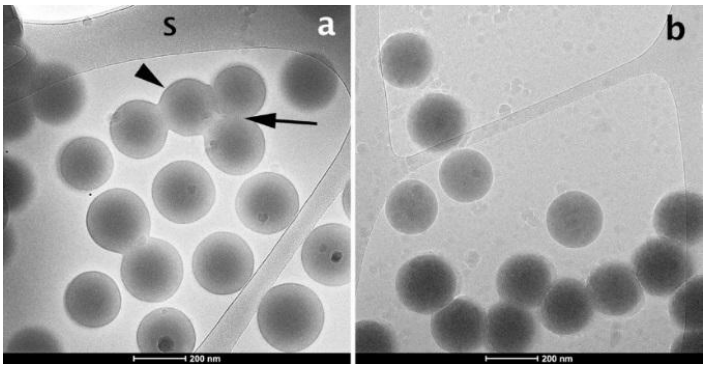

Fig. 7: Cryo-TEM pictures poly(VDF-*co*-PMVE) copolymers. In figure (a), the arrow head points to a dark layer surrounding the articles. The arrow points to a plane of fusion, where no dark layer is seen. The scale is 200 nm [104].Copyright 2020, Reproduced with permission from RSC.

i) Supercritical CO_2

VDF, HFP, TFE, CTFE and other fluoroalkenes are hydrophobic gases for which the medium plays an essential role. Among the media, supercritical CO_2 ($scCO_2$) is a dense fluid able to solubilize fluoropolymers [106], to carry out some radical copolymerizations of fluorinated monomers and comprehensively documented by DeSimone [107-108]. Since that discovery, other surveys, including those of VDF with various comonomers (e.g., acrylic acid [25], vinyl acetate [109], HFP [108-110]), have been reported.

More recently, Beuermann's team [110] extensively studied the kinetics of radical copolymerization of VDF with HFP and monitored the pressure and temperature influences on the homopolymerization of VDF, k_p, and on the copolymerizations of VDF and HFP, $<k_{p,COPO}>$ (Fig. 8).

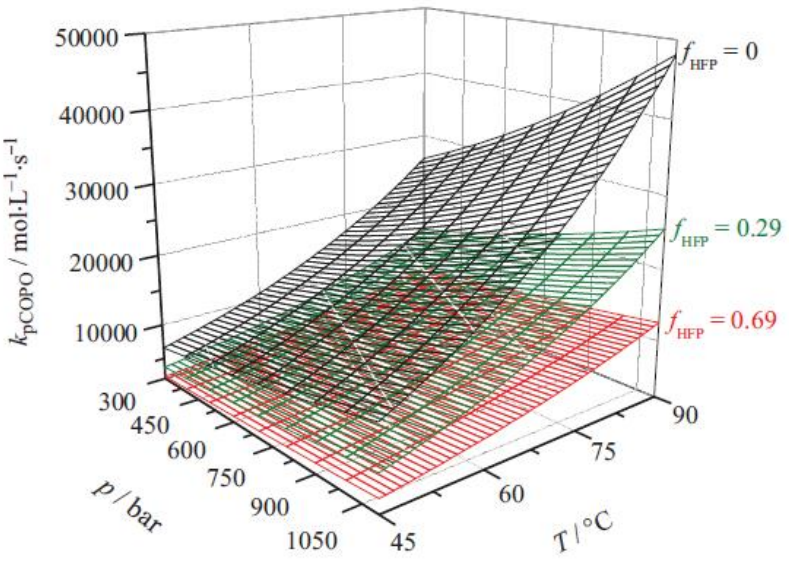

Fig. 8: Pressure and temperature dependences of VDF homopolymerization kp (black) and k $_{p,COPO}$ for the copolymerizations of VDF and HFP with initial molar feed ratio, f_{HFP}= 0.29 (green) and f_{HFP}=0.69 (red) [110]. Copyright 2018. Reproduced from with permission from Elsevier.

The knowledge of the composition of the remaining monomer enabled the authors to calcule kp,COPO versus time. The resulting variation of <kt,COPO> with the conversion is displayed in Fig. 9, the reaction conditions being supplied in the caption [110]. The left figure exhibits the monomer conversion versus time while that on the right side plots $<k_{t,COPO}>$ *vs* the monomer conversion. The temperature has a strong influence on the conversion versus time. In addition, a rather high impact on $<k_{t,COPO}>$ can be observed. If pressure and temperature are kept constant, f_{VDF} variation from 0.45 to 0.65 has a small influence on the conversion vs time and <kt,COPO>. In all cases, $<k_{t,COPO}>$ is reduced with an increasing monomer conversion and hence an increasing viscosity in the medium. The initial values for $<k_{t,COPO}>$ ranged between $1.5x10^9$ and $6.3x10^9$ Lmol^{-1} s^{-1}. These low conversions are close to the physically meaningful limit for diffusion-controlled rate coefficients, which is considered to be due to the low viscosity system made of $scCO_2$ and the gaseous monomers.

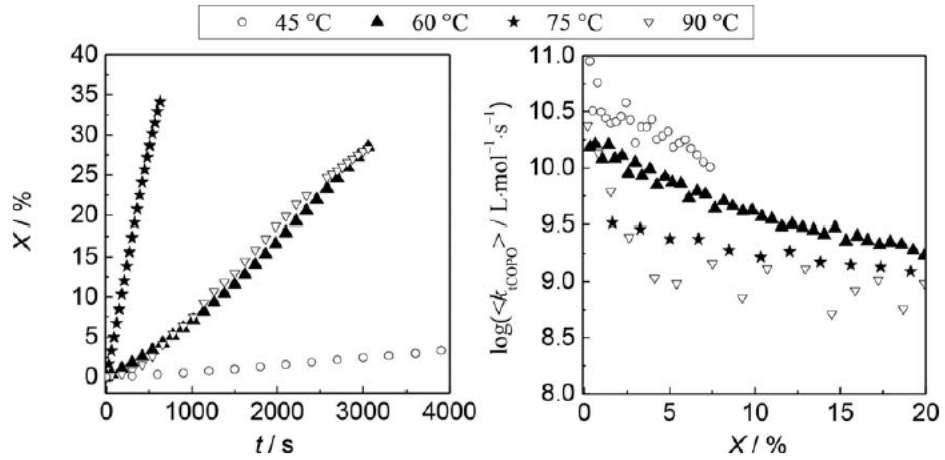

Fig. 9: Conversion *versus* time (left) and log(<$k_{t,COPO}$>) *vs* conversion (right) in the radical copolymerizations of VDF with HFP with f_{VDF}=0.45 in 56 wt% CO_2 at 75 °C and 1100 bar [c(TBPP)=0.084 mol L^{-1}] and at 45, 60, 75 and 90 °C; [c(DTBP)=0.504 mol L^{-1}] where TBPP and DTBP stand for *tert*-butyl peroxypivalate and di(*tert*-butyl) peroxide, respectively [110].

3.1.4. Radical copolymerization of VDF with aromatic fluorinated monomers

Aromatic monomers are also stabilized by mesomery (Q>1) and thus are more reactive than fluoroalkenes. This is why the radical copolymerization of styrene [as well as (meth)acrylates and butadiene) have not been successfully achieved. To decrease such a reactivity, original 2-trifluoromethyl styrene [111] (as well as 2-trifluoromethyl acrylate) [34-35] have been suggested. They are inactive in radical homopolymerization.

Trifluorovinyloxy parabromobenzene [112] or sulfonyl chloride [113] (Scheme 28) could be interesting monomers to obtain copolymers devoted to potential fuel cell membranes. But their poor reactivity (even suspecting to induce some inhibition) and β-scission [112], occurring from the trifluorovinyloxy end radical during the polymerization, led to low ionic exchange capacities and poor conductivities. Nevertheless, the terpolymerization of such aryl monomers with VDF and CTFE (or HFP) yielded more successful results.

Similarly, the radical copolymerization of α-trifluoromethyl styrene with either VDF or HFP or CTFE failed but its terpolymerization with VDF and CTFE (Scheme 27) led to ca. 50 % yield [111].

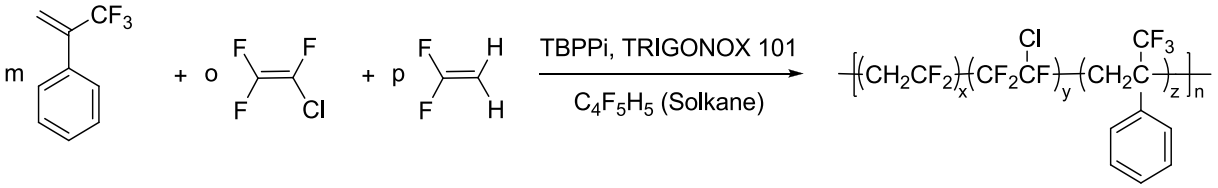

Scheme 28: radical terpolymerization of chlorotrifluoroethylene (CTFE) and VDF with α-trifluoromethyl styrene (TBPPI and Trigonox [101] stand for *tert*-butyl peroxypivalate and 2,5-bis(*tert*-butylperoxy)-2,5-dimethylhexane, respectively). [111]

Similarly, it was required to proceed with a terpolymerization to favor the incorporation of trifluorovinyl oxyaryl monomer in the copolymer [112] (Scheme 28).

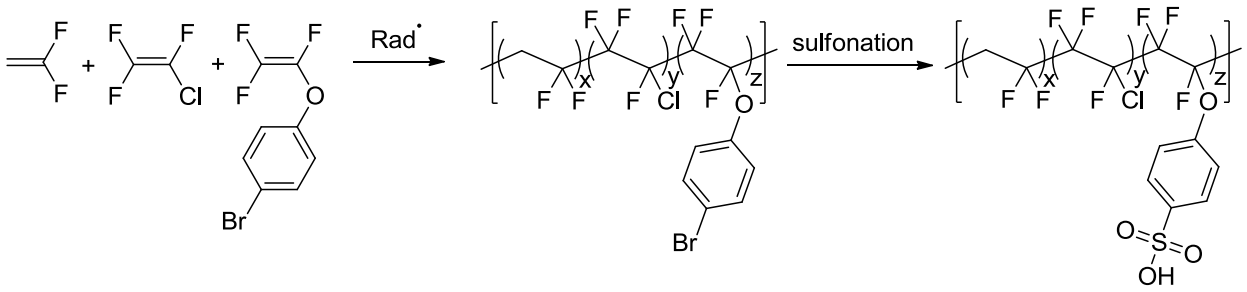

Scheme 29: original fluorinated copolymers bearing sulfonic acid by termonomer-induced copolymerization of trifluorovinyl oxyparabromobenzene (TFVOPBB) with CTFE and VDF.[112]

3.1.5. Terpolymerization Involving VDF

Besides such above examples, the literature is also abundant on the terpolymerizations involving VDF, as reveiwed by Hull et al. [114] on industrially produced THV® terpolymers (usually based on TFE, VDF and HFP). Similarly, poly(TFE-*alt*-P) copolymer is a well-known elastomers (though with a high Tg value of ca. -5 °C) marketed by AGC under the Aflas® trademark. Hence, inserting VDF led to poly(TFE-*ter*-P-*ter*-VDF) terpolymers as a new generation [115-117] of elastomers with lower Tg values and base resistance. Advantageoulsy, the presence of VDF units, as a possible weak points because of hydrogen atoms, favors some crosslinking, well comprehensively reviewed by Moore [17], Logothetis [46], Schmiegel [52] or Taguet et al. [118].

Cure site monomers (e.g., $F_2C=CFOR_FX$ with X= Br, I, CN, OCN [17,46,47,52]) were copolymerized with VDF (and eventually other fluorinated comonomers) to lead to novel elastomers after crosslinking. In addition, the radical terpolymerization of MAF with VDF and HFP [72] led to original Viton®, Dai®el, Dyneon® Elastomers or Tecnoflon® marketed by Chemours (formerly DuPont), Daikin,

Dyneon and Solvay Specialty Polymers, respectively, bearing carboxylic acid side functions (Scheme 30).

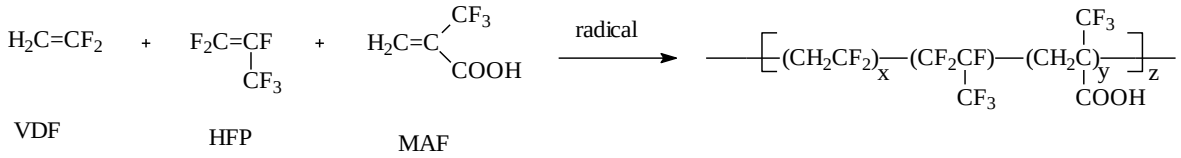

Scheme 30: radical terpolymerization of 2-trifluoromethacrylic (MAF) with VDF and HFP [72].

Furthermore, more recent studies on improving the ferroelectric properties of poly(VDF-*co*-TrFE) copolymers have been reported with the insertion of a third monomer [92] (section 7.6.3) and MAF monomer was also successfully incorporated in the terpolymers [119] without disturbing the ferroelectric properties displayed from the processed poly(VDF-*co*-TrFE) copolymer films. This was also observed for other non-functional [120] (Scheme 31) or functional comonomer (such as trifluorovinyl alkyl trialkoxysilane [92], methyl α,β-difluoroacrylate, itaconic acid, and dimethyl vinyl phosphonate [121-122]).

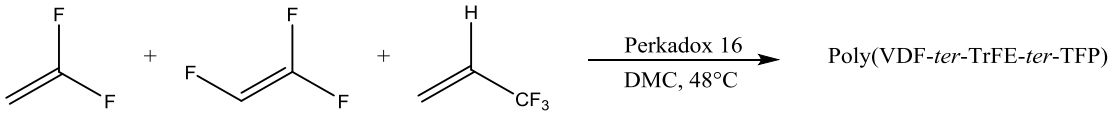

Scheme 31: radical terpolymerization of VDF with TrFE and 3,3,3-trifluoropropene [120] (where Perkadox and DMC stand for bis(*tert*-butyl cyclohexyl) peroxydicarbonate and dimethyl carbonate, respectively).

Presently, poly(VDF-*ter*-TrFE-*ter*-CTFE) and poly(VDF-*ter*-TrFE-*ter*-CFE) terpolymer (where CFE stands for chlorofluoroethylene) are commercially available [11].

To enhance the chemical, thermal and mechanical properties, cure site monomers (CSMs) have been terpolymerized with VDF and other fluoroalkenes [17,22,46,52,118,123,124]. These monomers are reactive in radical copolymerization and a post crosslinking is applied from the functional group borne by the CSM, such as cyano (at high temperatures), bromo (or iodo) in presence of peroxide and

triallyl(iso)cyanurate, etc, as well explained in these above reviews. These are usually trifluorovinyl comonomers to preserve the fluorinated backbone thus maintaining outstanding properties.

As mentioned above, CF_3SO_2K could be oxidized by a persulfate to release a $CF_3°$ radical able to also initiate the terpolymerization of VDF with HFP and PMVE, thus yielding poly(VDF-*ter*-HFP-*ter*-PMVE) terpolymers under aqueous conditions (Scheme 32) [89-90].

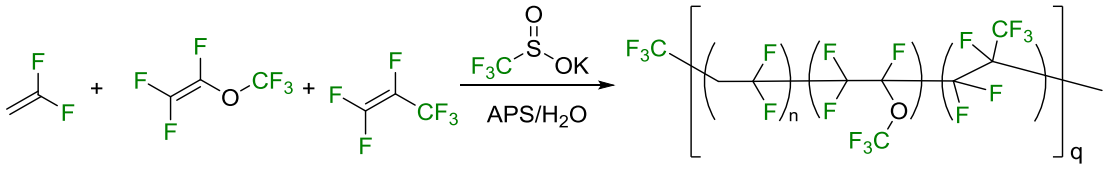

Scheme 32: terpolymerization of VDF with HFP and PMVE, initiated by CF_3SO_2K and APS (where APS stands for ammonium persulfate) reproduced from American Chem. Soc. [90]

3.1.6. Kinetics of Copolymerization of VDF with various comonomers

The kinetics of copolymerization aims at supplying a comparison of the reactivities of comonomers about VDF. This is also based on the Q, e scheme (where Q is related to the resonance and e to the inductive effects, (also in section 2.1.2.1.) for which several recent values have been supplied in a book chapter [126]) Usually, four main competitive equations of propagation of macroradicals onto either VDF or the comonomer [16] but more recent work, well exemplified on the copolymerization of VDF with HFP [110] relies on five equations. The intrinsic reactivity of both comonomers can be obtained from the determination of their reactivity ratios, r, listed in Table 1, showing that the reactivity ratio of VDF could be lower than those of certain functional comonomers [109,120,127-154].

The experimental data points of instantaneous VDF molar content in the copolymer (F_{VDF}) *versus* that in the feed (f_{VDF}) were plotted and fitted by the Mayo Lewis equation. F_{VDF} and f_{VDF} were estimated from the average copolymer composition determined by ^{19}F NMR spectroscopy and from the composition of the initial monomer feed, respectively. The diagrams of composition for (VDF;M)

couples was already reported [16] while the monomer reactivty ratios are listed in Table 1. Fig. 10 represents more recent kinetic results [138].

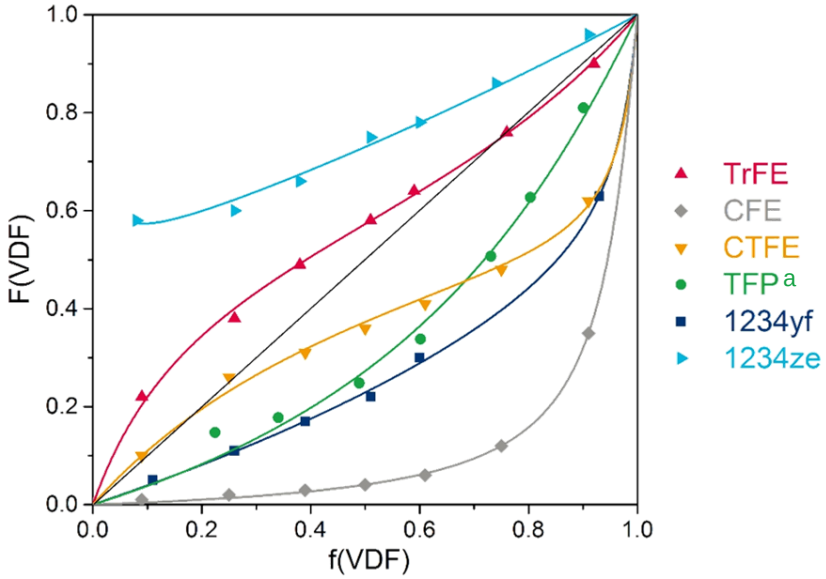

Fig. 10: Evolution of the instantaneous VDF molar fraction in the copolymer (F_{VDF}) *versus* the instantaneous VDF molar fraction in the feed (f_{VDF}), for the radical copolymerizations of VDF with various fluorinated comonomers. The data points (from sampling at low monomer conversion) were fitted using the Mayo-Lewis equation. [a]Experimental data from Kostov *et al.* [155] determined at 74 °C in solution copolymerization (in 1,1,1,3,3-pentafluorobutane as the solvent).

When r value is lower than 1, the radicals terminated by M_1 monomer have the tendency to cross-propagate onto M_2 rather than to homopolymerize. Indeed, a reactivity series of fluorinated monomers about VDF can be supplied from the traditional method to determine the relative reactivity of a macroradical onto several monomers. It compares $1/r_1$ values (or k_{12}/k_{11}) as the ratio of rate constants of crossed propagation to that of propagation (k_{11}). Thus, the higher the 1/r value, the more the radical is able to react onto the second monomer. Table 1 proposes the following series of relative reactivities of monomers to ~~~~~~~VDF• macroradical: $F_2C=CHC_6F_{13}$ < $F_2C=CHCF_3$ < $F_2C=C(CF_3)COF$ < HFP < PMVE < BDFE < PPVE < VDF < TrFE < $F_2C=CFCH_2CH_2Br$ < $F_2C=CFCH_2OH$ < $F_2C=C(CF_3)OCOC_6H_5$ < $F_2C=CFO(HFP)OC_2F_4SO_2F$< CTFE (recent value) < TrFE < BrTFE < $H_2C=CFCF_2OR_F$ < $H_2C=C(CF_3)CO_2H$ < $F_2C=CFCO_2CH_3$ < TFE < $F_2C=CFC_3H_6SCOCH_3$

< $F_2C=CFC_3H_6OAc$ < $H_2C=CHF$ ≈ CTFE (old value) < TFP < ethylene, although numerous kinetics still deserve to be investigated in similar conditions, to really supply a better comparison.

Monomer B	r_{VDF}	r_M	$r_{VDF}r_M$	$1/r_{VDF}$	Ref.
$H_2C=CH_2$	0.05	8.5	0.42	20.00	[127]
$H_2C=CHOCOCH_3$	-0.40	1.67	-0.67	-2.5	[109]
	0.50	2.0	1.00	2.0	[31]
$H_2C=CHCO_2H$	0.11	305	33.6	9.0	[25]
$H_2C=C(CF_3)CO_2H$	0.33	0	0	3.03	[72]
$H_2C=C(CF_3)CO_2tBu$	0.0399	0.0356	0.001	25	[39]
$FCH=CH_2$	0.17– 0.43	3.8 – 4.9	0.76–0.92	2.3-5.9	[128]
$H_2C=CHCF_3$	0.43	2.8	1.20	2.32	[120]
$H_2C=CFCF_2OR_F$	0.38	2.41	0.92	2.63	[129]
$FCH=CFCO_2R$	0.34	0.86	0.29	2.94	[32]
$F_2C=CHBr$	1.2	0.4	0.48	0.83	[75]
$F_2C=CFH$	0.70	0.50	0.35	1.43	[130]
	0.77	0.32	0.25	1.28	[120]
$H_2C=CFCF_3$	0.76	1.23	0.98	1.31	[131]*
	0.384	2.15	0.83	2.6	[132]*
	0.079	2.6	0.21	12.6	[133]
$H_2C=C(CF_3)_2$	0.136	0.047	0.007	7.3	[38]
trans-$FCH=CHCF_3$	1.67	0	0	0.59	[134]
$F_2C=CHCF_3$	9.0	0.06	0.54	0.11	[135]
$F_2C=CHC_6F_{13}$	12.0	0.90	10.8	0.08	[136]
$CFCl=CF_2$	0.73	0.75	0.35	1.37	[137]
	0.17	0.52	0.54	5.88	[138]
	0.069	0.80	0.06	14.5	[139]
$BrCF=CF_2$	0.43	1.46	0.63	2.33	[137]
$CF_2=CF_2$	0.23	3.73	0.86	4.35	[137-138]
	0.32	0.28	0.09	3.13	[140]
$CF_3-CF=CF_2$	6.70	0	0	0.15	[141]
	2.45	0	0	0.40	[142]
	2.90	0.12	0.35	0.34	[143]
	4.8	0	0	0.21	[144]
	5.13	0	0	0.19	[145]
	3.2	0	0	0.30	[66]
	3.3	0	0	0.30	[146]
$F_2C=CFOCF_3$	3.40	0	0	0.29	[147]
	2.5	0	0	0.40	[148]*
$F_2C=CFOC_3F_7$	1.15	0	0	1.75	[149]
$F_2C=CFO(HFP)OC_2F_4SO_2F$	0.57	0.07	0.04	1.02	[125]
$CF_2=CFCH_2OH$	0.83	0.11	0.09	1.20	[149]
$CF_2=CF(CH_2)_2Br$	0.96	0.09	0.09	1.04	[54]
$CF_2=CF(CH_2)_3OAc$	0.17	3.26	0.59	1.00	[150]

$F_2C=CF(CH_2)_3SAc$	0.60	0.41	0.25	1.60	[151]
$CF_2=CFCO_2CH_3$	0.30	0	0	3.33	[36]
$F_2C=C(CF_3)COF$	7.60	0.02	0.15	0.13	[152]
$F_2C=C(CF_3)OCOC_6H_5$	0.77	0.11	0.08	1.31	[153]
$CF_3C(O)CF_3$	4.1	0.1	0.41	0.25	[154]

Table 1: Monomer reactivity ratios for the radical copolymerization of VDF with other comonomers (M) (* indicates results from RDRP copolymerization).

The reactivity ratios of VDF, fluorinated comonomers, ethylene [127] and VAc [31,109] are listed in Table 1, deduced from the diagram of composition (Fig. 9). It displays the tendency of the copolymerization of various (VDF; comonomer) pairs. The obtained polymer/monomer composition curves can lead to a classification into four main families: i) that for which $r_{VDF} > 1$ and $r_M < 1$ (case when M is HFP [66,139-144], perfluoroalkyl vinyl ether [146], pentafluoropropene [134], 1234ze [133], $F_2C=CHBr$ [75], and $C_6F_{13}CH=CF_2$ [135]), ii) that for which $r_{VDF} < 1$ and $r_M > 1$ [case of ethylene, VAc, CTFE, TFE, BrTFE, 1234yf and $F_2C=CF(CH_2)_3$-XAc (X = S or O)), iii) case where $r_{VDF} < 1$ and $r_M < 1$ (e.g., $F_2C=CFCH_2OH$, $FCH=CFCO_2R$ and $F_2C=C(CF_3)OCOR$); and finally, iv) case where alternation occurs ($r_{VDF} \sim 0$ and $r_M \sim 0$ for HFIB, methyl trifluoromethacrylate (MTFA) and MAF).

The alternance may come from the steric hindrance of both bulky CF_3 and CO_2H groups in MAF, HFIB and hexafluoroacetone.

3.1.7. Conclusion

A wide variety of functional comonomers have been copolymerized with VDF successfully, whatever they are halogenated or not. Though the latter kind may induce some transfer reactions that lower the molar masses, many more fluorinated ones have been used and may explain why the first work started on perfluorinated ones. Kinetics of radical copolymerization led to the determination of their reactivity ratios and could be compared though the conditions were not the same as well as the technique utilized by the authors. Such poly(VDF-*co*-M) copolymers have been involved in many

applications (section 7). More recent techniques of controlled radical polymerizations have also been successfully applied on the copolymerization of VDF with other comonomers, summarized in the following section.

3.2. Reversible Deactivation Radical (Co)Polymerization (RDRP)

3.2.1. Introduction

Techniques on RDRP (or controlled radical polymerization, CRP) are available (photo-iniferters, nitroxides-mediated polymerization, atom transfer radical polymerization, reversible addition fragmentation transfer/macromolecular design interchange of xanthate, iodine transfer polymerization) and well-reported in many textbooks [156-159] and reviews [160-167] but not all of them can be adaptable for fluoroalkenes [168-173]. Though the great development of RDRP was reported in the mid-90ies (mainly on hydrocarbon monomers such as (meth)acrylates and styrene), the Daikin Company pioneered the concept of iodine transfer polymerization (ITP) in the late 70ies [174-175], regarded nowadays as a controlled one [176-178]. Industrially, in the 90ies, the Daikin Company started the production of the first controlled (co)polymers under such conditions [164, 176-178]. In addition, RDRP of (meth)acrylate and styrenes bearing fluorinated pendant groups has been reviewed [179-181].

3.2.2. Iodine Transfer copolymerization

Iodine transfer polymerization (ITP) is based on the fast reversible equilibrium between macromolecular dormant chain (terminated by an iodine atom, P_m-I or poly(VDF-*co*-M)-I) and active/living [P_m° or poly(VDF-*co*-M)°] radicals (Scheme 33). This is mainly due to the poor dissocation energy of the CF_2-I bond (ca. 45 kcal.mol^{-1}) [191].

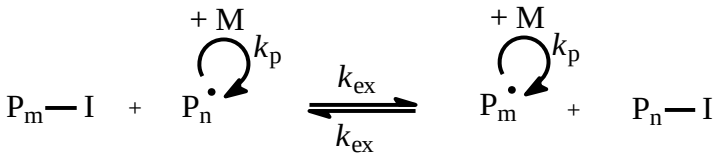

Scheme 33: Mechanism of reversible equilibrium between dormant iodinated macromolecular chain and active macroradicals in the iodine transfer radical polymerization (ITP) [176-178].

Lots of (VDF;M) monomer pairs have been tested in ITcopolymerization in various media: water for (VDF;HFP) [110,176-178,182] or (VDF;PMVE) [53, 148], sc CO_2, [173,184], solvents [184]), (VDF;1234yf) or (VDF;MAF) [186] in solution[130]) or IT terpolymerization involving "exotic" monomers as $F_2C{=}CFSF_5$ [186], or under visible photochemical initiation in presence of $Mn_2(CO)_{10}$ that acted as a catalyst [187].

One of the most exciting innovations from ITP deals with the preparation of thermoplastic elastomers (TPEs). Such A-B-A (or Hard-Soft-Hard) fluorocopolymers are phase segregated with crystalline zones and amorphous domains combining various advantages including broad temperatures of service. These fluorinated triblock copolymers are synthesised from a two step-procedure: first, a telechelic diiodofluorinated copolymer (usually an elastomeric I-Soft-I block made from various compositions of VDF/M [16, 177,189]) is produced and can be further used as a novel CTA in a second ITP (Scheme 34).

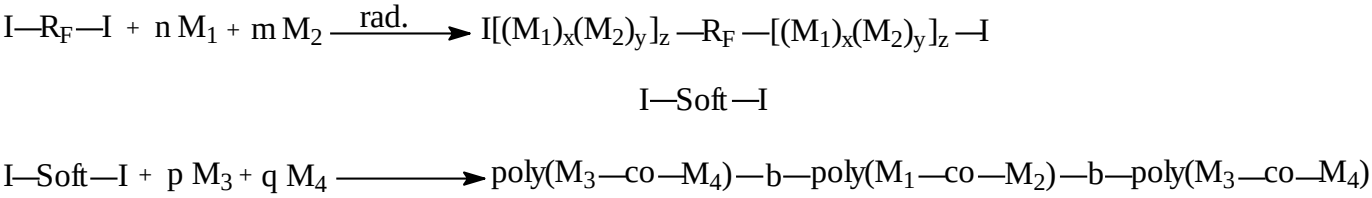

Scheme 34: iodine transfer copolymerization of various monomers for the synthesis of a thermoplastic elastomers [189].

ITP is versatile since various processes can be utilized (emulsion [190], suspension, microemulsion processes or in solution) and industrially scaled up. Daikin's pioneering works from 1979 [174-175] were confirmed by the DuPont Company (nowadays Chemours) and at Ausimont (now Solvay Specialty Polymers). *Quasi* exhaustive lists of fluorinated elastomers and thermoplastic elastomers have been reported [16,177,189,191] involving (fluoro)alkenes as VDF, HFP, TFE, PMVE, CTFE, ethylene and propylene. Typical combinations of comonomers by pair, or more comonomers allowed to tune the suitable sequence to be either amorphous (soft) or crystalline (hard) (see also section 7.3). For the preparation of block copolymers by such a copolymerization of two (or three or four) olefins, soft or hard segments could be prepared by varying the comonomer amounts and taking into account their reactivity ratios (Table 1). α,ω-Diiodoperfluoroalkanes enable to control the radical (co)polymerization of fluoroalkenes *via* ITP, « degenerative transfer » or « *pseudo*-living and branching technology [192].

Apostolo *et al.* [182] achieved a comprehensive study on the RDRP of VDF and HFP in microemulsion in presence of diiodoperfluoroalkanes. A kinetic model was established to identify the most appropriate operating conditions to produce poly(VDF-*co*-HFP) copolymers with desired features in terms of microstructure, especially branched macromolecules with uniform chain lengths and dispersities. Actually, a significant reduction of the dispersity, *Đ*, was observed (with a final value of 2.3 in contrast to 4-5 without any CTA).

A more recent study on ITP of fluoroolefins, achieved by Solvay Specialty Polymers [193], has claimed the aqueous IT terpolymerization of VDF (in large excess) with HFP (in ca. 1 mol% feed ratio) and acrylic acid (AA) with 1,4-diiodoperfluorobutane or diiodomethane (surprisingly claimed to be also an efficient CTA). The resulting poly(VDF-*ter*-HFP-*ter*-AA) terpolymer had molar masses higher than 470 $kg.mol^{-1}$ with low gel content and quasi no branching while the iodine containing chain-end was ranging from 0.1 to 5.0 $mmol.kg^{-1}$. That patent also indicated various end-groups as $-CH_2I$, $-CH_2OH$, $-CF_2H$ and $-CF_2CH_3$ while the particle sizes ranged between 20 and 350 nm. The melt

viscosity / average molar mass relationship for three terpolymers is depicted in Fig. 11, disclosing the results claimed in the patent (square) compared to those of two referenced terpolymers produced by conventional emulsion (full black circles) or suspension (empty circles) terpolymerizations [193]. The searched applications were for separators and membranes.

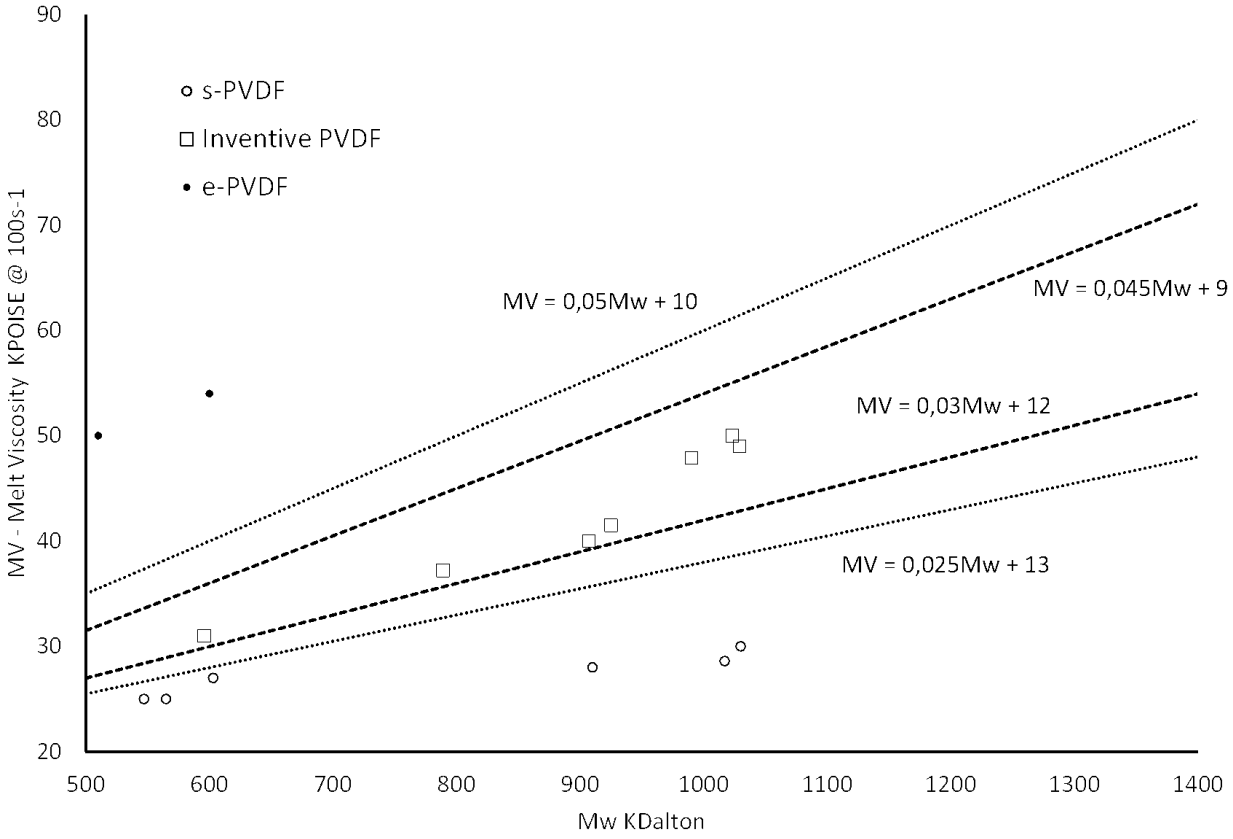

Fig. 11: melt viscosity *versus* molar masses for three poly(VDF-*ter*-HFP-*ter*-AA) terpolymers produced by ITP (where s-PVDF, e-PVDF and inventive PVDF stand for suspension, emulsion and disclosed in patent poly(VDF-*ter*-HFP-*ter*-AA) terpolymers, respectively) [193].

Another IT copolymerization consists of reacting VDF and PMVE in presence of 1,4-diiodoperfluorobutane leading to telechelic diiodo-poly(VDF-*co*-PMVE) cooligomers, the molar mass of which reached up to 5000 $g.mol^{-1}$and Tg values ranging from -63 to -35 °C [148]. The functionalization of these cooligomers was achieved to produce telechelic diols and then bis(acrylate)s

[194]. Two routes (Scheme 35) were suggested: i) by bis(ethylenation) of the poly(VDF-*co*-PMVE) cooligomers followed by oxidation of the iodine end-groups and ii) by radical addition of such diiodocooligomers onto allyl alcohol followed by the selective reduction of the iodine atoms in the resulting bis(iodhydrin). The latter strategy was more efficient since the oxidation also yielded formiate as a by-product and some deydrofluorination. These telechelic diols were acrylated prior to photocrosslinking (with various photoinitiators) yielding soft films of low Tg (ca -30 °C) with a high thermal stability [195].

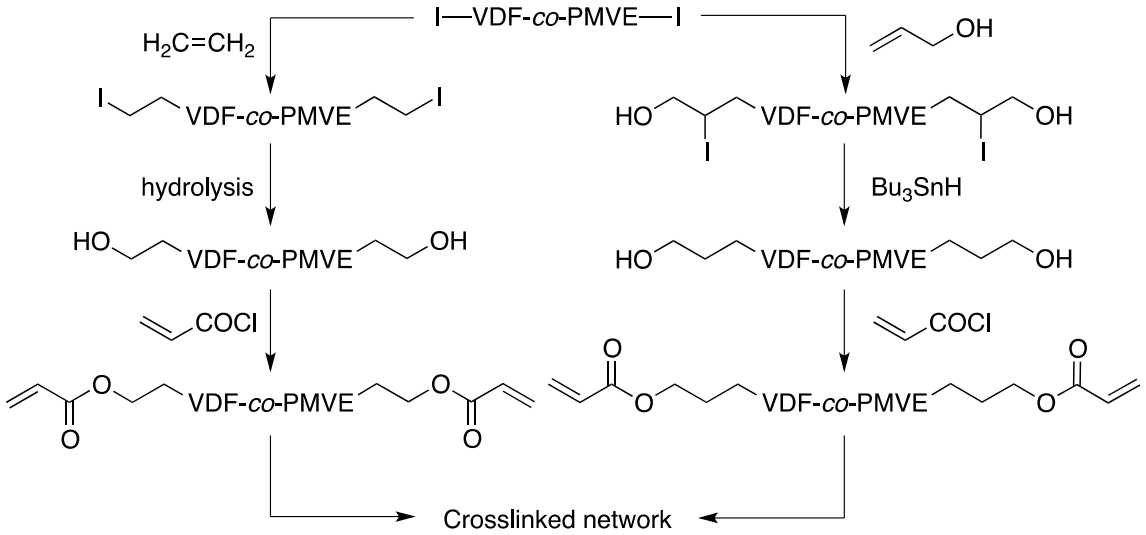

Scheme 35: Overall strategies to synthesize photocross-linkable telechelic diacrylate poly(VDF-*co*-PMVE) cooligomers (that contained C2 or C3 spacers)[194-195]. Copyright 2012, Reproduced with permission from the American Chemical Society.

A similar ITP strategy was later on applied for controlled poly(VDF-*co*-HFP) cooligomers, the molar masses of which reached 3000 $g.mol^{-1}$ and dispersity values lower than 1.3. These authors modified them into telechelic diol Mn<3000 g/mol) [185].

Related to a previous study, the bisethylenated telechelic diiodo-poly(VDF-*co*-PMVE) cooligomers were chemically changed into difunctional bis(azido) copolymers. The Huisgen's 1,3-dipolar cycloaddition of such bis(azido) derivatives with α,ω-dipropargyl ether hexafluorobisphenol AF, catalyzed by CuBr/bipyridine [196], led to novel fluoroaromatics based on soft poly(VDF-*co*-PMVE) moities (Scheme 36).

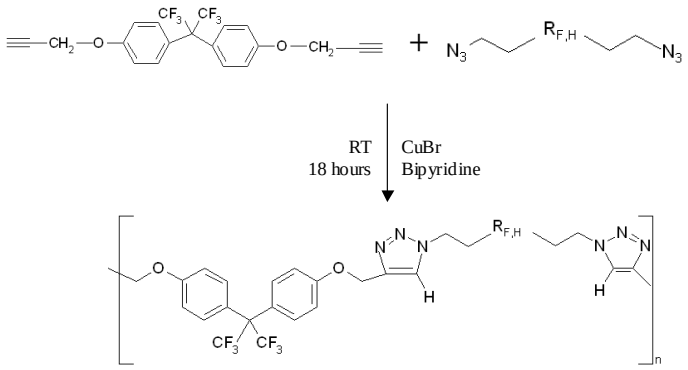

Scheme 36: Condensation of telechelic diazido poly(VDF-*co*-PMVE) cooligomers with aromatic α,ω-diyne ($R_{F,H}$ = C_6F_{12} or C_2F_4-[$(CH_2CF_2)_xCF_2CF(CF_3)]_y$ [196]. Copyright 2010. Reproduced with permission from the American Chemical Society.

Producing hybrid organic/inorganic materials is quite challenging, especially hybrid fluorosilicones. These diiodo-poly(VDF-*co*-PMVE) cooligomers induced some softness and a thermal stability, which is acheived by introducing a longer distance between the silicon atoms to reduce depolymerization by backbiting. Hybrid fluorosilicones based on organic soft poly(VDF-*co*-PMVE) copolymer and inorganic silicates were reported.[197]. The approach lies first on the radical addition of α,ω diiodo poly(VDF-*co*-PMVE) cooligomer onto vinyl methyl(alkoxy)silanes to lead to telechelic bis(methyl/ethoxy) poly(VDF-*co*-PMVE) copolymers (Scheme 37).

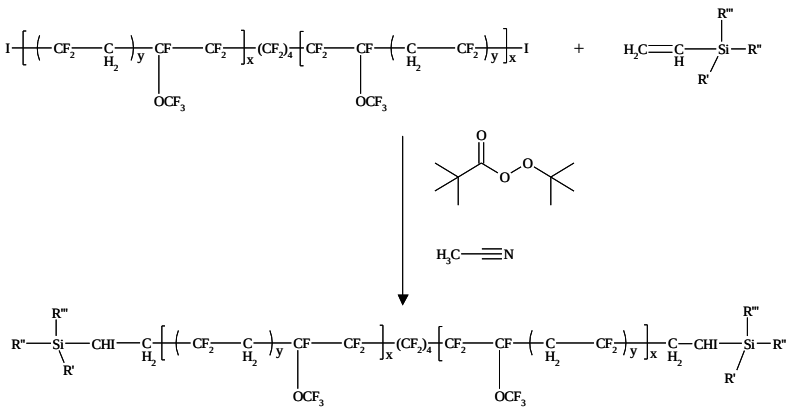

Scheme 37: radical addition of telechelic diiodo poly(VDF-*co*-PMVE) cooligomer onto vinyl methyl(alkoxy)silanes (R', R" and R'" designate methyl or OEt) [197].

The second step dealt with the hydrolysis/condensation of such telechelic silicon alkoxides based on poly(methylethoxysilane) end-groups (Scheme 38) in presence of acid and additives [such as

Ti(O-*i*Pr)$_4$]. The final product exhibited a nanomorphology with small inorganic domains which represent the crosslinked area (favoring better mechanical properties), and organic poly(VDF-*co*-PMVE) zones. The size of each domain depends on the number of crosslinking sites available, the reactivity of the crosslinker linked to the end-groups, and the molar mass of the polymer backbone [197]. This led to hybrid organic-inorganic crosslinked networks (Fig. 12).

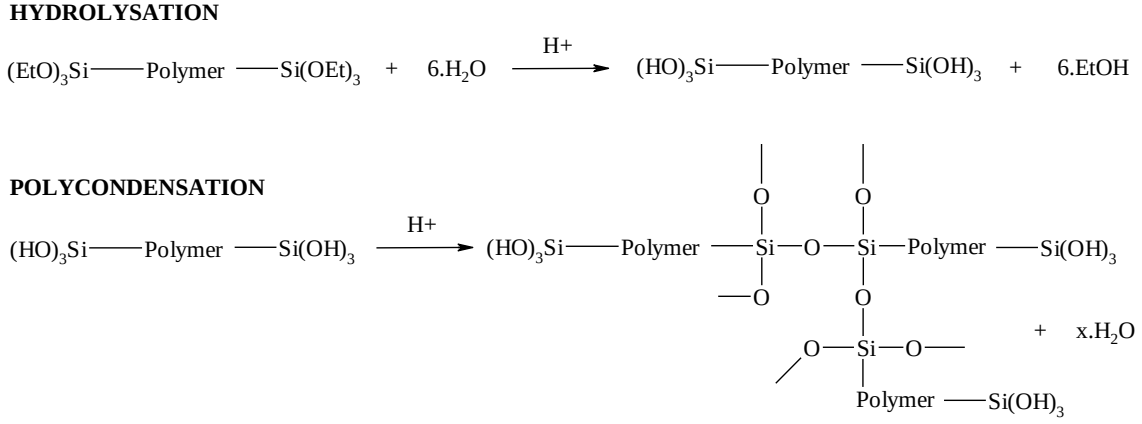

Scheme 38: Hydrolysis and polycondensation of telechelic bis(triethoxysilyl) functionalized poly(VDF-*co*-PMVE) copolymers.

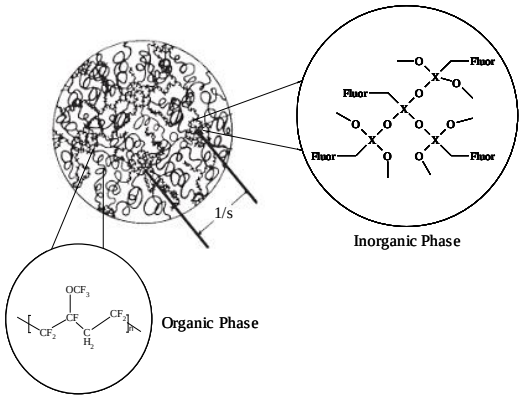

Fig. 12: Schematic representation of a typical hybrid organic-inorganic network, where X represents the inorganic phase (in this instance it could be Silicate) while the organic phase is represented by poly(VDF-co-PMVE) copolymer. The distance between inorganic phases is provided as 1/s [197].

The reaction conditions were optimized to establish a structure-properties relationship (thus improving mechanical and thermal properties of the resulting networks) (Scheme 38). While hybrid materials with higher Tg (ca. -10 °C) were obtained from bis(triethoxysilane) fluorinated copolymers,

those achieved from telechelic bis(dimethylethoxy) took too much time (ca. 5-7 days) to be produced. The best compromise was those involving telechelic bis(diethoxymethyl) copolymers with bis(ethoxydimethylsilane) functionalized poly(VDF-*co*-PMVE) copolymer (Fig. 13), and the incorporation of siloxane components to reach low Tg hybrids (-47 °C) with high thermal stability, good mechanical properties and *quasi* no swelling in boiling octane and acetone.

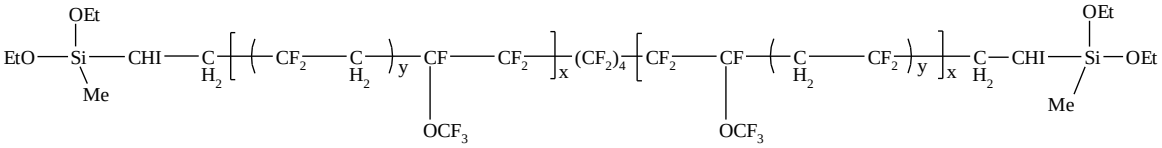

Fig. 13: structure of telechelic bis(diethoxymethylsilane) poly(VDF-*co*-PMVE) copolymer achieved from the radical addition of α,ω-diiodo poly(VDF-*co*-PMVE) onto vinyl diethoxymethylsilane [197].

Such materials display macroscopic elastic behavior and phase segregation of inorganic silicon domains and organic fluorinated ones (Fig. 14).

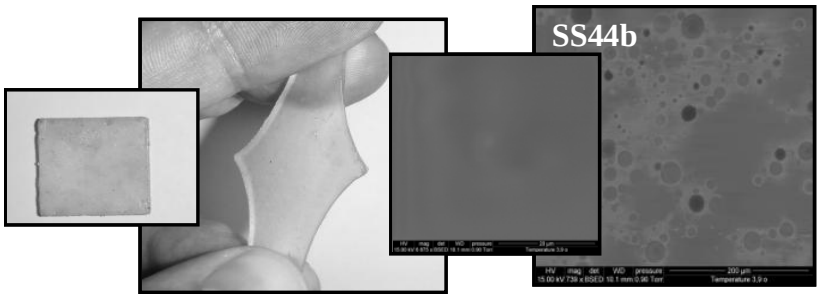

Fig. 14: macroscopic and scanning electron microscopy pictures of crosslinked network from telechelic (diethoxymethyl) and telechelic (ethoxybismethyl) poly(VDF-*co*-PMVE) copolymers showing two distinct phases: the dark regions on the right SEM picture are Si rich phases (evidenced by EDX). The bar scale is 200 μm [197].

3.2.3 Reversible addition-fragmentation chain-transfer Polymerization

Diffrently from ITP, RAFT is controlled by sulfur-containing CTAs, such as dithiocarbamates, xanthates and trithiocarbamates and relies on fast equilibria of two steps (Scheme 39). This technique

has also led to many surveys and is summarized in excellent reviews [155,160,164,198-200]. RAFT of fluorinated alkenes have been reported in the last 10 years, mainly controlled by xanthates (and called macromolecular design through interchange of xanthate) and summarized in recent reviews [171-173].

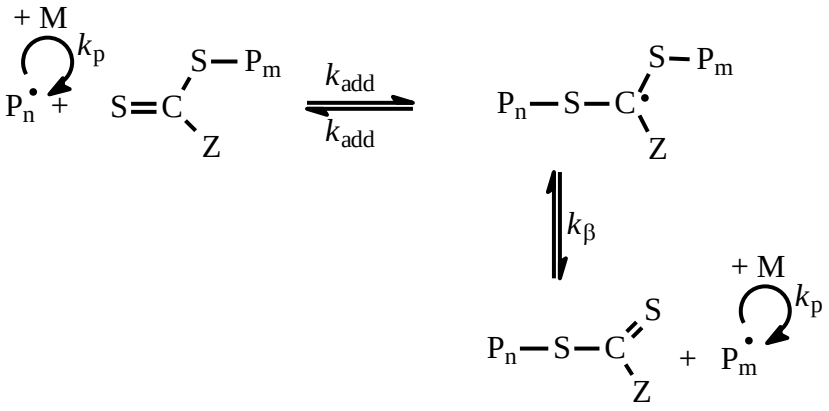

Scheme 39: Reversible addition-fragmentation chain transfer process (RAFT and MADIX)

As a matter of fact, quite a few studies have reported the RAFT copolymerization of VDF with various comonomers. First, Kostov et al. [201] achieved the step wise copolymerization of VDF with 3,3,3-trifluoropropene (TFP) followed by a poly(vinyl acetate), PVAc, block end-capping (Scheme 40). After hydrolysis, the poly(VDF-*co*-TFP)-*b*-poly(vinyl alcohol) displayed interesting surface activity to act as original surfactants with competitive critical micellar concentration (cmc) to that of PFOA.

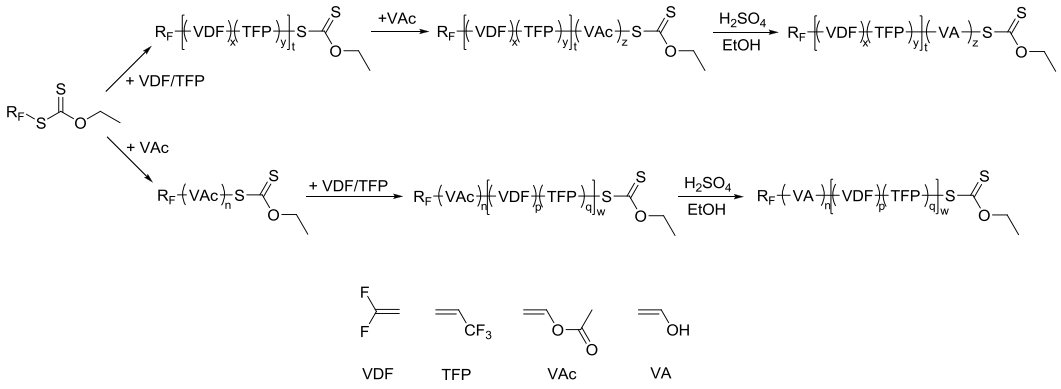

Scheme 40: Strategies for the preparation of amphiphilic block copolymers from the stepwise RAFT terpolymerization of VDF with 3,3,3-trifluoropropene (TFP) and vinyl acetate (VAc) [201] (where R_F stands for C_6F_{13}). Copyright 2012, Reproduced with permission from the American Chemical Society.

In addition, the RAFT copolymerization of VDF with *tert*-butyl α-trifluoromethacrylate (MAF-TBE) controlled by a linear [202-203] or cyclic [204] xanthate was achieved with the goal to design original emulsifiers between nanosilicates and commercially available poly(VDF-*co*-HFP) copolymers for polymer exchange fuel cell membranes (PEMFCs) by reactive extrusion ([205-206], section 7.6.1).

The same group also reported the RAFT terpolymerization of VDF with trifluoroethylene (TrFE) and 2,3,3,3-tetrafluoroprop-1-ene (1234yz) controlled by (macro)xanthate enabling to produce original block copolymers (Scheme 41) for potential electroactive polymers[207].

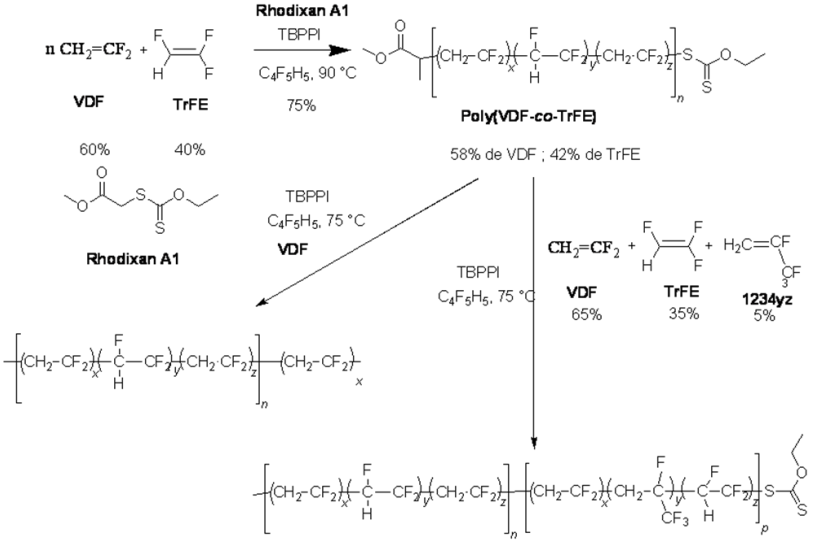

Scheme 41: RAFT terpolymerization of VDF with trifluoroethylene (TrFE) and 2,3,3,3-tetrafluoroprop-1-ene (1234yz) controlled with (macro)xanthate to obtain block copolymers [207].

The RAFT copolymerization of VDF with PMVE in presence of oligo(dimethyl acrylamide) macroxanthate CTA led to block copolymers (Scheme 42) as interesting surfactants for the polymerization in $scCO_2$ medium, the poly(VDF-*co*-PMVE) sequence being CO_2-philic [208].

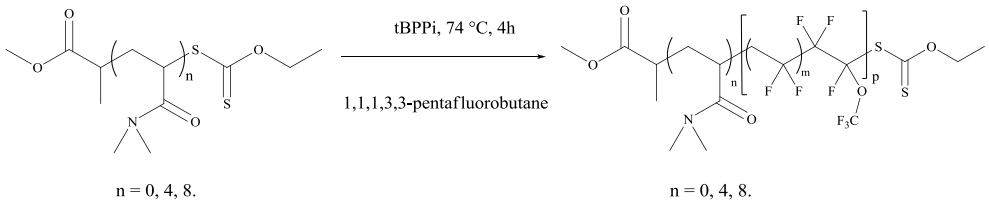

Scheme 42: RAFT copolymerization of VDF with PMVE in presence of oligo(dimethyl acrylamide) macroxanthate (where tBPPi stands for *tert*-butyl peroxypivalate) [209].Copyright 2012, Reproduced with permission from the American Chemical Society.

A more recent interesting article reports the RAFT of VDF in emulsion involving a specific oligo(ethylene glycol) xanthate that both controlled the polymerization of VDF and acted as a surfactant to favor its emulsion polymerization of VDF [209].

3.2.4. Organometallic mediated radical copolymerization (OMRP) of VDF

Another RDRP technique deals with the cobalt mediated radical copolymerization (CMRP) [166]. It was scarcely used on VDF by redox initiation using either oligo(VAc)-$Co(acac)_2$ [210] or a combination of bis(*tert*-butylcyclohexyl) peroxydicarbonate (P16) and $Co(acac)_2$ with an optimized control of the polymerization conditions ($[P16]_0/[Co(acac)_2]_0$ = 2/1, T= 60 ^oC) [211]. Recently, from such conditions, the CMR copolymerization of VDF with 2,3,3,3-tetrafluoroprop-1-ene (1234yf) led to controlled poly(VDF-*co*-1234yf) copolymers (Scheme 43) with molar masses reaching 12,200 g/mol^{-1} and low dispersities ($Đ$ = 1.33-1.47) [132].

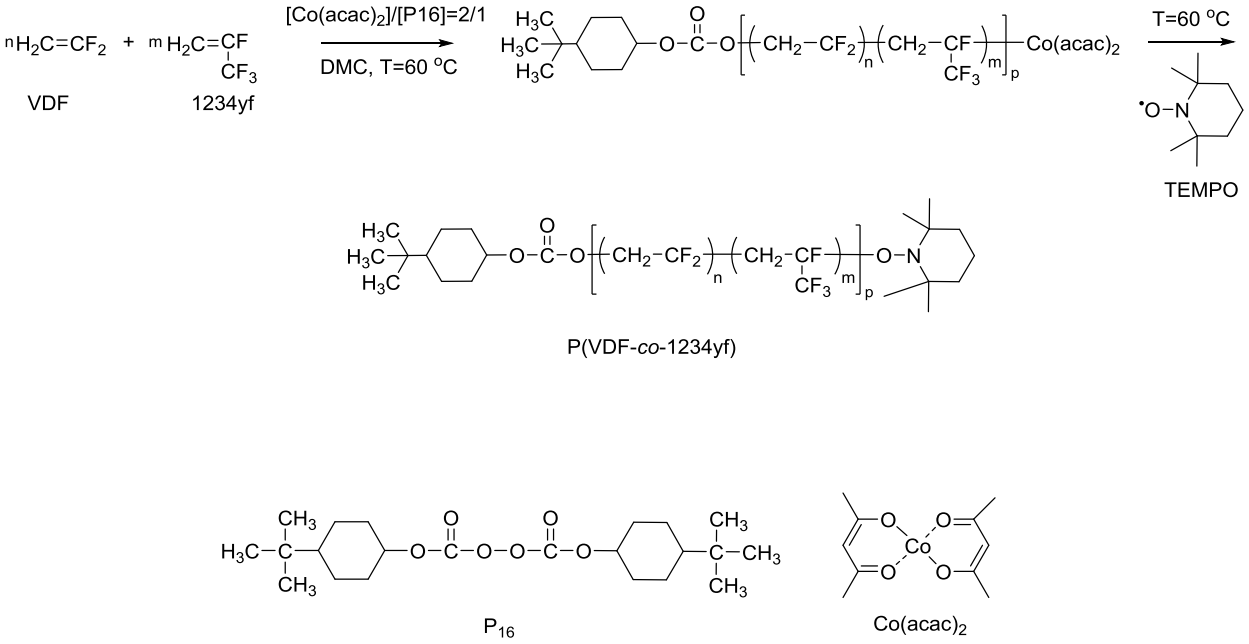

Scheme 43: Preparation of poly(VDF-*co*-1234yf) copolymers by Cobalt mediated radical copolymerization of VDF and 1234yf initiated by bis(*tert*-butylcyclohexyl) peroxydicarbonate (P16) and mediated by $Co(acac)_2$ in dimethyl carbonate (DMC) [132].

The control of the copolymerization was evidenced by the linear molar mass of the resulting copolymers-monomer conversion tendency (Fig. 15).

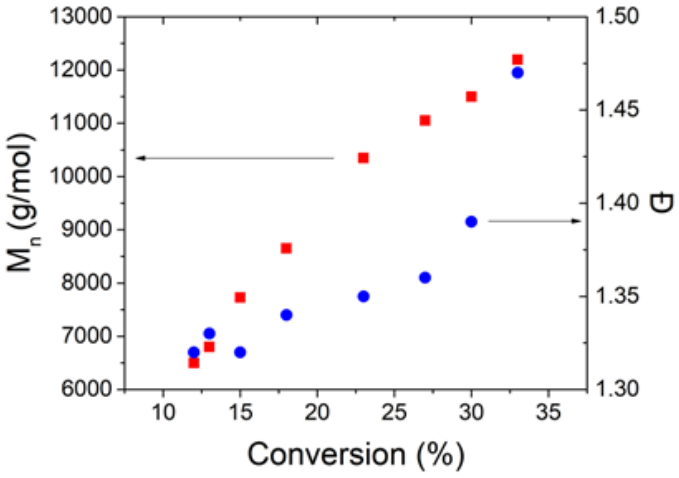

Fig. 15: molar masses (M_n) and dispersities ($Đ$) *versus* the comonomer conversions for the Cobalt mediated copolymerization of VDF with 1234yf. Conditions ($[VDF]_0/[1234yf]_0/[P16]_0/[Co(acac)_2]_0$=80/20/2/1 at T=60 °C [132].

3.2.5. Conclusion

Various strategies to produce well-defined copolymers based on VDF are available, some of them even reaching an industrial scale. The oldest and most developed technique concerns ITP mainly, whereas more recently RAFT and CMRP are promising strategies. Four recent reviews [170-173] on controlled radical polymerization (RDRP) of fluoroalkenes summarized the synthesis of well-architectured polymers including block (*via* ITP and RAFT) and graft copolymers [by surface intiated polymerization, radiation grafting, copolymerization with macromonomers, ATRP (mainly grafting of hydrocarbon polymer from poly(VDF-*co*-CTFE), coupled atom transfer radical coupling with the objective of self-assembly systems and various High Tech applications. These different routes are not repeated in that present review. However, the applications of these well-designed VDF-containing copolymers are thermoplastic elastomers which can preserve their unique performances over a wide range of temperatures (section 7.3).

3.3. Telechelic poly(VDF-*co*-M) copolymers

Telechelic oligomers or polymers are valuable building blocks for polycondensation, polyaddition or crosslinking, and a few of them, containing poly (or oligo)(VDF-*co*-M) have been reported. In addition to diols based on VDF and PMVE [section 4.1 (Scheme 35)] [195], fluorinated telechelic peresters [212], synthesized by oxidation of fluorinated acid chlorides [213] could initiate the dead end copolymerization of VDF and HFP leading to novel fluoroelastomers [212] (Scheme 44).

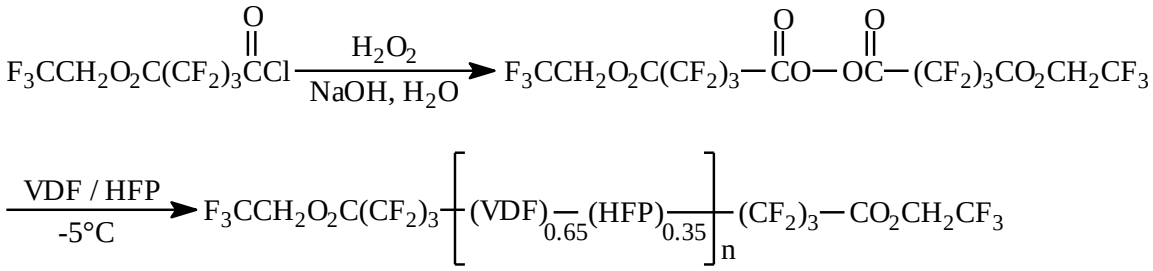

Scheme 44: dead end copolymerization of VDF and HFP in presence of fluorinated telechelic acyl peroxides [212].

The average molar mass assessed by vapor pressure osmometry reached 4,000 g.mol $^{-1}$.

Similarly, the same authors prepared new fluorinated initiators (Scheme 45) useful for the preparation of fluoroelastomers [214].

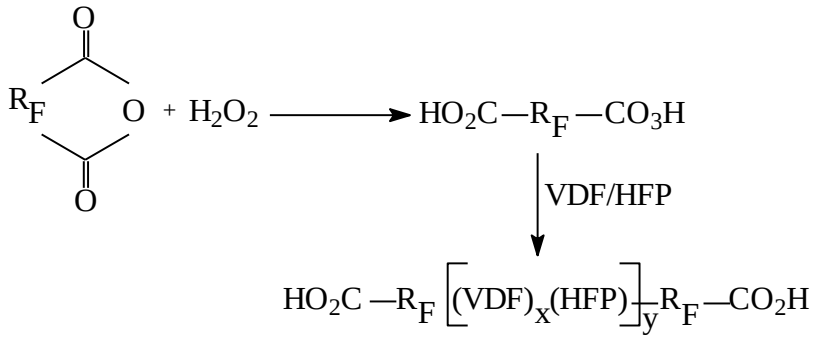

Scheme 45: synthesis of novel fluorinated anhydrides to release percarbonates able to intiate the copolymerization of VDF and HFP [214].

Later on, a Russian group synthesized other functional fluorinated peresters and studied their kinetics of thermal decomposition [215].

Moreover, Oka and Morita [216] also prepared bis(hydroxyl) telechelic poly(VDF-*co*-HFP) copolymers from $(tBuOCH_2CF_2CO_2)_2$, after a subsequent hydrolysis step of the resulting end-groups.

In addition, hydrogen peroxide was also involved in the synthesis of novel α,ω-difunctional poly(VDF-co-HFP) ($\overline{M}_n$ = 300-2000) in a two-step procedure [217] (G designates CH_2OH or CO_2H) (Scheme 46).

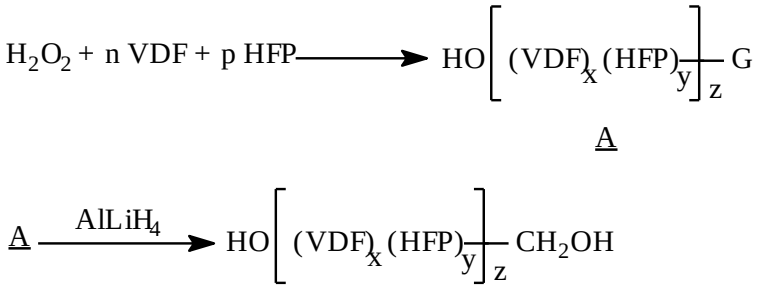

Scheme 46: radical copolymerization of VDF with HFP initiated by hydrogen peroxide (where G designates CH_2OH or CO_2H) [217]

However, more recently, that reaction was revisited, initiated by a AIBN/H_2O_2 mixture in presence of dimethyl carbonate (as the solvent) that induced much transfer [218] leading to the formation of many side products including fluorinated carbonates (ocurring with 92% selectivity toward the addition of carbonate radicals onto the VDF tail) well identified by NMR and Maldi Tof.

Other fluorinated telechelic oligodiols based on VDF and HFP units (with the structure $HOCH_2CF_2(CH_2CF_2)_p[CF(CF_3)CF_2]_qCF_2CH_2OH$) were claimed by Chan *et al.* [219] but the description of the detailed synthesis was not reported.

5. Crosslinking of Copolymers based on VDF

The process of crosslinking (also named curing) creates a three-dimensional network that turn the elastomer resitant for long-term mechanical service under a sustained stress or constant deformation (strain). Both these features are the main requirements for shock and vibration controls or sealing. Invariably the crosslinks are often the most vulnerable component of the cured elastomer. To crosslink VDF-containing copolymers, two distinct halogen elimination reactions have been reported: i) E2 mechanism involving simultaneous elimination of hydrogen and the adjacent fluorine provoked by the nucleophile reactant (base) that generates a double bond in the backbone, followed by a Michael addition of the excess of telechelic base [diamine or bisphenate such as gem(trifluoromethyl)bisphenate AF, BPAF [17,52,113] onto two double bonds of two different backbones, creating the crosslink; ii) E1 mechanism which may occur without any base but rather by ionization or radicals supplied by peroxides. The specific location is a cure-site monomer (CSM) having iodine or bromine substitution that is readily displaced by the peroxide radical via an ene reaction (onto triene as triallyl (iso)cyanurate involving quite stable triazine crosslinks) [17,46,113].

Three main strategies of crosslinking can be achieved and have been extensively reported [17, 46, 52, 113], either from an ionic process (first two ones) or via free radicals (last one): i) the diamine

cures, as the oldest one, involves a (CO_2) blocked diamine, hexamethylene diamine carbamate: thanks to its basic/nucleophilic behavior, a amine induces a dehydrofluorination in the VDF units leading to unsaturation, followed by a Micheal addition of the excess of amine onto the generated double bond; MgO is often used to trap the released HF; ii) dihydroxy cure (or bispenol AF), commercialized in the 1970's the normal crosslinking process in phase-transfer catalyzed bisphenol systems (as BPAF) that contain metal oxide or hydroxide acid acceptors like MgO or $Ca(OH)_2$ ([52]]; iii) Triazine (peroxide) crosslinking occurs at specific sites available on the cure-site monomer (CSM)[46,47]. Many examples from termonomers with the following structure $F_2C=CFOR_FX$ with X= Br, I, CN OCN, CN crosslinked *via* SnPh or from trialkoxysilane [220]. The CSM and curing mechanism was originally developed for an improved low-temperature poly(VDF-*co*-PMVE) fluoroelastomer. The quite acidic VDF and the ionic cure mechanisms (diamine and BPAF) creates cleavage of the trifluoroalkoxy group in PMVE units resulting in backbone cleavage, and a perfluoromethanol by product.

Regarding the properties, VDF units adjacent to perfluorocarbon monomers like TFE or HFP can be highly selectively attacked by base in both standard poly(VDF-*co*-HFP) or poly(VDF-*ter*-HFP-*ter*-TFE) co- and terpolymers ([114] and in base-resistant TFE and propylene (P)-containing terpolymers. The high VDF content needed for an adequate amine or bisphenol cure response of poly(VDF-*ter*-TFE-*ter*-P) terpolymers renders them less base-resistant than the newly developed, more highly fluorinated poly(TFE-*ter*-P-*ter*-TFP) composition because the 3,3,3-trifluoropropene (TFP) level is designed for efficient reaction and consumption during cure. In contrast, the residual VDF units in these terpolymers, not reacted during the cure, remained available for degradation by base during service.

Chen *et al.* [221] developed thermally self-curable poly(VDF-*co*-CTFE) fluoroelastomers functionalized with pendant TEMPO. This strategy involves two competitive processes, mainly occurring from the role of copper complex: i) the coupling reaction between poly(VDF-*co*-CTFE) macroradicals and TEMPO and ii) the dehydrochlorination of commercially available poly(VDF-*co*-CTFE) backbone (Scheme 47).

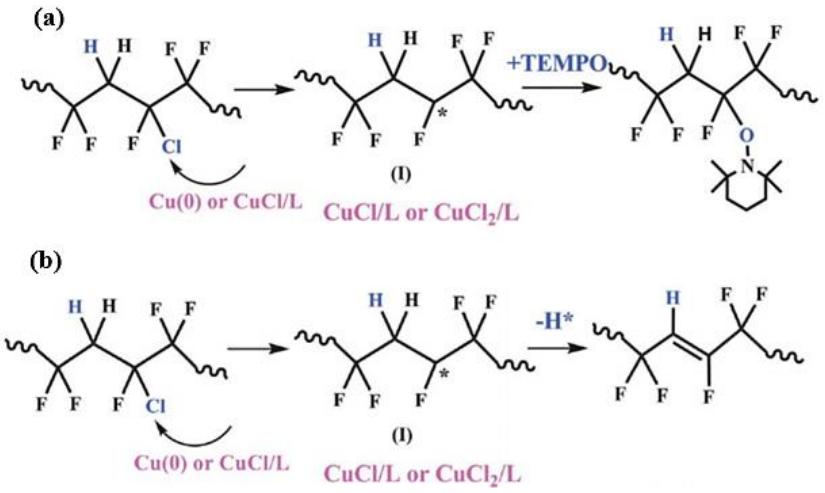

Scheme 47: (a) Grafting of TEMPO onto poly(VDF-*co*-CTFE) by an ARGET-ATRP process using poly(VDF-*co*-CTFE) as the initiator and (b) The dehydrochlorination of poly(VDF-*co*-CTFE) by the β-H elimination mechanism. [221]. 2014 Copyright. Reproduced with permission from RSC.

Many articles describe the thermal degradation of VDF-containing elastomers and copolymers. One example from Choi and Kim [249] reports the degradation of poly(VDF-*co*-HFP) copolymers. 2,3,3,3-Tetrafluoropropene (1234yf) can be formed from the VDF (head-to-tail)-HFP (head- to-tail) (hVDFt-hHFPt) heterosequence as well as from the VDF(tail-to-head)-VDF(head-to-tail) (tVDFh-hVDFt) homosequence (Scheme 48). Furthermore, 1234yf can be formed from the VDF(head-to-tail)-VDF(head-to-tail) (hVDFt-hVDFt) homosequence.

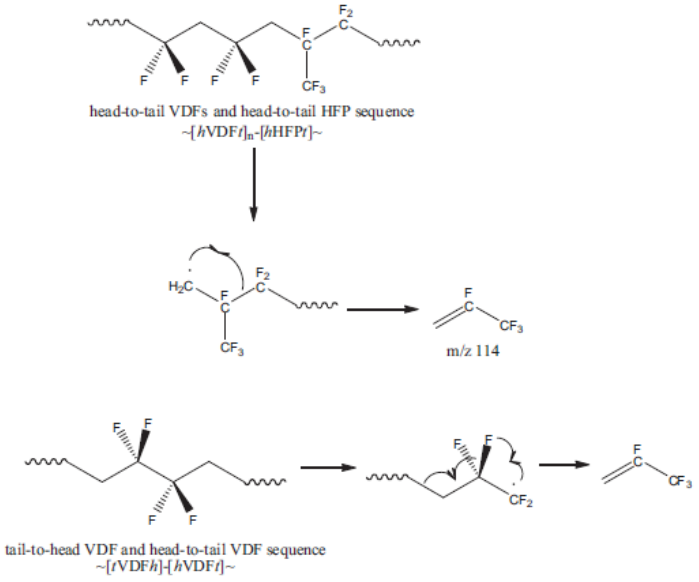

Scheme 48: Pyrolysis mechanism of poly(VDF-*co*-HFP) copolymers for the formation of 2,3,3,3-tetrafluoropropene (1234yf) from VDF–HFP heterosequence (--[hVDFt]-[hHFPt]--) and VDF head-to-head sequence (--[tVDFh]-[hVDFt]--) [222]. Copyright 2014, Reproduced with permission from Elsevier Science Ltd.

6. Are VDF-containing Copolymers of Low Concern Criteria?

6.1. Environmental issues and attempts of recycling fluorinated copolymers

Fluoropolymers are inert, stable, solid materials which have a high resistance against acids, oxidants, microbes, and photolytic and metabolic processes. Hence, they are thermally, chemically, and biologically inert and are not expected to degrade under environmental conditions or normal use and processing conditions. However, they are persistent but not bioaccumulative, not mobile and not toxic and therefore not regarded as substances of very high concern (SVHCs) from a regulatory perspective [95-96]. The tiny solubility in n-octanol and in water (< 10 mg/L also linked to their density almost double that of water) associated to their quite high molar masses indicate the inability of fluoropolymers to actively or passively penetrate into cell membranes [223-225]. Indeed, they are not mobile in the environment and therefore would not be expected to be found in sources of drinking water [96]. Actually, persistence on its own does not justify the need for specific risk management measures. Generally, during the processing of fluoropolymers, at quite elevated temperature, toxic gases can be generated. For instance, in the case of PTFE, as the temperature reaches around 450 °C, carbonyl fluoride and hydrogen fluoride can be produced in air [226], while in the case of VDF-copolymer, HF can also be released. Their extreme persistence and both the emissions and the aid-processing associated with their production, use, and disposal can be an issue for environmental and human health [95-96].

Widely used by regulators, polymers of low concern (PLC) criteria have been established around the world and documented by OECD expert groups as an appropriate hazard assessment methodology for polymers in-use and can effectively identify low risk fluoropolymers to help prioritize regulatory action. Physical, chemical, thermal, and biological stability are important criteria for a

polymer to be considered a PLC as well as for physico-chemical properties reflecting the state of the polymers. To meet the PLC assessment criteria for particle size, a powder must be 5 μm or greater in size (as median mass aerodynamic diameter). VDF-containing copolymers (including fluoroelastomers) generally satisfy the particle size PLC criterion.

As a matter of fact, at the end of industrial or consumer use, these copolymers may be disposed *via* the following routes: landfill, incineration (e.g., waste-to-energy facilities), or reuse / recycling. There is sufficient data demonstrating that fluoropolymers such as PTFE do not degrade in the environment or release substances of toxicological or environmental concern [94].Additionally, the life-cycle stages of fluoropolymer creation (aka manufacturing) and disposal at the end of industrial or consumer use (i.e. end-of-life) are important to consider. The primary focus in these life-cycle stages is generally non-polymer PFAS from the manufacturing process or fluoropolymer degradation in end-of-life disposal.

Though their tonnage is small, searching strategies to recycle fluoropolymers is still a great challenge, as well as to decompose them in a green way. Various VDF-containing copolymers have undergone some mineralization into fluoride anions under subcritical water (section 4.2) whereas quite a few surveys have reported their recycling. But recycling of fluoropolymer products and articles containing fluoropolymers is difficult to achieve since separation of the fluoropolymer from the end products is not always possible [94]. This is due to the fact that they are used predominantly in small components of larger finished articles involving a wide variety of materials.

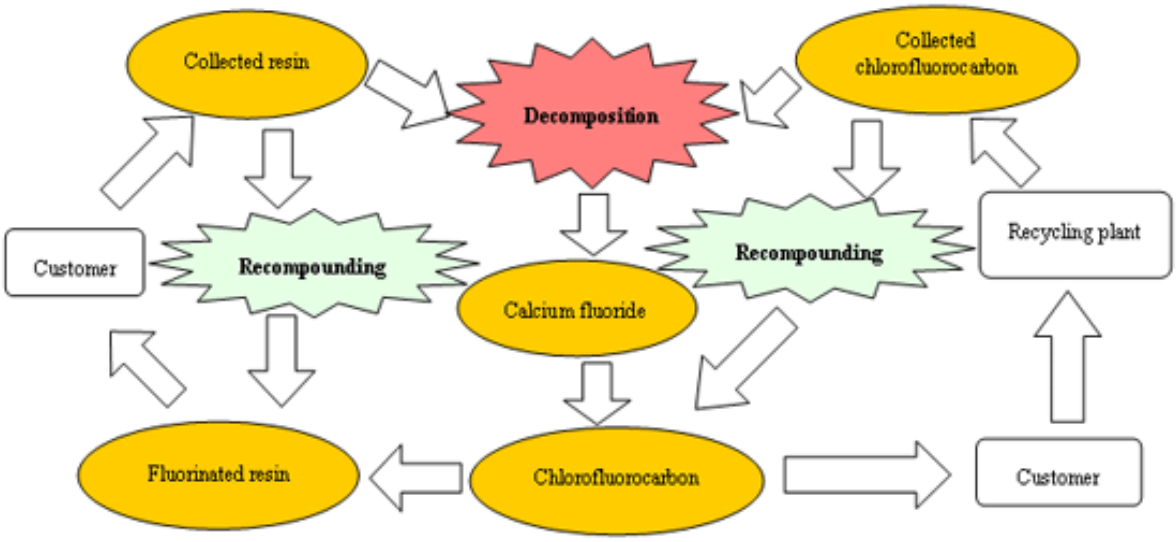

Fig. 16: Chain of collecting, recycling and recompounding chlorofluorocarbons and fluoropolymers at AGC Company [228]

Several options to recycle fluoropolymers are possible. In *primary recycling*, solid fluoropolymer waste is ground and later fed back into the manufacturing cycle of fluoropolymers. Recycled fluoropolymers may be used in high-end application when suitably collected, cleaned and reprocessed. In *secondary recycling*, solid fluoropolymer waste is ground, followed by degradation to approximately 1% of the original degree of polymerization by using gamma rays, electron beams or thermo-mechanical degradation. The recovered material can be utilized in the manufacturing of new fluoropolymers. Lastly, in *tertiary recycling* or up-cycling, solid fluoropolymer is ground, then pyrolyzed at a temperatures above 600 °C generating back the monomers which can further be purified by distillation, and then reused to produce new fluoropolymers [227]. For the primary and secondary processes, recycling treatments can be achieved by the fluoropolymer manufacturers themselves (onsite), or at a larger scale, mainly by specialist recycling companies. The up-cycling needs to be co-located to a fluoropolymer fabrication plant that utilizes the recycled monomer. Primary and secondary recyclings are limited, due to the presence of fillers, colorants or dies, and other materials involved in the final items (e.g., plasticizors and antistatics). Further, recycling may not be convenient route for all end-of-life components, as they are used predominantly in small components of larger finished items.

Therefore, collecting and dismantling for recycling might not be feasible for all products [94]. However, up-cycling treatment is applicable to some articles containing fluoropolymers, such as pipe liners in chemical plants, as well as other plant components as pumps, tank liners, seals, hoses, and many other fluoropolymers components. These are the products for which the high amounts of fluoropolymers are used offering significant recycling potential.

Indeed, because of the difficulty in handling the gas generated in the thermal decomposition process, fluorinated resins have been considered extremely difficult to recycle, and when deemed as non-recyclable, it has been treated as industrial waste. Indeed, the Asahi Glass Company (now AGC), in collaboration with Nittetsu Chemical Engineering, has claimed a recycling process of fluorinated resin since 2001 [228]. In the new procedure, the collected fluorinated resin is decomposed into calcium fluoride, extracted and then recompounded to produce fluorinated resins (Fig. 16). Activities relating to recycling technology include the reuse of chlorofluorocarbons emitted from electric home appliance manufacturing plants and glass bulbs for cathode ray tubes.

A similar technology has also been developed at Dyneon Company [94] and better described by Schlipf and Schwalm [227] or by the FluoropolymerGroup [229], as well as reviewed (Fig. 17) [230].

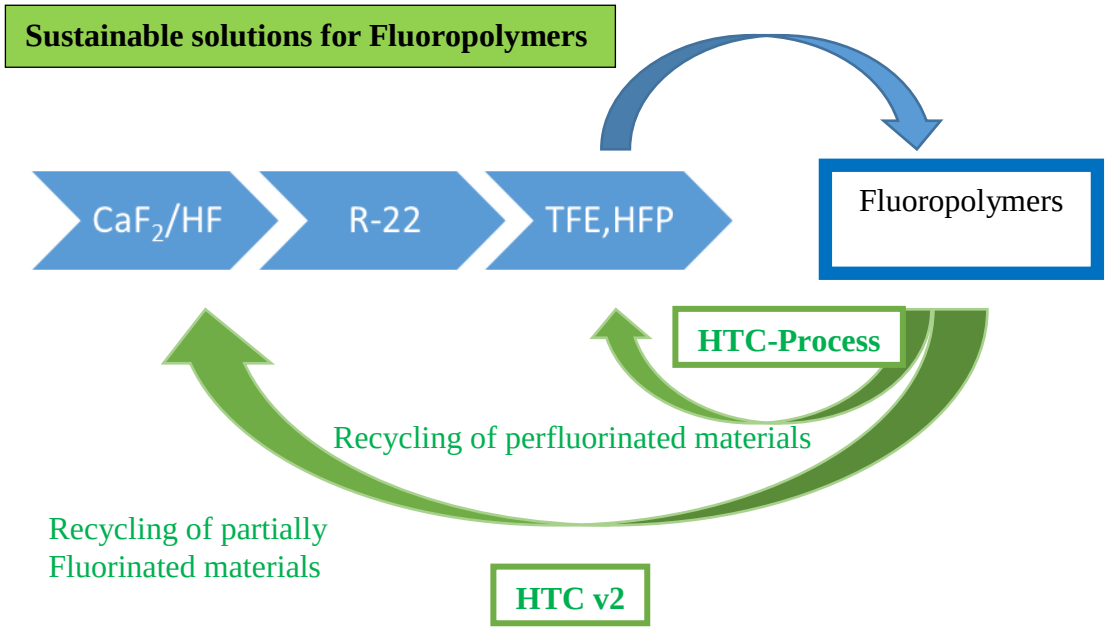

Fig. 17: Fluoropolymer recycling loop (adapted from [230])

4.2. Mineralization of VDF-containing copolymers

The mineralization of various fluoropolymers, extensively reported by the Hori's team, was processed in subcritical water, regarded as a high-pressure liquid water, the temperature ranging between 100 ºC and its critical temperature, 374 °C (at pressures higher than 22.1 MPa). In these conditions, water displays high diffusivity, low viscosity and ability to hydrolyze many organic compounds including biomass, reactions using subcritical or sc water are considered environmentally benign in chemical engineering with the aim of developing a technique for the recycling of fluorine element [231].

For saving energy consumption, lowering temperature that enables complete mineralization was achieved by the same team, from a similar technology [232] from poly(VDF-*co*-HFP) and poly(VDF-*co*-PMVE) copolymers treated in sc water by addition of $KMnO_4$. As known, $KMnO_4$ is a safe oxidizing agent, used at drinking water treatment plants to remove iron component and to control the formation of trihalomethanes and other disinfection by-products [231].

Actually, a *quasi*-complete mineralization of poly(VDF-*co*-HFP) and poly(VDF-*co*-PMVE) copolymers could be achieved at 250 ºC in presence of H_2O_2. Scheme 49 supplies a proposed mechanism [233]. Compared to the above method , the reaction temperature allowing a complete mineralization could be reduced by 50 ºC. In addition, Hori's team examined the formation of CaF_2 from the reaction solutions to close the loop on the fluorine reaction chain, since CaF_2 is the source for fluorinated compounds. [232].

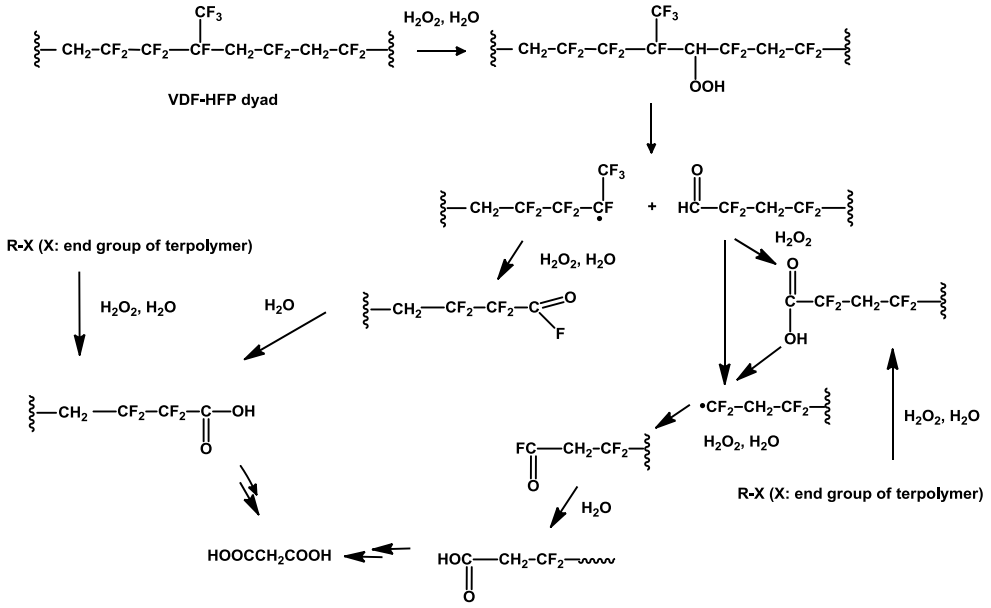

Scheme 49: Proposed mechanism for the H_2O_2-induced decomposition of poly(VDF-*ter*-HFP-*ter*-TFE) terpolymer.[233]. Copyright 2017. Reproduced with permission from Elsevier.

This strategy was extended to the mineralization of poly(VDF-*co*-MAF) copolymers [234] and poly(VDF-*ter*-HFP-*ter*-TFE) fluoroelastomer [233].

7. Applications

Thanks to their remarkable properties, VDF-specialty polymers have been used increasingly in applications where most hydrocarbon-based polymers fail, such as chemical processing, oil wells, motor vehicle engines, nuclear reactors, and space applications (Fig. 18) [235-241].

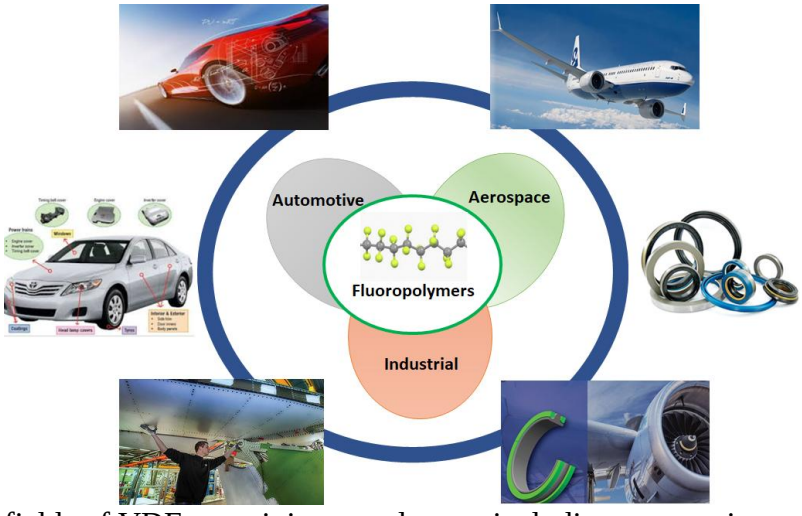

Fig. 18: Application fields of VDF-containing copolymers including automotive, aerospace and industrial areas [235-241].

7.1. Functional Coatings

Goldbach et al. [4] comprehensively reviewed the use of VDF copolymers for coating applications. More recently, the conventional radical terpolymerization of VDF with PFSVE and CTFE (Fig. 19) led to novel functional coatings stable in highly corrosive media (piranha solution) endowed with good surface properties [242].

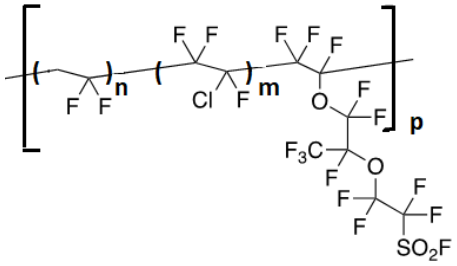

Fig. 19: structure of poly(VDF-*ter*-CTFE-*ter*-PFSVE) terpolymers for specific coatings stable in piranha solution [242].

7.2. Fluorinated elastomers

Fluroelastomers are among the best materials for use in the marine, automotive, aerospace, oil, and chemical industries where they are used as gaskets, seals, O-rings and fuel hoses. As mentioned in section 5, four fluoroelastomers (A Type, B Type, GFLT Type and GLT Type [17]) have evidenced their extreme chemical resistance with quite few or no swelling in aeronautic fluids (such as skydrol®[241]) are currently characterized with severe specifications to pass the tests.

Many articles and patents report the synthesis, properties, processing and applications of VDF-containing elastomers summarized in various text books [17,20,46] and reviews [47,114,191,243].

Based on the composition of VDF content, poly(VDF-*co*-M) copolymers can be semi-crytsalline or amorphous [16-17,21,46-47,66] (Fig. 3).

Table 2 lists non-exhaustive commercially available VDF-containing fluoroelastomers produced from major companies, their fluorine content and several properties. Indeed, all FKM designate elastomers based on VDF with or without any cure site monomer (CSM) and represent the largest category (>80%) of fluoroelastomers.

Company	**Trademark**	**Comonomers in copolymer**	**%F**	**T_g (°C)**	**Advantages/drawbacks**
Chemours	Viton®	VDF/HFP and VDF/HFP/TFE			Good chemical resistance at high T
3M	3M Elastomers®	VDF/HFP	64	-18	Resistance to oxidation, solvents, flames
SolvaySP	Tecnoflon®	VDF/HFP/TFE	70	-7, -13,	May swell
Daikin	Dai-el®			- 21	High thermostability, better resistance to swelling
Solvay	FKM®	VDF/HFP/TFE	67	-16	Better mechanical properties
Specialty		with CSM	Variable		E protects from alkaly attack
Polymers		VDF/HFP/TFE/E (5%)	Variable	-40	Resistance to oxidative attack
		VDF/PAVE			
SolvaySP	Tecnoflon®	VDF/$HCF{=}CFCF_3$	Variable		Heat and solvent resistance
3M	Kel F®	VDF/TFE/$HCF{=}CFCF_3$	62-70		Vulcanization: better heat and chemical resistance
		VDF/CTFE	Variable	-15	

Table 2: Fluoroelastomers: trademarks and properties. Adapted from [191,234,235,243] (where CSM and SolvaySP stand for cure site monomer and Solvay Specialty Polymers, respectively).

Regarding the glass transition temperature (Tg) values, Beginn et al. [144] studied the influence of HFP amount in poly(VDF-*co*-HFP) copolymers produced in $scCO_2$ medium and observed a *quasi* linear dependence (Fig. 20). In contrast, quite a few data of their melting points (Tm) were supplied [244]. Indeed, these fluorinated copolymers cannot contain any HFP molar percentage higher than 50% [52] because of the absence of propagation of HFP (r_{HFP}=0 as listed in Table 1).

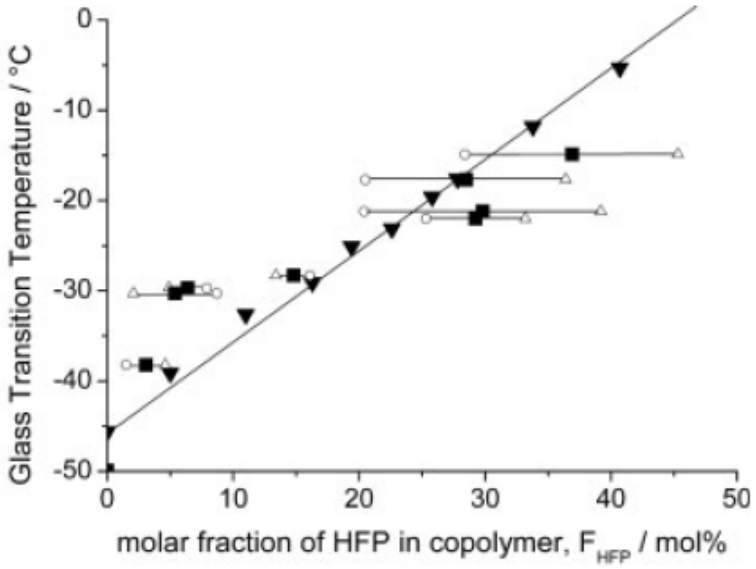

Fig. 20: evolution of glass transition temperature (Tg) vs the HFP content in poly(VDF-*co*-HFP) copolymers achieved in $scCO_2$ medium. [144]. 2005 Copyright. Reproduced wih permission from Wiley.

Two major properties of elastomers are heat and oil resistances. Wang and Legare [245] proposed a comprehensive chart (Fig. 21) that displays the top right side materials (FFKM and FKM) are the most appropriate candidates for both high thermal and chemical inertness performances. Actually, all of the fluoroelastomers are capable to bear thousands of hours of service life at 200 °C. One of the FFKM (based on TFE majorly) can reach a temperature of service as high as 300 °C. Useful service life is often strongly influenced by design and application. In terms of physical properties, the strong ionic attraction between adjacent hydrogen and fluorine atoms contributes substantially to the room-temperature strength of fluoroelastomers. Thermal stability varies within the different fluoroelastomers. The VDF-containing elastomers are slightly less stable than FFKM due to thermally induced dehydrofluorination.These elastomers should not be used in a totally confined environment. Improvements in crosslink stability have been made over the past 45 years [46,52].

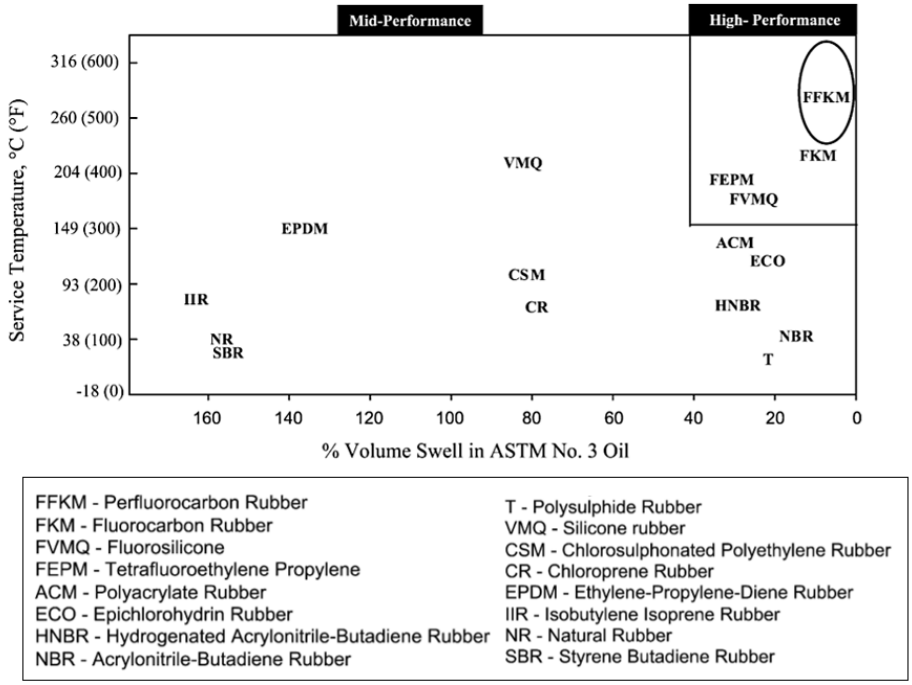

Fig. 21: Relative heat and oil resistance of various elastomers (ASTM D2000). [245]. Copyright 2003. Reproduced with permission from Elsevier.

Wang and Legare [245] also compared the mechanical properties of such materials with those of poly(TFE-*alt*-propylene) and fluorosilicones (Table 3). Usually, fluoroelastomers have low temperature properties dictated by several characteristics: the size of the fluorine atom, the fluorinated substituent (e.g., trifluoro and trifluoroalkoxy groups) and various intermolecular forces because of the high electronegativity of fluorine atoms. In contrast to FKM and FFKM which are the hardest, fluorosilicones display much more mobility (Tg = -65 °C for poly(methyl-3,3,3-trifluoropropyl siloxanes) as for polyphosphazenes [191,246], thanks to the -SiO-SiO- flexible moieties and have also the highest compression set.

The compositions of the elastomers can be determined by NMR spectroscopy as carefully studied by Rinaldi's team. Indeed, two interesting articles report in-depth characterizations of poly(VDF-*co*-HFP) copolymers [247] and poly(VDF-*ter*-HFP-*ter*-TFE) elastomers [248].

Property	**Fluoroelastomers**

	FFKM®	FKM®	Aflas®	Fluorosilicone®
100 % Modulus (MPa)	6.2-13.1	2.1-15.2	2.5-3.5	1.0-6.1
Tensile strength (MPa)	14.5-16.8	9.0-18.6	18.0-20.0	6.2-8.6
Elongation (%)	120-240	100-500	250-350	100-500
Compression set (%) 70 h, 200 °C	35-50	≥10	45-50	60
Hardness (Shore A)	70-95	90-95	65-75	50-75
Brittle temp. (°C)	-40 to -30	-59 to -18	-40	-66

Table 3: Mechanical properties of different fluoroelastomers. [46-47,243,245]. (Aflas® is a poly(TFE-*alt*-P) alternating copolymer marketed by AGC).

Currently, five FKM kinds of elastomers are differentiated by trademarks and are classified according to the following types: i) Type 1: copolymer based on HFP and VDF (containing 66 wt% Fluorine) with the best balance of overall properties; ii) Type 2: Terpolymer made of TFE, HFP and VDF endowed with a higher heat resistance, best aromatic solvent resistance of the VDF containing fluoroelastomers (68-69.5 wt% F); iii) Type 3: Terpolymer containing TFE, a fluorinated vinyl ether (e.g. PMVE), and VDF with improved low-temperature performance, higher cost (62- 68 wt% F); iv) Type 4: Terpolymer of TFE, propylene and VDF with improved base resistance, higher swell in hydrocarbons, decreased low-temperature performance (with 67 wt% F); v) Type 5: Pentapolymer based on TFE, HFP, ethylene, PMVE and VDF with improved base resistance, low swell in hydrocarbons, improved low-temperature performance.

Besides FKM elastomers, FFKM are not based on VDF units to overcome base issues and its designation is "*Perfluoro rubbers based on TFE and perfluoroalkyl, or perfluoroalkoxy vinyl ethers* [17,52,124].

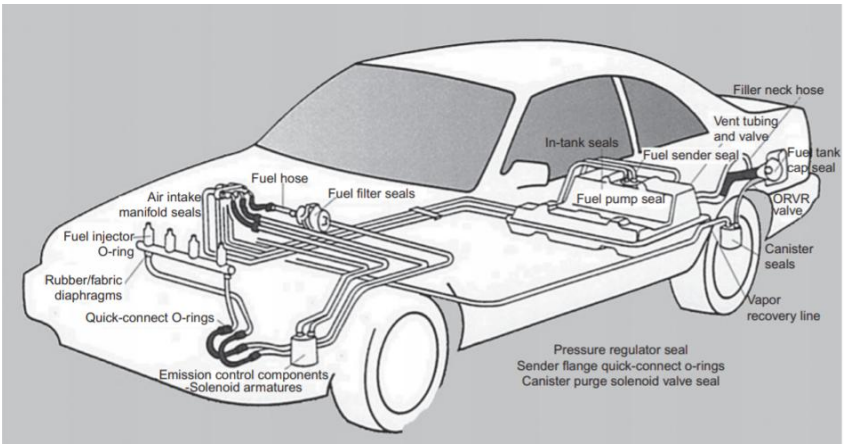

Fig. 22: Fluoroelastomers used in fuel systems. [238] Reproduced with permission of Elsevier.

Articles based on fluorocarbon elastomers, involved in many applications for cars and aerospace industries, have been listed in various documents [17,21,46-47,241].

7.3. Thermoplastic Elastomers

Fluorinated thermoplastic elastomers (TPEs) have been produced for several decades from ITP (section 3.2.1). Various well-documented books [2,249] and reviews [176-178,191,243] have aready summarized their syntheses, properties and applications which are not recalled in that present review. Further, numerous applications in high tech areas such as aerospace, aeronautics and engineering or in optics, arising from their outstanding properties. These TPEs are useful as O-rings, hot melts, pressure-sensitive adhesives, tough transparent films, sealants having good chemical and ageing resistance, protective coatings for metals, or even for denture plates (Dai-el® T530, marketed by the Daikin Company is claimed not to display any erythrocyte hemolysis or cytotoxicity, and does not generate any harmful substances). They can find applications as pressure sensitive adhesives, electrical devices (e.g., conductors), fuel hoses for engines, O-rings and shaft seals. Usually, the central elastomeric sequences display molar masses higher than 30,000 while those of the plastomeric (or hard) blocks (> 10,000), although Yagi *et al.* [250] already claimed molar masses of TPEs up to 1,000,000 $g.mol^{-1}$.

As a consequence, original TPEs composed of soft and hard segments (same as the well-known polystyrene-*b*-polybutadiene-*b*-polystyrene (SBS) triblock copolymers), are currently produced in a *pseudo*living fashion by stepwise ITP (Scheme 50).

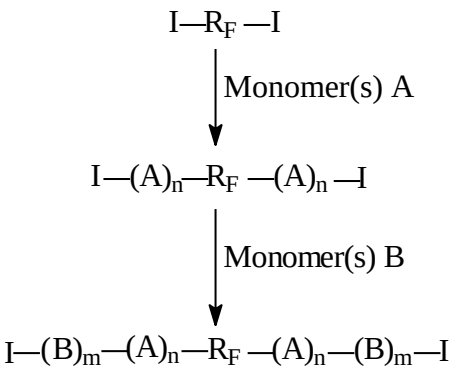

Scheme 50: synthesis of thermoplastic elastomers via a two step-procedure (polyA yielding a soft sequence while PolyB is a hard block) [189,191].

The TPEs display negative glass transition temperature, Tg, and high melting temperatures, Tm, sometimes higher than 250 °C [249]. Fig. 23 represents the heterogenous morphology in which both amorphous and crystalline zones coexist, the crystalline domain inducing some physical crosslinkings.

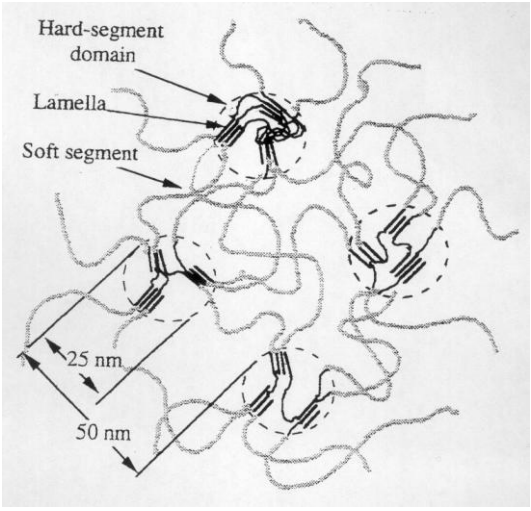

Fig. 23: schematic representation of a thermoplastic elastomer with amorphous and crystalline zones [189,191]

Beside block copolymers, commercial graft copolymers are also available: one example is Cefral®, marketed by the Central Glass Company [251] being currently produced from a two-step process: i) the first one leads to fluorinated macroinitiators (MacroPerCa) from the suspension terpolymerization of two fluoroolefins and *tert*-butyl peroxyallyl carbonate (TBPAC that bears a peroxycarbonate group) (Scheme 51). The trick was to achieve the reaction at low temperature without decomposing the peroxycarbonate function. The second steps deals with the polymerization of VDF initiated by the MacroPerCa at 95 °C, giving graft terpolymer (in 81–91%) consisting in a an elastomeric backbone (Tg ca. -20 °C) and PVDF thermoplastic grafts (Tm= 155–160 °C).

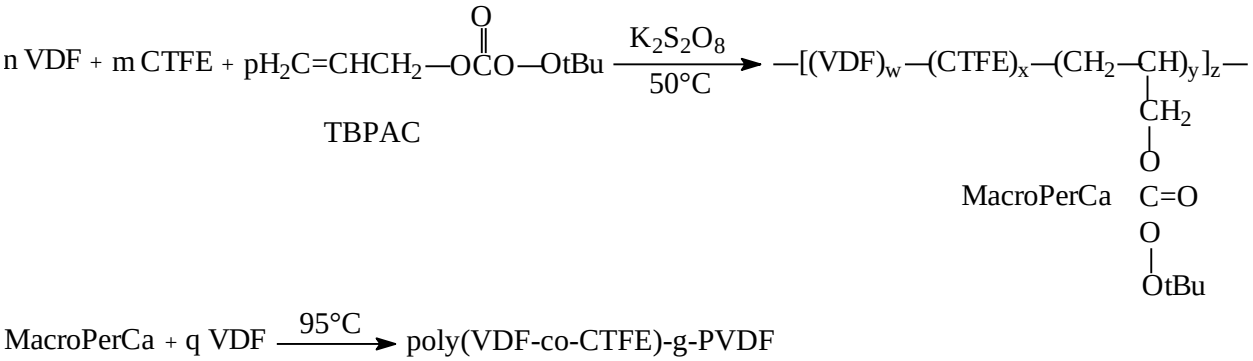

Scheme 51: synthesis of graft thermoplastic elastomers from the radical terpolymerization of allyl *tert*-butylperoxycarbonate (TBPAC) with VDF and CTFE at low temperature followed by the PVDF grafting at higher temperature.[251]

The patent claims several examples of novel TPEs based on various molar percentages of VDF, CTFE, HFP, and MacroPerCa, and the massic yields of the resulting co-/terpolymers reached ca. 60–80%. Tg values of poly(VDF-*ter*-CTFE-*ter*-TBPAC) and poly(VDF-*ter*-HFP-*ter*-TBPAC) were -21 and -19 °C, respectively. Regretly, neither the molar masses nor the comonomer amounts in the terpolymers were supplied. In addition, reaching high molar mass-terpolymers from the first step may be questionable, because of unavoidable allylic transfer from TBPAC, hence yielding oligomers. Furthermore, no information on possible presence of "free" PVDF chains produced by the direct initiation of VDF from *tert*-butoxy radicals (released from dangling MacroPerCa) was mentioned.

7.4. Composites

VDF-copolymers/filler composites have been reported in many articles and patents and this is quite difficult to summarize all surveys reported in that area. The fillers are of various nature: metals, nanoparticles and ionic liquids.

For example, Heidarian et al. [252] prepared fluoroelastomers (FEs) nanocomposites filled with carbon nanotube (CNT) and their properties were compared with those of carbon black (CB) filled- or unfilled-FEs. Though tanδ in the glassy state was lower but higher in the rubbery state, the CNT/FE and in comparison to others (in their glassy and rubbery states), the storage modulus was higher. The authors reported that the crystalline part of FE and CB/FE were mostly in α-form. However, CNT together with shear and high temperature, induced γ-crystallinity in the FE. X-ray diffraction (XRD) results also corroborated DSC and DMA results and showed that CNT induced a γ-crystallinity increase in FE while the α-phase crystallinity decreased compared to others and XRD, DSC and DMA results for FE and filler/FE confirmed such results. The same group extensively studied the influence of CNT into FE [253-254]. More recently, Shamsuri et al. [255] comprehensively reviewed the preparation and uses of composites based on poly(VDF-*co*-HFP) copolymers blended with at least 20 different ionic liquids (ILs) *via* various processes (the most commonly used being to soak the copolymer in the IL, or solution blending in low boiling point polar aprotic solvent like acetone, or by means of a hot-pressing machine to shape the blends). These authors also listed several nanofillers such as graphene oxide (GO), multi-walled carbon nanotubes (MWCNTs), octadecylamine modified montmorillonite (OMMT), TiO_2, sodium montmorillonite (NaMMT), poly(vinyl pyrrolidone) grains or succinonitrile (SN). Indeed, the nature of the IL and the nanofiller has a great influence on the crystalline, chemical, thermal and mechanical and properties of the resulting composites.

In addition, because of the electrostatic interaction between the anion of the ionic liquid and PVDF moieties, the absorption bands of the CH−CF−CH stretching vibrations in the composites shifted to higher wavenumber regions compared to those of neat PVDF [256]. The authors also observed that

PVDF mixed with MWCNTs-[Emim][NTf2] provides high tensile strength and elongation composites, as well as high melting temperature with good interaction of their components. However, as displayed in Fig. 24b, independently of the fluorinated matrix, the incorporation of the IL induced a lower thermal stability of the polymer to 394 °C in PVDF, followed by poly(VDF-*co*-HFP) (391 °C), poly(VDF-*co*-TrFE) (393 °C) and poly(VDF-*co*-CTFE) (354 °C). This is an indicative of the IL imidazolium interaction with the CH_2-CF_2 units in the fluorinated matrix. The thermal degradation of IL [C2mim][TFSI] is within the range of thermal degradation values of the polymer, starting from ca. 400 °C.

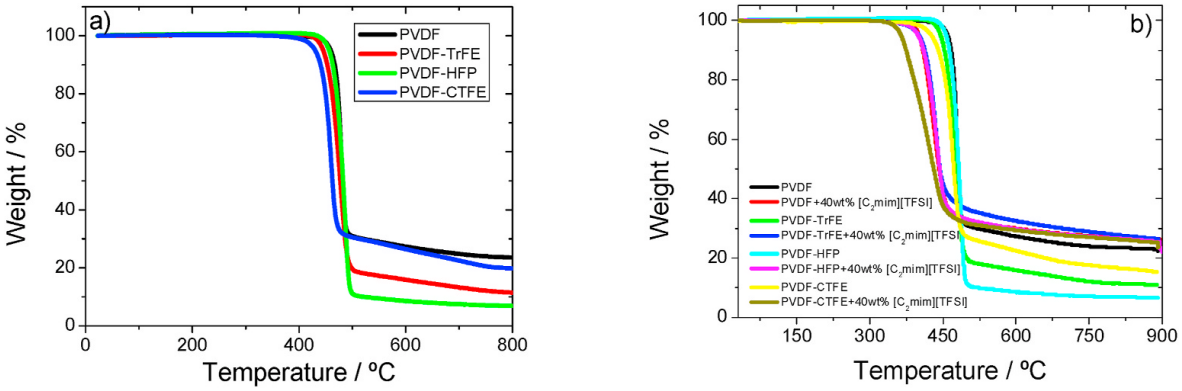

Fig. 24: TGA thermograms for: a) neat PVDF, poly(VDF-*co*-TrFE), poly(VDF-*co*-CTFE) and poly(VDF-*co*-HFP) copolymers at a heating rate of 10 °C.min^{-1}; b) PVDF and VDF co-polymer composites comprising 40 wt% of the IL [C2mim][TFSI] at the same heating rate. [256]. Copyright 2021. Reproduced with permission with Elsevier.

IL/fluoropolymer composites varying the polymer matrix [poly(VDF-*co*-TrFE), poly(VDF-*co*-HFP) and poly(VDF-*co*-CTFE) copolymers] and [Emim][TFSI] content [257] showed that, independently of the polymer matrix, the thermal degradation for the IL/polymer composites occurs in a single step degradation process, the degradation mechanism and the residual weight for the composites being not significantly affected by the IL content and polymer type. Overall, the degradation temperature decreases with increasing IL content, suggesting that the interaction of CH_2-

CF_2 with the imidazolium ring leads to the decrease of the thermal stability, regardless of the type of fluorinated polymer [257].

In addition, Yang et al. [258] studied the efficient compatibilization role of perfluorooctyltriphenylphosphonium iodide IL as a potential interfacial agent in poly(VDF-*co*-CTFE) copolymer/graphene composite films. In fact, because of the absorbtion of this IL on the surface of graphene oxide (GO) and reduced graphene oxide (rGO), two series of poly(VDF-*co*-CTFE)/GO-IL and poly(VDF-*co*-CTFE)/rGO-IL composites with different loading amounts were processed. Differences in the interaction model between GO with IL and rGO with IL were observed. Subsequently, the interfacial effect of IL on the properties of poly(VDF-*co*-CTFE)/graphene composites, such as crystallization, chain segmental relaxation behavior, dispersion, and the final dielectric properties (Fig. 25) were also investigated. Actually, rGO-IL imposed different effects on crystallization behavior, and subsequent dielectric properties of composite materials compared to GO-IL because of different interactions of IL with GO or rGO. Furthermore, the authors observed that such poly(VDF-*co*-CTFE)/IL-modified graphene composites displayed high dielectric permittivity and low dielectric loss: the relative permittivity at 1 kHz of composite loaded with 2.70% rGO-IL increased up to 20.3 compared with that of 11.0 for the pristine matrix, whereas tan δ worthed 0.032 [ca. the same value as that of the pristine matrix (tan δ = 0.030)]. In addition, dielectric breakdown strength was significantly reduced.

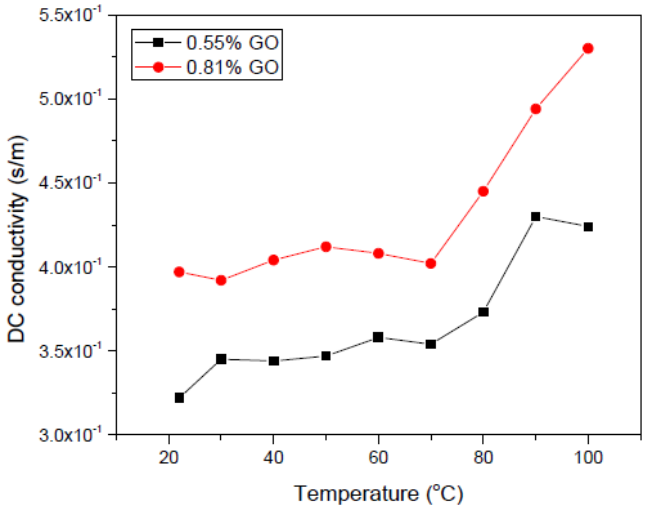

Fig. 25: Direct current (DC) conductivity *versus* the temperature of poly(VDF-*co*-CTFE)/graphene oxide (GO) at different GO loadings [257]. Copyright 2019. Reproduced with permission from MDPI.

7.5. Membranes

7.5.1. Membranes for water treatment

Besides Energy, one of the major greatest challenges facing the 21st century aims at supplying sustainable feedstocks of clean drinkable and freshwater water, at reasonable costs. Membrane technology continues to dominate the water purification processes thanks to its energy efficiency. Nevertheless, a need is searched to improve membranes which are more selective, less prone to various types of fouling, have higher flux, and are more resistant to the chemical environment. [259-260]. Nearly 68% of the water on earth is seawater, while ~ 30% exists in glacier forms or as a groundwater reservoir and only 2–3% is distributed to the world's population as fresh and grey water, respectively. From the UN document [261–263], ca. 2.4 billion population suffer freshwater crisis (estimated to be 3.9 billion by 2050) every year. Thus, a wide global interest on freshwater reclamation from brackish water has to be developed to overcome these issues.

Rajput et al. [264] designed novel crosslinked cation exchange membranes (CEMs) for brackish water desalination *via* electrodialysis, in three steps: first, a dehydrofluorination of poly(VDF-*co*-HFP) led to unsaturated copolymers (or kind of macromonomers) which were reported to further copolymerize with styrene and divinylbenzene (DVB) followed by a sulfonation (Fig. 26). However,

that copolymerization needs minute characterization and it is expected some deeper insight to well evidence such a reaction for which the inner hindered double bond should not be so reactive.

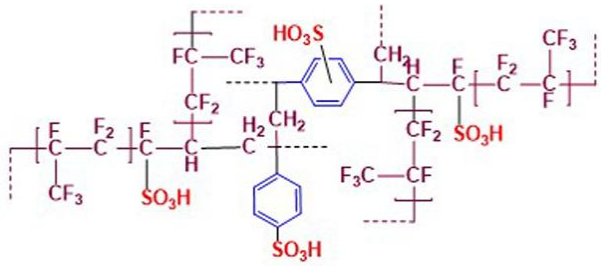

Fig. 26: structure of the obtained network by radical copolymerization of DVB/styrene with dehydrofluorinated poly(VDF-*co*-HFP) copolymer followed by sulfonation [264]. Copyright 2021, Reproduced with permission from Elsevier.

The membrane containing 45% styrene-DVB (*i.e.*, CEM-45) exhibited water uptake (52%) and ionic conductivity (up to 19 $mS.cm^{-1}$) at 30 °C. Dynamic current-voltage characteristics were evaluated for membranes: CEM-45 showed ca. 205% and 63.6% higher limiting current density (45.8 $A.m^{-2}$) relative to CEM-35 (15.0 $A.m^{-2}$) and CEM-40 (28.0 $A.m^{-2}$). FE-SEM evaluated that membranes possess symmetric lunar patched morphology which could have influence on Ilim, plateau potential and plateau current attributed due to triggered interfacial affinity with brackish water. All membranes displayed excellent thermal and mechanical stabilities up to 220 °C and 10 MPa, respectively [264]. Desalination properties were studied in term of the current efficiency, ionic flux and high salt removal efficiency (up to 93%) was achieved with a significant power consumption (1.19 kWh kg^{-1}) and current efficiency (75%) from CEM-45 membrane. Regarding the electrodialysis performance, CEM-45 was suitable for brackish water desalination.

The authors also studied the stress-strain (Fig. 27) and viscoelastic properties of copolymer pristine membranes (CPMs) and CEM membranes. For CPM-x membranes the prominent region is a proportional plastic region, while for CEM-x membranes, the viscoelastic nature is well seen and highlighted two distinct regions (proportional plastic and elongating elastic regions) [264]. For CEMs, void filling and plasticizing water effect are key parameters. In addition, strong Van der Waal forces of interaction in the crosslinked system via -SO_3H functions linked to water was possible.

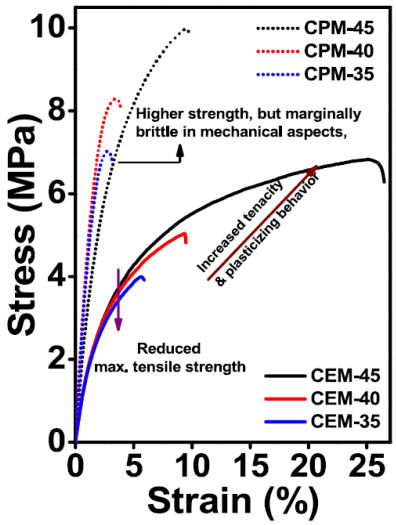

Fig. 27: Engineering stress (MPa) vs. Engineering strain (%) behavior of poly(VDF-*co*-HFP)-*g*-(St-DVB) *co*-polymer pristine membrane (CPMs) and cation exchange membrane (CEMs) (where 35, 40 and 45 stand for the styrene-DVB composition).[264] Copyright 2021, Reproduced with permission from Elsevier.

Salt removal performance and rate of change in relative magnitude of ionic carried out for 210 min and evidences that three CEMs efficiently reduced from 5800 ppm of brackish water to ca. 450 ppm, in 210-360 min. Faster salt reduction rate depends on a higher membrane flux due to relatively higher membrane potential and transport properties. Fig. 28b exhibits the ionic flux in concentrate compartment in the process of electrodialytic desalination. It reveals that the ionic flux with CEM-45 is higher than that from CEM-40 and further CEM-35. This tendency of salt reduction is even steeper after 90 min being assigned to the lowering of ionic fluxes as well as the reduced influence of diffusion-gradient concentration.

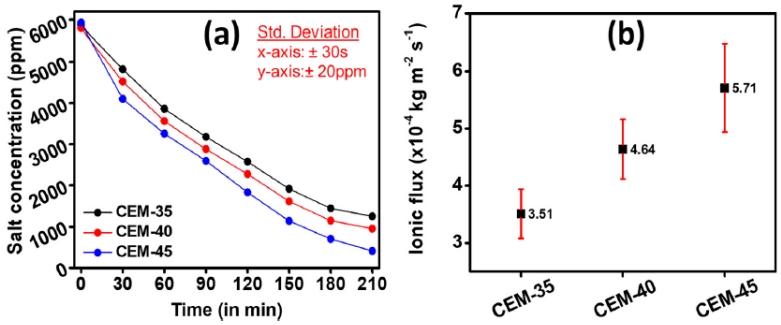

Fig. 28: Electrodialysis results (a) salt concentration profile and filtrate compartments *versus* time (b) cumulative ionic flux during electrodialytic desalination for 3 CEM membranes (where 35, 40 and 45

stand for the styrene-DVB composition).[264].Copyright 2021, Reproduced with permission from Elsevier.

7.5.2. Vacuum membrane distillation

Yadav et al. [265] prepared flat sheet membranes based on poly(VDF-*co*-HFP) and poly(ethylene glycol) (PEG) of various molar masses and concentrations by solution blending with antifouling features for distillation. They optimized the porosity, pore size distribution, hydrophobicity and dimensional stability of such membranes to find out the best conditions for vacuum membrane distillation (VMD) desalination. The membrane porosity and thus permeate flux increased with the PEG concentration. Particularly, the membrane, composed of 20 wt% poly(VDF-*co*-HFP) and 10 wt% PEG-400, showed superior performance (>99.8% salt rejection and flux for 4% NaCl feed water of 19.72 l $m^{-2}h^{-1}$) (Fig. 29) in comparison to other PVDF based flat sheet membranes reported in the literature. From a three-dimensional comprehensive computational fluid dynamics model, these authors also predicted the vapor flux profile in the VMD process with a suitable accuracy. [265]

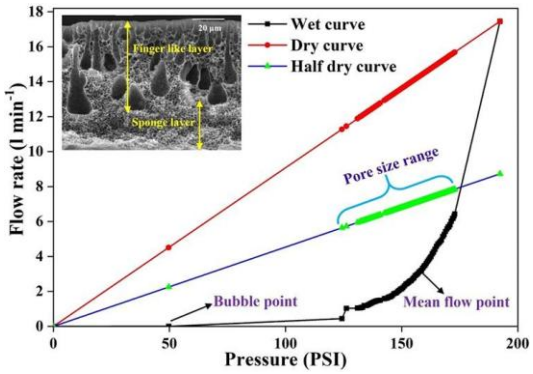

Fig. 29: pore size and pore size distribution of poly(VDF-*co*-HFP)/PEG-400 membrane by capillary flow porometer wet, dry and half-dry curves (inset is a SEM picture of cross-section of such membranes).[265]. Copyright 2021. Reproduced with permission from Elsevier.

From another strategy, the same group [266] recently synthesized novel grafted poly(VDF-*co*-HFP) membranes with tuned hydrophobic and anti-fouling characteristics for desalination of high saline water by VMD process. Different functional groups or monomers as tri(methoxy) silane, 4-methyl styrene, and 2,3,4,5,6-pentafluorostyrene (PFSt) were used as side-chain grafting onto the fluorinated backbone. Membrane performances were achieved by permeate flux, fouling resistant

nature, water contact angle and long-term durability. Among different prepared membranes, PFSt grafted poly(VDF-*co*-HFP) membrane was regarded as a promising candidate for desalination of high saline water by VMD process (with a 36% increase-permeate water flux compared to that of pristine membrane), high salt rejection (99.99%), anti-fouling property by simple water washing, and satisfactory durability.

Another strategy for water purification is the direct contact membrane distillation (DCMD). For such a peculiar application, many articles have reported that various VDF-copolymers can be electrospun to provide materials with enhanced performances and recently reviewed [267].

Lalia et al.[268] optimized the formation of nanofibrous poly(VDF-*co*-HFP) membranes followed by a hot-pressing post-processing that could increase the pore size, the pore distribution and the membrane thickness. The efficiency of the membranes in DCMD applications was evidenced by the liquid entry pressure. In addition, these authors used nanocrystalline cellulose as filler for the same electrospun fluoropolymer and hot-pressed nanofibrous membranes.[269] The obtained membranes exhibited improved mechanical properties alongside high flux rate and salt rejection. Such a fluorinated copolymer was also involved in multilayer structured membranes, consisting in a thick layer (60 μm) of electrospun poly(VDF-*co*-HFP) fibers as the substrate and a thin outer layer (20 μm) of PVDF/CNT with improved superhydrophobic properties [270]. The presence of CNT further enhanced the surface roughness yielding higher water contact angles compared to that of pristine poly(VDF-*co*-HFP) electrospun membrane. Furthermore, better flux performance and salt rejection than for those of a commercially available PVDF membranes were noted.

7.6. Materials for Energy

This section deals with non-exhaustive applications of various systems for clean energy: fuel cells, Lithium ion batteries, electroactive (piezo- or ferroelectric) devices, dye sensitizor solar cell and photovoltaics.

7.6.1 Fuel Cells Membranes

Fuel cells (FCs) are clean energy devices which convert the electrochemical (e.g. an oxidation-reduction of a fuel and comburent) energy into to electrical energy without releasing greenhouse gases. Fuel cell electric vehicles (FCEVs) are powered by a fuel that can be either hydrogen (for proton exchange membranes [271]) or hydroxides (for solid alkaline FC [272,273]). The membranes are the key components of FCs and several types can be offered: proton, alkaline and quasianydrous ones. Though less mature than Lithium ion batteries (as an energy storage system), Toyota [274] and Hyundai have already launched the production of FC Mirai and Hyundai Nexo cars since a couple of years.

7.6.1.1. Protonic fuel cell membranes

For proton exchange membrane for fuel cell (PEMFC), sulfonic acids are required and advantageously electron-withdrawing CF_2 group adjacent to this function enables to make it quite acidic. In contrast to poly(TFE-*co*-PFSVE) copolymers (PFSVE stands for perfluoro(4-methyl-3,6-dioxaoct-7-ene) sulfonyl fluoride), currently leading to perfluorosulfonic acid (PFSA; e.g., Nafion®, Flemion®, Fumion®, Aciplex® or Aquivion®) membranes [271] the radical copolymerization of VDF with PFSVE has been reported by various authors [125, 275-280]. First pioneered by the DuPont Company [275-276], it was further reported by academic groups [125,277-280] but these studies reported that the proton conductivities and performances in fuel cells were lower than those of PFSA. While the patent claims copolymers with PSEPVE contents ranging between 0.5 and 50 mol%, no examples mention copolymers with a high PSEPVE content (the highest amount was a 1:10 in PSEPVE:VDF molar ratio) [276]. The copolymer having the lowest VDF amount contained 77.7 mol% VDF and 22.3 mol% PSEPVE [125]. Sayler and Thrasher [279] reported that the use of VDF in the copolymer favors two major drawbacks: i) methylene groups are not stable against radical attack and may decompose in presence of peroxide radicals at the high temperatures inside a fuel cell and ii) the hydrolysis cannot be achieved in presence of KOH (or NaOH) inducing some dehydrofluorination (thus

releasing hazardous HF from the copolymer backbone). The adopted strategy was to prepare them from VDF as opposed to TFE, hence these limitations able to be overcome. Because of their low reactivity ratios (r_{PFSVE} =0.07 and r_{VDF}=0.57 at 120 °C [125]), Sayler suggested the possibility to prepare *quasi* alternating poly(VDF-*alt*-PFSVE) copolymers and to carry out this copolymerization in bulk. Then, the direct fluorination of the resulting material enabled to obtain a perfluorinated material stable up to 350 °C, allowing for the benefits from using VDF to prepare high molar masses with low EW polymer without the drawback of the poorer chemical stability. Hickner's group [278] could crosslink these poly(VDF-*co*-PFSVE) copolymers and the resulting membrane exhibited methanol permeability of 1.89×10^{-9} cm^2/s, which was over 2 orders of magnitude lower than Nafion 117 with a methanol permeability of 1.92×10^{-6} cm^2/s in the same conditions.

A further study on the radical terpolymerization of PFSVE with VDF and CTFE (Scheme 52) was attempted in order to increase the Fluorine content in the copolymer but the conductivity was not better than in the above materials [125].

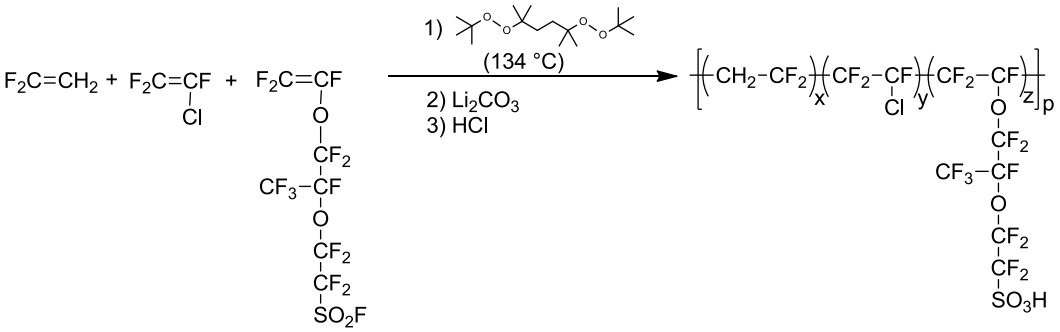

Scheme 52: Radical terpolymerization of perfluoro(4-methyl-3,6-dioxaoct-7-ene) sulfonyl fluoride (PFSVE) with VDF and CTFE.[125]

Actually and as mentioned in section 5, the crosslinking of ionomers enables to enhance the chemical, thermal and mechanical stabilities [281-282]. PFSA generally requires either the conversion of the sulfonic acid side chain or the synthesis of a terpolymer containing cross-linkable functional groups [283].

In the case of ionomers based on VDF, terpolymerizations of VDF with PFSVE and a CSM were reported and two examples are described hereafter. The first one used vinyl triethoxysilane (VTEOS) as CSM (Scheme 53), the microstructures (i.e. the content of the three comonomers incorporated within the terpolymers) of which were assessed by NMR spectroscopy [284].

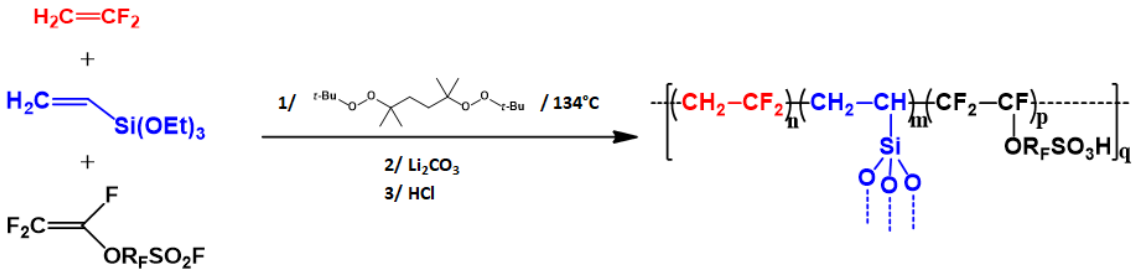

Scheme 53: Radical terpolymerization of VDF with PFSVE and vinyl triethoxysilane (VTEOS) (with R_F: $CF_2CF(CF_3)OC_2F_4$) as precursors of fuel cell membranes crosslinked by hydrolysis of triethoxysilane side groups [284].

These terpolymers of 5 compositions (containing VTEOS amount ranging from 3 to 8 mol.%), were further crosslinked in acidic medium. Additionally, as VDF units are quite sensitive in basic media, the sulfonic acid functions of these poly(VDF-*ter*-PFSVE-*ter*-VTEOS) terpolymers were achieved from $–SO_2F$ groups in PFVES units into $–SO_3Li$ in presence of Li_2CO_3 and then acidified to offer hybrid organic/inorganic membranes. The proton conductivities of such hybrid organic/inorganic $SiO_2–SO_3H$/ terpolymer membranes were 21 $mS.cm^{-1}$ at room temperature under 100% RH (IEC values of 0.4–0.5 $meqg^{-1}$) were two times less than that of Nafion NRE212) and reached 12 $mS.cm^{-1}$ at 120 °C [284]. Indeed, $–SO_3H$ groups were linked to water molecules thus forming a continuous pathway for proton hopping by the Grotthuss mechanism. The arrangement of the ionic domains in the hybrid interface seemed to contribute to a fast proton transfer by forming a continuous conduction path at high temperatures.

The second one involves a cyano CSM (Scheme 54) to favor a post thermal crosslinking *via* triazine function that induced both chemical and thermal stabilities (Scheme 55) with improved electrochemical characteristics (proton conductivity of 58 $mS.cm^{-1}$ at 80 °C and 100% RH) [285].

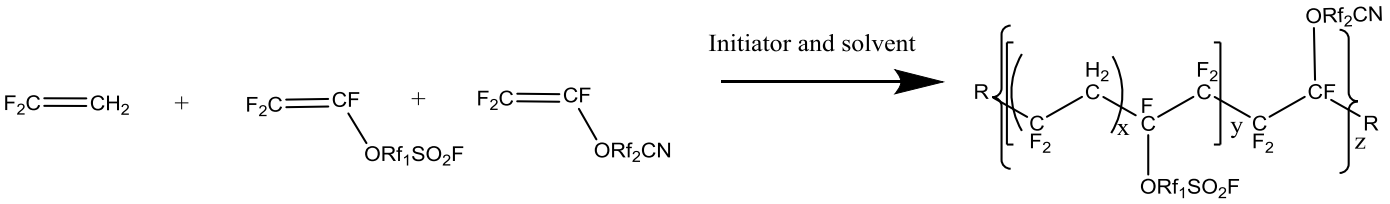

Scheme 54: radical terpolymerization of VDF with PFSVE and a cyano fluorinated monomer (where Rf and R_1 stand for $CF_2CF(CF_3)OCF_2CF_2$ and $OC(CH_3)_3$, respectively (or $C(CH_3)_3$, or CH_3, or OSO_3K) whereas the counter-cation is H^+ or K^+ [285].

Such a crosslinking was inspired from previous studies well-reported by Logothetis' review [46] and claimed by Yandrasits et al. [286].

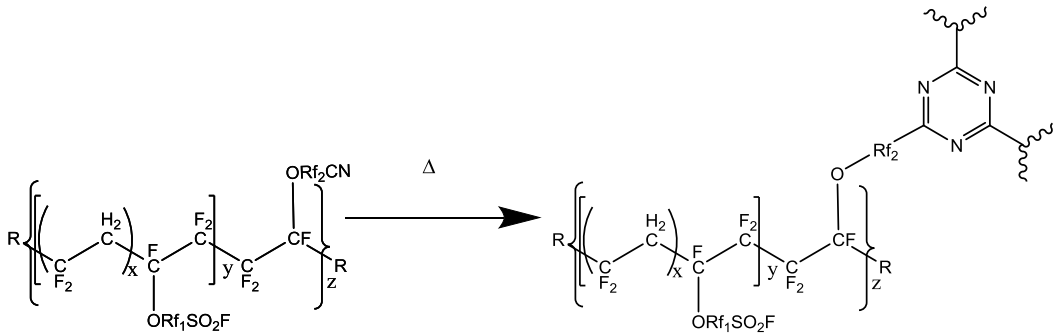

Scheme 55: radical terpolymerization of VDF with PFSVE and a perfluorocyano cure site monomer followed by a post thermal crosslinking generating a triazine function [285]. Copyright 2019, Reproduced with permission from RSC.

In addition, many fluoropolymers have been chemically modified to get fuel cell membranes from various strategy: i) via ATRP polymerization of hydrocarbon monomers (e.g. styrene) from the cleavage of C-Cl bond in poly(VDF-*co*-CTFE) copolymers, most of these studies being summarized in recent reviews [171-172]; ii) by radiografting of poly(VDF-*co*-M) copolymers (after irradiation *via* electron beam, ^{60}Co, X rays or other sources of ionization followed by a grafting of a functional monomer [287]); or iii) by "grafting onto" techniques [170-171]. One example yielding FC membranes

based on VDF dealt with the etherification of primary alcohol dangling groups [from the reduction of carboxylic acid of TFMAA (or MAF) units in poly(VDF-*ter*-HFP-*ter*-TFMAA) terpolymers] with paraphenol sulfonic acid, *via* a Mitsunobu reaction (Scheme 56) [288].

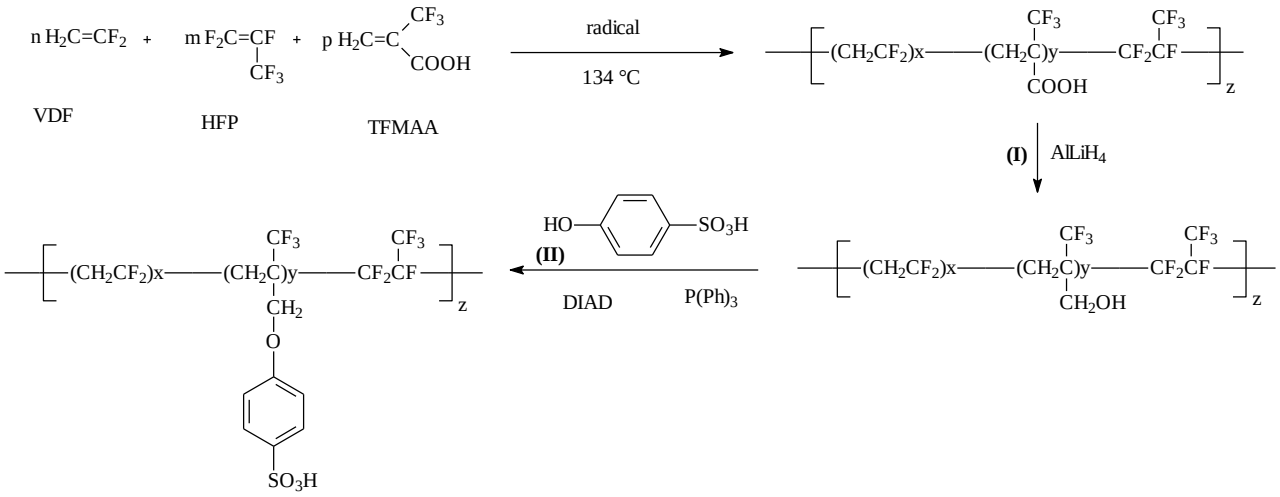

Scheme 56: Synthesis of poly(VDF-*ter*-HFP-*ter*-TFMAA) terpolymers, reduction of carboxylic acid into primary alcohols, and grafting of aryl sulfonic acid (where TFMAA (or MAF) stand for α-trifluoromethacrylic acid). [288]. Copyright 2012, Reproduced with permission from the American Chemical Society.

Usually, membranes are processed from casting (dissolution of copolymers in a solvent, spreading on a substrate, followed by evaporation to obtain the film) and finding environmental friendly techniques is challenging. A recent study used reactive extrusion of commercially available poly(VDF-co-HFP) copolymer or grafted with maleic anhydride (MA) [poly(VDF-*co*-HFP)-*g*-MA] (Fig. 30) with functional sulfur-containing silanes in presence of a few percents (up to 5%) of poly(VDF-*co*-MAF) copolymers [205-206]. The process was first optimized on a bis screw Lab and then further scaled up on extruder (with 400 g batch). After extrusion, the rods were pressed into films by heated rolling mills. Then, the mercapto groups in the hybrid organic/inorganic membranes were oxidized to get sulfonic acid functions which favored the proton-conducting exchanges.

The effect of the addition of such compatibilizers depending of the concentration of functional groups on the final morphology and electrochemical properties was studied (Table 4). Their water uptakes (limited up to 15 wt%), IECs (ranging between 1.0 and 1.3 meq.g^{-1}) and conductivities (up to

78 mS.cm^{-1} at room temperature and 100% RH) when 5 wt% of poly(VDF-*co*-MAF) was involved in the reactive processing were observed. The conductivity reached 54 mS.cm^{-1} when poly(VDF-*co*-HFP)-*g*-MA-0.75 was used (Fig. 30) which is comparable to that of Nafion® NR112 (52 mS.cm^{-1} in similar conditions of temperature and RH) highlighting the crucial role of the interface and its impact on the accessibility to the sulfonic acid functions [205,206] of such hybrid membranes produced in a clean process.

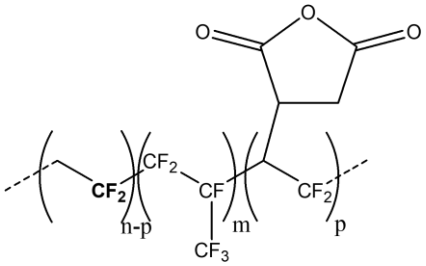

Fig. 30: Structure of the poly(VDF-*co*-HFP)-*g*-MA produced by grafting maleic anhydride (MA) onto poly(VDF-*co*-HFP) copolymer

Sample	poly(VDF-*co*-HFP)-*g*-MA-0.12	poly(VDF-*co*-HFP)-*g*-MA-0.22	poly(VDF-*co*-HFP)-*g*-MA-0.38	poly(VDF-*co*-HFP)-*g*-MA-0.62	poly(VDF-*co*-HFP)-*g*-MA-0.75
Thickness (µm)	65	75	95	90	98
Water uptake (%)	12.5	12.8	13.4	13.7	13.8
IEC Indirect dosing (meq/g)	0.80	0.90	1.02	1.10	1.20
IEC Elemental analysis (meq/g)[a]	0.90	1.00	1.01	1.12	1.25
Conductivity (mS/cm)	8	20	27	35	54

Table 4: Physical properties of poly(VDF-*co*-HFP)-*g*-MA/ SiO_2 composites depending of the MA concentration [205,206].

a) Ionic exchange capacity (IEC) from Sulfur elemental analysis

In addition, the combination of VDF co-polymers with ionic liquids (ILs) has been extensively explored for applications due to the tailorable and active properties of the polymer-IL composite

material. ILs, commonly defined as salts comprising cations and anions [289], display interesting characteristics such as high chemical and thermal stability, high ionic conductivity, low melting temperature, wide electrochemical potential window and negligible vapor pressure. Additionally, ILs present high ionic conductivity, flame retardancy and non-volatility and when they have a high ionic conductivity and flame retardancy, are attractive for electrochemistry applications, including fuel cell membranes.

ii) Solid Alkaline Fuel Cell membranes from poly(VDF-*co*-HFP) Copolymers

Solid Alkaline Fuel Cell (SAFC) is a promising device that does not require noble catalysts as for protonic ones [272-273]. However the membranes must be stable in hydroxides media so that VDF-containg copolymers are usually not stable in such a medium. However, a few articles have reported the crosslinkingby 1,4-diaminobutane of poly(VDF-*co*-HFP) copolymers bearing 1-chloromethyl amido moities (Scheme 57) to process alkaline exchange membranes [290]. However, these membranes were not compared to commercially available Tokuyama membranes and no information of the base sensitivity of such membranes in basic medium was supplied.

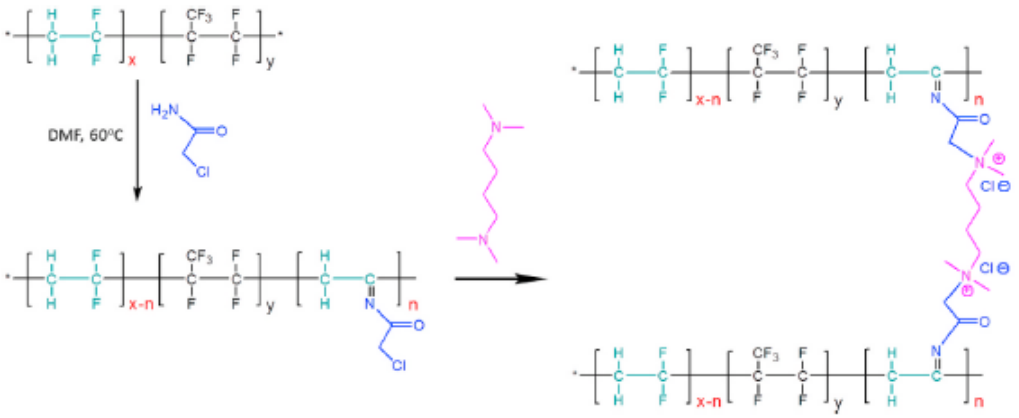

Scheme 57: preparation of crosslinked Alkaline Exchange Membranes based on quaternized poly(VDF-*co*-HFP) copolymer [290]. Copyright 2021. Reproduced with permission from Elsevier.

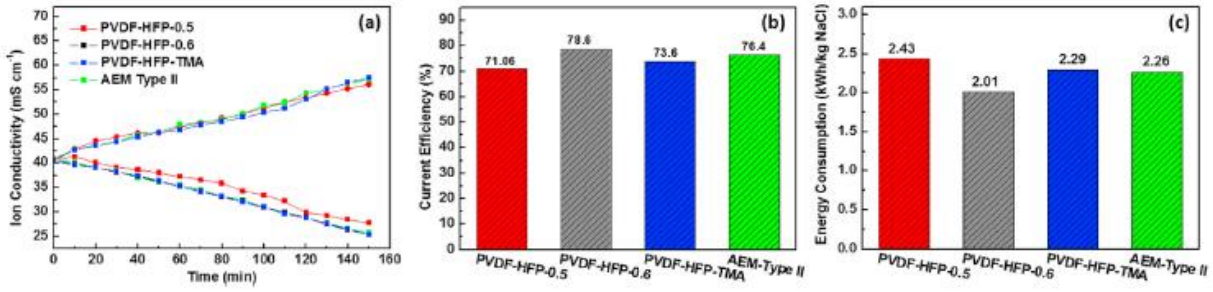

Fig. 31: The ion conductivities of NaCl solutions in various membraness (a), current efficiency (a) and energy consumption (b) of ED fabricated with poly (VDF-*co*-HFP)-X (X = 0.5 and 0.6) AEMs and Alkaline Exchange Membranes-Type II within 150 min. [290]. Copyright 2021. Reproduced with permission from Elsevier.

Other surveys report the copolymerization of dehydrofluorinated VDF-based copolymers with vinyl benzyl ammonium chloride or vinyl imidazole for SAFC membranes was also adopted by McHugh et al. [291]. The resulting membranes display ion-exchange capacity (IEC) and hydroxide conductivity values of 1.82 meq.g^{-1} and 48 mS.cm^{-1} compared to commercially available Fumapem® FAA-3-50 (2.02 meq.g^{-1} and 40-45 mS.cm^{-1}, respectively) [292].

However, the authors do not comment on the durablility of these membranes under hydroxide medium that is questionable since dehydrofluorination may occur on remaining VDF units.

In addition to such fuel cell membranes, a specific example deals with the use of sulphonated poly(VDF-*co*-HFP) copolymer / graphene oxide composite cation exchange for water splitting process for hydrogen production [293].

7.6.2. Electrolytes for Lithium Ion Batteries

Because of their chemical, electrochemical and thermal stabilities, another promising application of VDF-containing copolymers deals with lithium ion batteries (LIBs), especially specific components as binders (especially at the cathode), separators [4] and electrolytes [294]. Although LIBs are revolutionary in portable devices, new transportation means and grid sector, nowadays the graphite anode-based LIBs have reached their theoretical limit and cannot meet the increasing demand. Thus,

alternative battery designs with higher energy density are searched. Hence, lithium-metal batteries (LMBs) are quite promising: actually, replacing the graphite anode by lithium metal enables to enhance specific energy and energy density (~35% and ~50%, respectively). However, this generation of batteries still suffers from several issues, such as dendrite growth (leading to short circuit of the battery), corrosion of metallic Li, short lifetime and low columbic efficiency.[295-296] The dendrite outgrowth is mainly caused by the instability of the solid electrolyte interphase (SEI) on the lithium anode. A stable SEI limiting and preventing the dendrite formation can thus highly enhance the applicability of LMBs. In this regard, fluorinated SEIs are still encouraging candidates, allowing both the modulation of the deposition of Li (homogenously) and the increase in the safety of the batteries [297].

Poly(VDF-*co*-HFP) copolymer has been applied as separator membranes and gel polymer electrolytes (GPEs) where the larger amorphous content allows retaining higher liquid electrolytes amounts and, consequently, increasing ionic conduction and ionic diffusion [298]. Poly(VDF-*co*-HFP) GPEs have also been prepared using different fillers, such as, lithium nonafluorobutanesulfonate (LiNfO) and ionic liquid (IL) as 1-butyl-3-methylimidazolium nonafluorobutanesulfonate ([Bmim] [NfO]). The thermal stability of the different GPEs is significantly reduced compared to neat poly(VDF-*co*-HFP) and is affected by the different LiNfO/[Bmim][NfO] wt percentage within the polymer matrix indicating that the incorporation of the LiNfO/[Bmim] [NfO] leads to an increase of the segmental motion and flexibility of the poly(VDF-*co*-HFP) host polymer matrix and a reduction of the degree of crystallinity and the melting temperature [299].

Further with the same copolymer, Singh et al. [300] used 1-butyl-3-methylimidazolium bis(trifluoromethanesulfonyl)imide as IL, with and without the Li-salt (having $TFSI^-$ anion) [299]. The insertion of IL into the copolymer electrolyte (i.e. copolymer + 20 wt% LiTFSI) modified various physicochemical parameters (Tm, Tg, thermal stability, the crystallinity-rate, and ionic transport behavior) of such materials. The ionic conductivity of these GPE membranes increased with increased

IL concentration, reaching 2 x 10^{-3} S.cm^{-1} at 30 °C and 3 x 10^{-2} S.cm^{-1} at 130 °C (Fig. 32). GPE membrane containing higher IL loading (ca. 70 wt% of IL) exhibited high ionic transference number (higher than 0.99) and cationic transference number (ca. 0.22) over a wider electrochemical window.

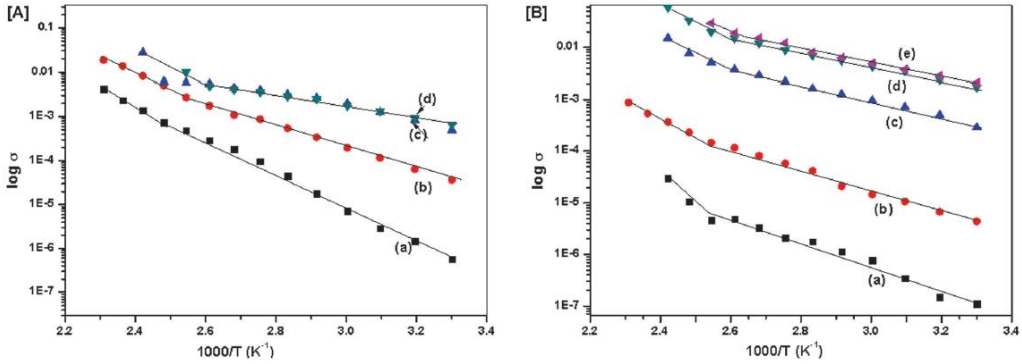

Fig. 32: (A) ionic conductivity of the polymer gel electrolyte membranes poly(VDF-*co*-HFP) copolymer + x wt% 1-butyl-3-methylimidazolium bis(trifluoromethanesulfonyl)imide (BMIMTFSI) vs composition and temperature. (a) x = 20, (b) x = 40, (c) x = 60 (d) x = 80 and (B) (poly(VDF-*co*-HFP) + 20% LiTFSI) + x wt% BMIMTFSI (a) x = 20, (b) x = 40, (c) x = 60 (d) x = 70 respectively.[299]. Copyright 2015. Reproduced with permission from RSC.

In addition, Suleman et al. [301] reported poly(VDF-*co*-HFP)/SN/[Emim][CF_3SO_3] composites (where Emim stands for 1-ethyl-3-methylimidazolum ionic liquid), with a decrease of the crystallization rates because of its major amorphous nature. Moreover, their melting temperature significantly increased up to 21% compared to that of the pristine fluorinated copolymer. This arises from the phase transition of the composite that occurred from the ordered phase to the disordered phase. In addition, because of the interactions between the nitrile group of SN and the poly(VDF-*co*-HFP) backbone [301] in such composites, the absorption band of the amorphous phase in the composite became considerably narrower in comparison to that of the amorphous phase of neat halogenated copolymer.

In addition, IL-containing well-designed triblock copolymers, synthesized by RAFT polymerization of imidazolium methacrylate in presence of a telechelic poly(VDF-*co*-HFP) copolymer as the macroCTA (Fig. 33) [302]. These original structures with pendant imidazolium cations led to matrix for liquid electrolytes, promoting the adsorption of electrolyte and lithium salt dissociation

[306]. These triblock copolymers were single-phase materials and the anionic counterion has notable impact on the thermal properties, ionic conductivity (reaching up to 0.5 $mS.cm^{-1}$) and segmental dynamics of the polymers.

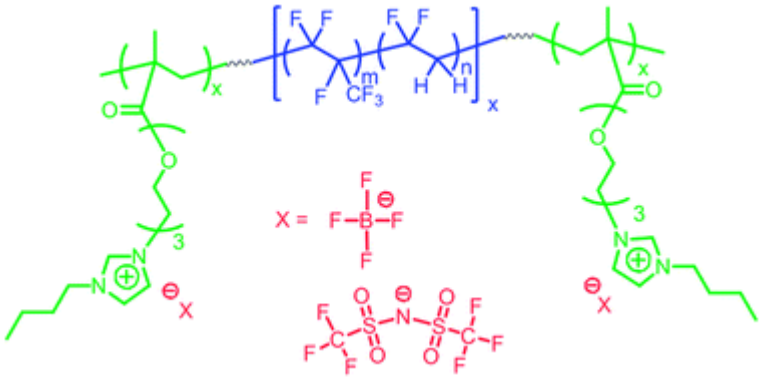

Fig. 33: structure of triblock copolymers from RAFT polymerization of imidazolium methacrylate with telechelic poly(VDF-*co*-HFP) copolymer as the macroCTA [302]. Copyright 2012. Reproduced from RSC.

Furthermore, poly(VDF-*co*-HFP) copolymer has also been used as a binder to prepare cells based on $Li(Ni_{0.5}Mn_{0.3}Co_{0.2})O$ (NMC) as the active material [4,303]. Compared to commercially available PVDF, this copolymer can efficiently reduce the peak temperature of preheated cells by up to 36 %, making it more suitable in fire safety applications [303].

Huang et al.[304] prepared novel cellulose acetate/poly(VDF-*co*-HFP) core/shell fibers through co-axial electrospinning. The fluorinated copolymer was chosen with a low crystallinity to favor better conducting properties for LIB separator application. In addition, $Li_{0.33}La_{0.557}TiO_3$ was added into the FP solution to yield a filled shell (Fig. 34:4). Excellent thermal stability, satisfactory electro-chemical performance, improved electrolyte wettability, and acceptable mechanical properties were obtained. Furthermore, the electrospun membrane had lower interfacial resistance and higher ionic conductivity than commercially available Celgard® 2300 separator.

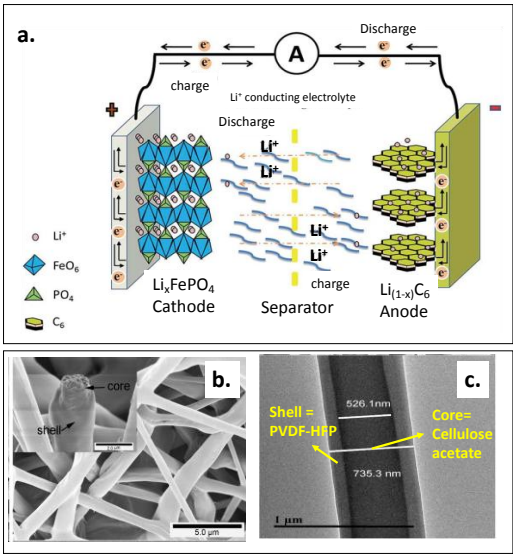

Fig. 34: a. Sketch of a Lithium-ion battery.[305] b. SEM and c. TEM images of co-axial cellulose acetate/Poly(VDF-*co*-HFP) core-shell nanofiber separators for LIBs.[304]. Copyright 2015, Reproduced with permission from the American Chemical Society.

Wang et al. [306] improved the mechanical properties of poly(VDF-*co*-CTFE) copolymer membranes by electrospinning involving Sb_2O_3 nanoparticles. In addition to the enhanced ionic conductivity, the composite electrospun membranes displayed lower interfacial resistance and valuable electrochemical stability compared to those of conventional PE separators. They also showed good flame retardancy properties and excellent thermal stability and resistance to shrinkage.

Besides poly(VDF-*co*-M) copolymers (M = HFP or CTFE) mentioned above, poly(VDF-*co*-VDMP) cooligomers are valuable materials which, mixed with LiTFSI, are regarded as interesting SPEs [64]. While the conductivity reached up to 1.9×10^{-2} mS cm^{-1} at 20 °C and 0.2 mS.cm^{-1} at 60 °C, their electrochemical stability window, evaluated by linear sweep at a scan rate of 1 mV/s (Fig. 35) were electrochemically stable in a wide range of potentials varying between 2.9 V and 4.7 V vs Li/Li^+. The degradation was noted above 5.0 V assigned to possible oxidation corrosion of stainless steel working electrode.

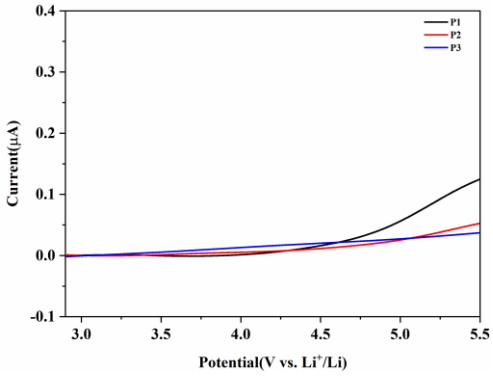

Fig. 35: Linear sweep voltammetry performed on the SPEs prepared from P1 (90 mol% VDF), P2 (70 mol% VDF), and P3 (ca. 50 mol% VDF) poly(VDF-co-vinyldimethoxyphosphonate-VDPM) with VDMP/Li^+ 2:1 molar ratio at scan rate of 1 mV/s [64]. Copyright 2020, Reproduced with permission from Wiley.

Scheme 14 reports the synthesis of novel 2-trifluoromethacrylate bearing specific function. To ensure some Li conductivity, triethylene glycol 2-trifluoromethyl acrylate (MAFTEG) was prepared and then copolymerized with VDF enabling the resulting PVDF-*g*-$(EO)_3$ copolymers to be blended with 1-propyl-1-methyl pyrrolidinium bis(fluorosulfonyl)imide (PyrFSI) in lithium bis(trifluoromethanesulfonyl)imide (LiTFSI) (Li/Pyr 1:9 mol ratio) [74]. This process led to several gel polymer electrolytes (GPEs) which displayed competing ionic conductivities above 0.2 $mS.cm^{-1}$ at room temperature and close to those of pyrrolidinium RTIL in its liquid form (1-2 $mS.cm^{-1}$). Additionnally, these ionic conductivities increased with silica nanoparticles amount up to 5 $mS.cm^{-1}$ at 20 wt% before decreasing (Fig. 36) [74].

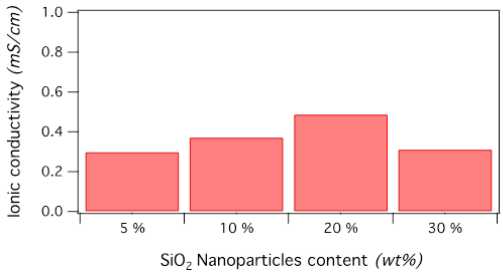

Fig. 36: Ionic conductivities of poly(VDF-*co*-MAFTEG) copolymer (9 mol% MAFTEG) as gel polymer electrolytes for different contents of silica nanoparticles [74]. Copyright 2015. Reproduced with permission from RSC.

The GPE appears to be electrochemically stable in a wide range of potentials varying from 1.5 V to 4 V vs. Li^+/Li (Fig. 37) making such GPE suitable with 4 V class Li-batteries [74]. Anodic peaks

are observed at 4 and 5 V. The first peak is attributed to the oxidation of MAFTEG groups at the interface with the electrodes while the second one at 5 V is thought to be due to the decomposition of FSI/TFSI anions.

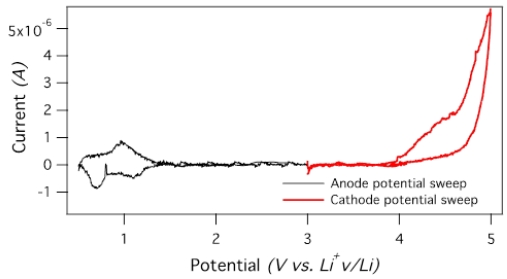

Fig. 37: Cyclic voltammetry response of the poly(VDF-*co*-MAFTEG) copolymer (9 mol% MAFTEG) as gel polymer electrolyte containing 20 wt% of SiO_2 nanoparticles [74]. Copyright 2015. Reproduced with permission from RSC.

More rencently, copolymers of VDF with perfluoro -2-methyl-3-oxa-5-sulfonimido[-3-oxa-5-sulfonyl fluoride] vinyl ether (VEPFSIS) bearing both sulfonimide and Lithium sulfonate (reaching molar masses up to 128 kg mol^{-1}) [307] were cast into self-standing membranes and then swollen by a 50/50 v/v ethylene carbonate/propylene carbonate mixture (Scheme 57). They led to single-ion polymer electrolytes with satisfactory conductivity (up to 10^{-4} S cm^{-1} at 30 °C), high Li^+ transport number (ca. 1), excellent interfacial stability *vs.* Lithium SIPE, electrochemical stability up to 4.3 V *vs.* Li^+/Li and and used as both electrolyte and cathode binder for high voltage Lithium metal polymer batteries (LMP) demonstrating promising cell performance with an excellent reversibility upon continuous lithium plating/striping cycles [307].

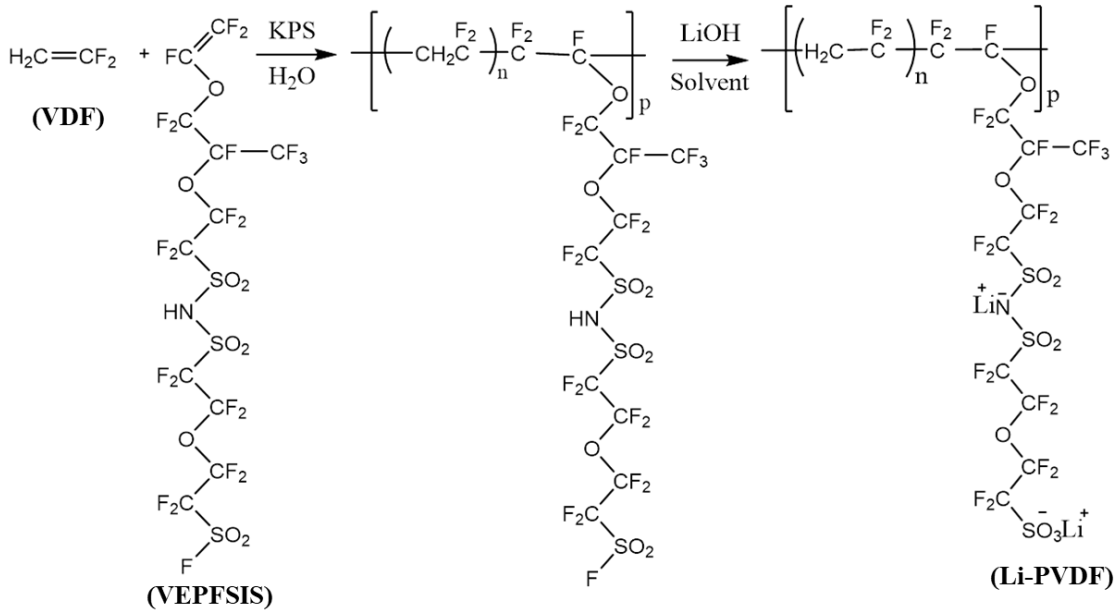

Scheme 58: Radical copolymerization of VDF and perfluoro -2-methyl-3-oxa-5-sulfonimido[-3-oxa-5-sulfonyl fluoride] vinyl ether (VEPFSIS) and modification of SO_2F into SO_3Li with the formation of single-ion conducting copolymer, Li-PVDF [307].

Finally, in contrast to their extensive use as electroactive copolymers (section 7.6.3), poly(VDF-*co*-TrFE) copolymers have also been invoved as GPE [308] or separator [309].

7.6.3. Electroactive Polymers (EAPs): Piezoelectric/Ferroelectric/Dielectric Devices and Actuators

i) Introduction

PVDF displays five polymorphs, namely α, β, γ, δ and ε for which the β crystalline phase is electroactive and regarded as the most intriguing conformation in which the molecules are in an *all-trans* chain conformation and are packed in an orthorhombic unit cell [11-13]. The β crystal phase of PVDF forms a planar zigzag positioning the Fluorine atoms one one side and the Hydrogen ones on the other side. Films based on PVDF are too rigid with low air permeability, and their application are limited for flexible tactile force sensors. Furthermore, these films also request an electrical, mechanical or thermal treatment [12] for improving the *β*-phase content [310]. Molar masses (M_ns) of PVDF have

also a key influence in such polymorphs: the β phase percentage increases from 90 to 96 % when M_n evolves from 180 to 700 kg.mol^{-1} [311-312]. As a matter of fact, VDF-containing copolymers, mainly poly(VDF-*co*-TrFE) copolymers exhibit very good electroactive (piezo-, pyro, and ferroelectric) properties, accompanied by high deformability and chemical resistance, especially in corrosive and harsh environment. They are promising materials in transducers, sensors, actuators [312-315], organic electronics [316], field-effect transistors, haptics, in biomedical devices [317], organic ferroelectric synapses in advanced neuromorphic systems [318] and energy harvesting and storage [319-320] (Fig. 38).

Generally, tactile sensors based on the sensing mechanisms are classified in several groups such as piezoelectric, piezoresistive, triboelectric, capacitive, and optical sensors [315,321]. Poly(VDF-*co*-TrFE) is considered to be the most studied and used electroactive VDF-copolymer, existing sponteously in β-crystal phase and with a high crystallinity for a TrFE mol% of 20-50 from melt or by solvent casting without any need of stretching [322-323]. Actually, the bulky TrFE induces an increase of the interchain distances.

Indeed, in contrast to PVDF sensors which exhibit poor thermal interference, poly(VDF-*co*-TrFE) materials are regarded as satisfactory functional materials for flexible tactile sensors, thanks to their higher *β*-phase content, better stability and sensitivity and lower detection limit [313,322].

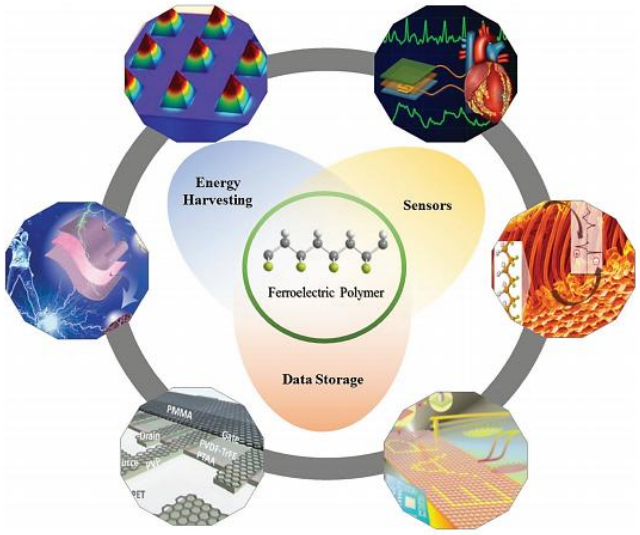

Fig. 38: Applications of ferroelectric polymer in flexible electronics, including data storage, energy harvesting, and sensors [319]. Copyright 2017. Reproduced with permission from Wiley.

ii) Electroactive poly(VDF-*co*-TrFE) copolymers

Table 5 exhibits relevant characteristics of poly(VDF-*co*-TrFE) films [324]. The presence of TrFE units in the copolymer can be viewed as defects, and in all cases, when the defect concentration increased, the ferroelectric β phase became less stable with respect to the paraelectric phase [322]. Recently, Zhu's team [325] reported the important role of the amorphous zone in such a copolymer to enhance the piezoelectric properties.

P(VDF-*co*-TrFE)	T_c [a] (°C)	T_m [b] (°C)	Crystallinity (%)		d_{33}	C_{11}
			DSC	DRX	(μC/cm^2)	(GPa)
Spin coating [c]	106	150	30	43	26	11-12
Solvent casting [d]	101	150	30	43	26	11-12

Table 5: DSC and XRD parameters of the first heating, piezoelectric coefficient (d_{33}) and elastic constant (C_{11}) of poly(VDF-*co*-TrFE) films (VDF/TrFE mol. content: 70/30). Copyright 2014. Adapted with permission from [324].

[a] Curie temperature, [b] melting temperature, [c] Thickness: 3-15 μm, [d] Thickness: 15-300 μm

In addition, enhancing electroactive features could be achieved by inserting nanofillers. For example, Hadji *et al*. [326] dispersed alumina nanoparticles (Al_2O_3) in poly(VDF-*co*-TrFE) copolymer matrix, and the resulting nanocomposites exhibited high piezoelectric coefficients after polarization under high electric field without any stretching. Piezoelectric measurements indicate that the resulting film could be filled by up to 10 wt % of alumina while they retained high piezoelectric properties and increased their elastic constant (C_{11}) by more than 20% (Fig. 39).

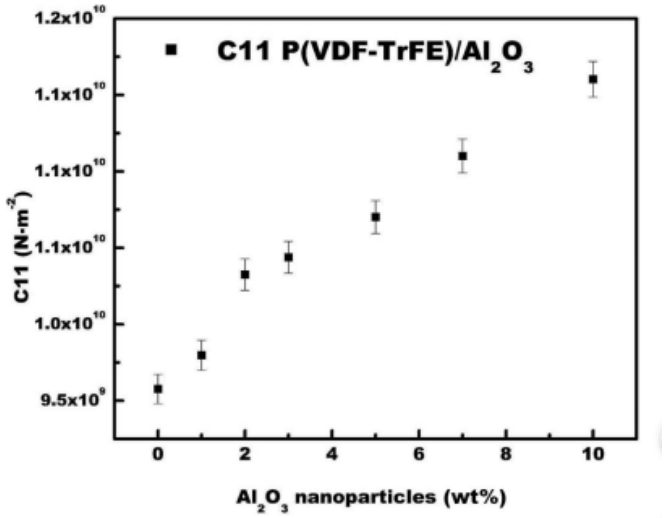

Fig. 39: Variation of elastic constant (C_{11}) *versus* alumina concentration in poly(VDF-*co*-TrFE)/Al_2O_3 composites [326]. Copyright 2012. Reproduced with permission from IEEE.

Thevenot et al. [327] processed flexible ferroelectric films made of poly(VDF-*co*-TrFE) copolymer softened by diethyl phthalate (DEP) as a plasticizer and studied their morphology, piezoelectric, mechanical, thermal, and crystalline properties. The authors reported that the elastic constant was reduced up to 30% while increasing the remanent polarization and the piezoelectric coefficient (Fig. 40) thanks to the lubricant property of DEP, helping the orientation of the crystallites. Furthermore, they noted a decrease of the coercive field from 46 to 32 $V.\mu m^{-1}$ after annealing at 138 °C for a DEP amount ranging from 20 to 50 wt%. Interestingly, a sensor was produced and electrically tested, evidencing that the softening of the copolymer induced a greater amplitude range of deformations of the device. The combination of the flexibility with high ferroelectric properties of such a plasticized VDF copolymer made a promising material for biomedical sensor applications.

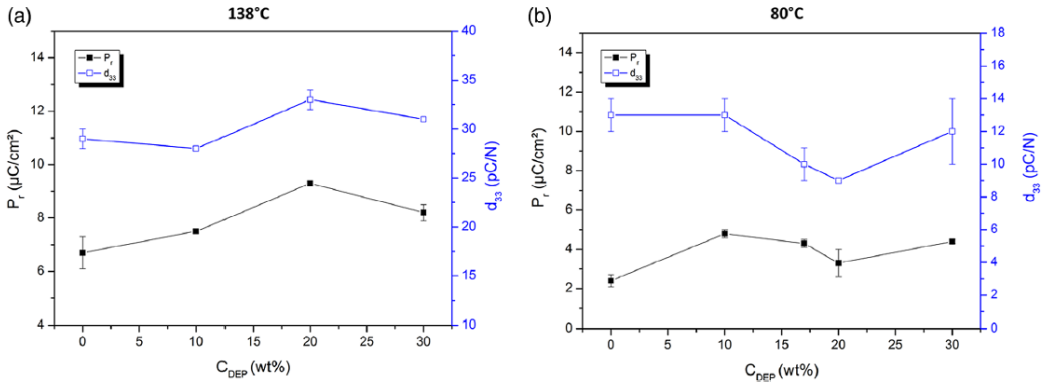

Fig. 40: Variation of the piezoelectric coefficient (d_{33}) and the remanent polarization Pr of poly(VDF-*co*-TrFE)/ diethyl phthalate (DEP) films *versus* DEP concentration for the annealing at (a) 138 and (b) 80 °C. The error bars are the standard deviation from the average of at least three measurements [327]. Copyright 2021. Reproduced with permission from Wiley.

On the other hand, electrospun VDF-based copolymers have featured some flexibility, high *β*-phase content and are highly porous (breathable). Therefore, in form of ultrathin fibrous membranes, they can be used as functional layers for dynamic tactile membranes. Their properties can further be enhanced by aligned fibers orientation and addition of nanofillers.[321] A flexible pressure sensor involving poly(VDF-*co*-TrFE) electrospun mat, with the fluorinated nanofibers wrapped by reduced graphene oxide (rGO) sheath, was sandwiched between two PDMS thin films (

Fig. 41) [328] proposed as an e-skin and a wearable diagnostic device for real-time health monitoring. Indeed, sensor application in cardiovascular disease diagnosis or speech recognition was evaluated by monitoring the blood pressure, engaged muscle traction and movement. The results evidenced valuable characteristics as a very fast response time (5 ms), ultrahigh sensitivity (15.6 kPa^{-1}) with low detection limit (1.2 Pa), low operating voltage (1.0 V), high stability and durability (over 100,000 cycles) [328].

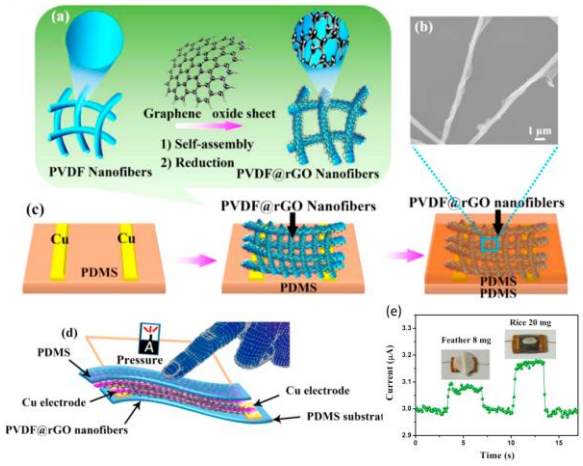

Fig. 41: Wearable sensor made of poly(VDF-*co*-TrFE) nanofibers. a. Sketch of the mechanism for the formation of PVDF fibers coated by reduced graphene oxide (rGO) nanosheets, followed by electrostatic interaction; b. Field emission scanning electron microscopy (FESEM) image of the rGO nanosheets coated poly(VDF-*co*-TrFE) fibers; c. schematic illustration of the fabrication of a flexible pressure sensor; d. schematic of a typical pressure sensor; e. transient response to the loading and removal of a feather (8 mg) and a rice (20 mg), the fronted corresponding to a pressure of only1.2 Pa. [328]. Copyright 2016, Reproduced with permission from Elsevier.

In addition, Loos' team [329] designed original P2VP-*b*-poly(VDF-*co*-TrFE)-*b*-P2VP triblock copolymer from the Huisgen CuAAc click-coupling between poly(vinyl pyridine) (P2VP, produced by RAFT of 2-vinyl pyridine) with alkyne end-groups and telechelic bis(azido) poly(VDF-*co*-TrFE) (Scheme 59). These authors also studied their phase separation that did not induce any drastic changes in the shape of the displacement-electric (D–E) loops. Changing P2VP by PSt of the same molar mass induced different switching characteristics significantly. Indeed, D–E loops became narrower, with a tendency toward a linear dielectric contribution, with almost zero remnant polarization while the maximum polarization lower than that of P2VP-*b*-poly(VDF-*co*-TrFE) 70:30.

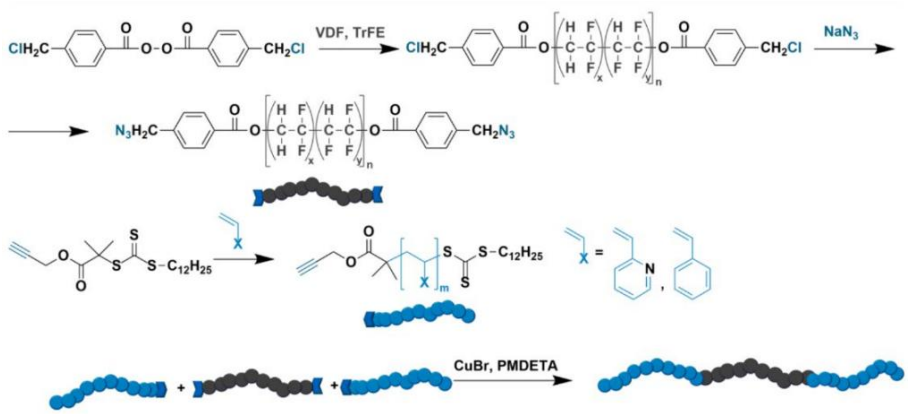

Scheme 59: Sketch of synthesis of poly(M)-*b*-poly(VDF-*co*-TrFE)-*b*-poly(M) triblock copolymers (where M stands for styrene or 2-vinylpyridine) by CuAAc click-coupling of telechelic bis(azido) poly(VDF-*co*-TrFE) and P2VP or PSt (with an alkyne end-group) obtained by RAFT polymerization of VP or styrene.[329], Copyright 2019. Reproduced with permission from Nature Publishing House.

Three non-exhaustive studies from less used electroactive VDF-containing copolymers are suggested below.

First, a structurally ferroelectric poly(VDF-*co*-HFP) copolymer at low HFP content and hence lower crystallinity compared to that of PVDF, led to materials with a polarization of 0.08 $C.m^{-2}$ (for 5mol% HFP) [322].

In addition, poly(VDF-*co*-HFP) blended with different [Emim][NTf2] IL contents [where NTf2 represents bis(trifluoromethane)sulfonamide] providing composites with novel electroactive properties for possible actuators [330]. Both the crystallinity-rate and the mechanical properties (tensile stress and Young's modulus) of the blends decreased because of the strong interaction of the IL with the polar units inducing a plasticizing behavior of the blends. In addition, the thermal properties, such as the melting temperature of the blends, decreased owing to the plasticization effect of the IL and its complexation with the poly(VDF-*co*-HFP) backbone. On the other hand, the chemical properties, as the characteristic absorption bands of the β-phase content of the blends increased, which was due to the nucleation of β-phase through the electrostatic interactions between the imidazolium cations of the IL and the negatively polarized CF_2 groups of poly(VDF-*co*-HFP) [330]. Hence, the authors deduced that

such a fluoropolymer/[Emim][NTf2] blend granted low tensile stress and Young's modulus blends, as well as low melting temperature. Third, because of the large dipole moment of 1234yf monomer (2.4 D), both strong spontaneous polarization and dielectric responses were observed in highly-crystalline poly(VDF-*co*-1234yf) copolymers, as approached by Asandei et al. [331]. The results were obtained from the combination of density-functional theory (DFT) and modern theory of polarization calculations of the polar properties for such a copolymer crystal models, with contributions to the total polarization from individual fluorinated comonomer units and polymer chains.

iii) Electroactive poly(VDF-*ter*-TrFE-*ter*-M) terpolymers

Many poly(VDF-*ter*-TrFE-*ter*-M) terpolymers have been synthesized by direct terpolymerization of the three monomers in order to tackle how M termonomer may induce some features in the morphology (crystallization and crystal lattice) and favor an orientation of the dipoles (Fig. 42) for better electroactive properties of the resulting films. In addition to the Van der Waals radii of the atoms, the dipole moment of the termonomer units is also considered to understand the final electroactive properties. CTFE (that has a weaker dipole moment, 0.64 D) compared to that of 1-chloro-1-fluoroethylene (CFE, 1.8 D) [332,333] led to most innovating investigations. This difference induces various electroactive properties because it also leads to differences in the pinning force and in the response of the terpolymer to an electric field.

CTFE meets both essential criteria to well copolymerize with VDF and to introduce defects (Fig. 42) within the crystal that promotes relaxor ferroelectric (RFE) properties. The RFE behavior of polymers is thought to be caused by the formation of FE nano-domains and by the pinning of mobile dipoles of the poly(VDF-*co*-TrFE) segments in *all-trans* conformation [322,333]. The formation of nano-domains arises from the bulky chlorine atom that introduces in the terpolymer chain a gauche type linkage which acts as a kink and limits the growth of large FE domains as in the case of poly(VDF-*ter*-TrFE-*ter*-CTFE) terpolymers (Fig. 42). Thus, the formation of γ crystalline phase with $tttg^{+}tttg^{-}$ conformation shifts the Ferro to Paraelectric transition (also called the Curie transition) near ambient temperature. In

the operating conditions of devices, this characteristic is important for the electroactive response of the RFE terpolymer as the dielectric constant is at its maximum at T_C.

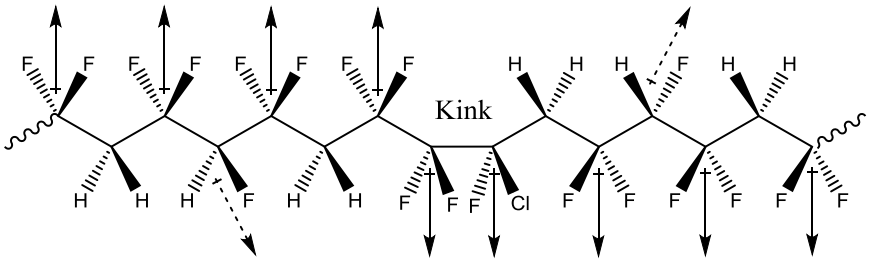

Fi 42: Kink inserted from a CTFE unit along the poly(VDF-*co*-TrFE) backbone in poly(VDF-*ter*-TrFE-*ter*-CTFE) terpolymer. Arrows indicate the dipole moments of carbon atoms bearing electro-attractive atoms. Dashed-line arrows and solid line arrows indicate weak dipoles and stronger dipoles, respectively.

Chung's team [91-92] pioneered the synthesis of poly(VDF-*ter*-TrFE-*ter*-CTFE) terpolymers, designing these materials with a small CTFE content and noting that its incorporation induced a significant decrease of the melting and Curie transition temperatures while the crystallinity-rate remained high. Nowadays, such terpolymers are commercially available from aqueous process of terpolymerization achieved with appropriate initiators [11].

Another strategy reported by Zhang *et al*. [11,335] aimed at obtaining such above terpolymers without handling hazardous TrFE gas, in two steps (Scheme 60): first, a radical copolymerization of VDF with CTFE followed by the reduction of the chlorine atoms in poly(VDF-*co*-CTFE) copolymers to partially modify CTFE units into TrFE ones. These authors studied the influence of the TrFE amount on the dielectric constant at 1 kHz (where ε=57 at 90 °C) and noted that when the TrFE content decreased, the dielectric constant peak shifted from about 40 °C to 100 °C, while the peak shape evolved from a broad flat to a narrow peak at about 90 °C, then broadened.

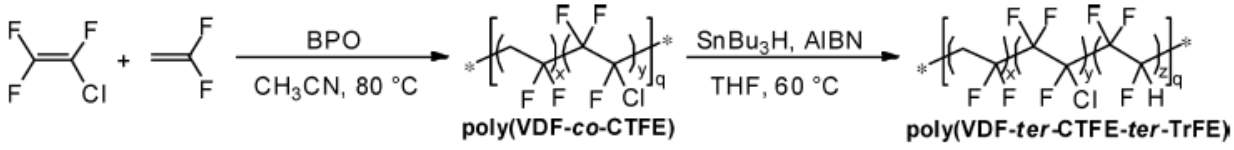

Scheme 60: Preparation of poly(CTFE-*ter*-TrFE-*ter*-VDF) terpolymers by radical copolymerization of VDF and CTFE, followed by partial reduction of chlorine atoms in CTFE units [334-335].

Actually, hydrogenation process of poly(VDF-*co*-TrFE) copolymers involved an environmentally friendly and controllable hydrogenation procedure of poly(VDF-*co*-CTFE) (via atom transfer chain transfer [335] to avoid using hazardous tributyltin hydride and tributyltin chloride. Various poly(CTFE-*ter*-TrFE-*ter*-VDF) terpolymers of different compositions synthesized from both above routes are gathered in a ternary diagram (Fig. 43) [11].

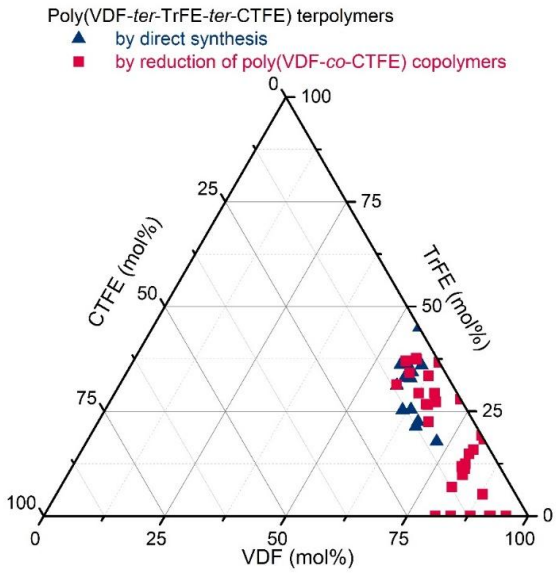

Fig. 43: VDF/TrFE/CTFE ternary composition diagram in mol % for poly(VDF-*ter*-TrFE-*ter*-CTFE) terpolymers. Blue triangles correspond to terpolymers produced by direct radical terpolymerization while the red squares designate terpolymers obtained by reduction of the chlorine atoms in poly(VDF-*co*-CTFE) copolymers [11]. Copyright 2017. Reproduced with permission from Elsevier.

In addition, Bargain et al. [336] reported that, depending on the CTFE content (from 0 to 10 mol %), poly(VDF-*ter*-TrFE-*ter*-CTFE) terpolymers exhibit ferroelectric (FE) or RFE properties at low temperature whereas they all present a paraelectric (PE) behavior at high temperature. The thermal evolution of their electroactive properties is related to reversible crystal-crystal transitions. By studying these structural transitions for three different terpolymers composed of various CTFE contents (0, 4.4 and 9.7 mol %), using simultaneous SAXS-WAXS experiments along thermal cycles, the same group [336] highlighted two types of crystalline phases at low temperature with their proper crystal-crystal

transition: the first one contained all-trans conformations (orthorhombic FE phase) with a discontinuous transition towards the hexagonal PE phase whereas the second one incorporated gauche disordered conformations (orthorhombic defective ferroelectric (DFE) or RFE) transits continuously towards the same hexagonal PE phase. In the film containing 4.4 mol % CTFE, these authors noted a coexistence of both these simultaneous phase transitions, one discontinuous (FE to PE) and one continuous (RFE to PE), while the continuous one only existed in the higher CTFE amount. RFE properties were precisely observed in the temperature range of the structural RFE to PE transition [0 °C, 40 °C]. By coupling electric displacement−electric field (D−E) loop measurements, thermo-mechanical experiments (DSC and DMA) and dielectric spectroscopy, these authors suggested a model to explain this RFE-PE continuous crystal-crystal transition in these terpolymers.

The appearance of these RFE properties arised from a disorder in the all-trans sequences and in the dipoles organization along the chains, thus to a modification in the crystalline state [337].

Poly(VDF-*ter*-TrFE-*ter*-M) terpolymers (where M stands for CFE or CTFE) display RFE properties with the most studied compositions corresponding to CFE or CTFE contents close to 8 mol% [337,338]. Subtle CFE or CTFE incorporation within the FE crystals, from the introduction of conformational disorder [337,339], led to RFE properties *via* the pinning effect [338]. Whereas other termonomers, as 3,3,3-trifluoropropene [120] or trans-1,3,3,3-tetrafluoropropene [340], expelled out of the FE crystals, decreased the crystal ratio and degraded the ferroelectric properties. At room temperature, the RFE crystal structure is orthorhombic with inter-chain distances higher than in the FE crystals and with the absence of intra-chain order [336,338]. Using in-situ SAXS-WAXS experiments, recent work proved the existence of a structural transition from the orthorhombic RFE phase to the high temperature hexagonal PE phase [336]. This structural transition is a continuous crystal-crystal transition, covering a wide temperature range from 20 to 50 °C, also highlighted by a broad maximum of dielectric constant in the same temperature range. As with the T_C, the physical transition from RFE

to PE state was related to a structural transition, evidencing the strong impact of crystal structure on macroscopic properties.

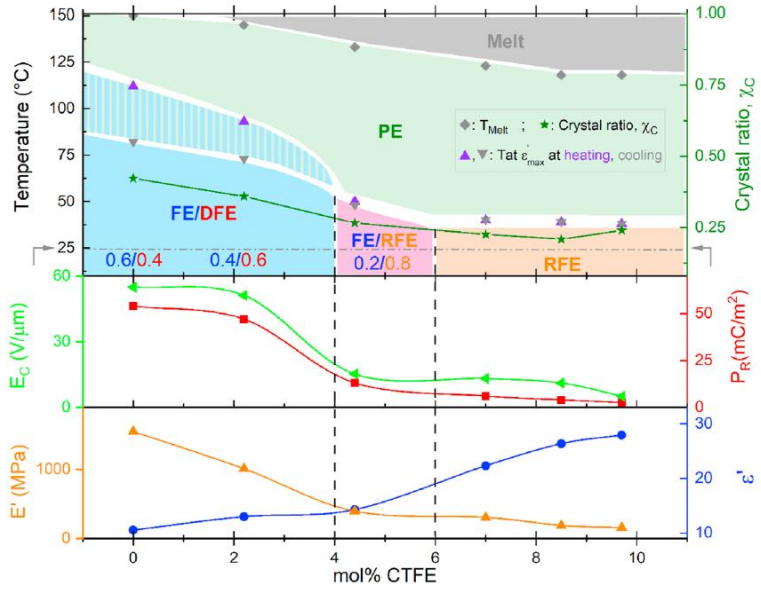

Fig. 44: Temperature *versus* mol% CTFE phase diagram of annealed poly(VDF-*ter*-TrFE-*ter*-CTFE) terpolymers. In the upper part, the phase diagram is deduced from experiments presented in ref. [336-337]. In the lower part, the crystallinity (χ_C) (green star, top figure), the coercive field EC,(green triangle), the remnant polarization PR (red square, middle figure), the storage modulus E' (at 1 Hz) (orange triangle, bottom figure), and the dielectric constant ε′ (at 1 kHz), (blue circle), are measured at 25 ◦C for the various CTFE amounts.[337]. Copyright 2021. Reproduced with permission from Elsevier.

An actuator device reported by Capsal's team contained bis(2-ethylhexyl) phthalate (DEHP) plasticizer [341], which is not certificated as biocompatible for surgical procedures. To meet the stringent medical requirements, diisononyl phthalate (DINP) plasticizer (10%) was chosen instead of the above one because of its biocompatibility, safety for the patients and of its exceptional ability to signifcantly enhance the electromechanical performances of the poly(VDF-*ter*-TrFE-*ter*-CFE) terpolymers (62.2/29.4/8.4 mol.%, respectively) in low-cost fexible guidewire tip for endovascular surgery [342]. The authors found the best compromise required to ensure enough radiation for microbial deactivation (and thus to minimize the bacterial, fungal, or viral disease transmission) and maintain the suitable properties of the materials. Actually, electromechanical performances and

thermal/dielectric properties of β-irradiated terpolymer-based sterilization treatment did not cause any signifcant risk to the neat/plasticized terpolymers, confirming the reliability of such electrostrictive materials for medical device development [342].

Polymer	S_M (%)	Y (GPa)	$YS_M^2/2$ (J/cm^3)	k_{33}
Piezo Poly(VDF-*co*-TrFE)	0.2	3.3	0.01	0.27
High-Energy Electron Irradiated P(VDF-*co*-TrFE)	-5.0	0.4	0.50	0.30
Poly(VDF-ter-TrFE-ter-CTFE)	-4.0	0.4	0.32	0.28
Poly(VDF-ter-TrFE-ter-CFE)	-4.5	1.1	1.10	0.55

Table 6: Comparison of the electromechanical properties of poly(VDF-*co*-TrFE) co- and terpolymers. Reproduced with permission of [344].

* S_M, Y, $YS_M^2/2$, and k_{33} stand for the maximum strain observed in the material, the Young's modulus, the elastic energy density (a parameter normally used to compare different electroactive materials) and the thickness electromechanical coupling factor, respectively. For electrostrictive polymers, the value of k_{33} presented here is the value at high field (where CFE stands for 1-chloro-1-fluoroethylene)[344].

Indeed, poly(VDF-*ter*-TrFE-*ter*-CFE) terpolymers have the highest room temperature permittivity value (ca. 50 at 1 kHz) [342] or even 60 at room temperature [344] for VDF/TrFE/CFE composition of 59.5/36.5/4.0 mol%. Moreover, the resulting terpolymers led to better electromechanical performances such as electromechanical coupling factor (0.55) and elastic energy density (1.1 J/cm^3) [343] than those of poly(VDF-*co*-TrFE) copolymer (Table 6).

Zhang *et al.* [345] reported PVDF/poly(VDF-*ter*-TrFE-*ter*-CFE) terpolymer blends and compared to those of neat polymers, displaying much higher dielectric constants and electric displacement at high electric fields. At 100 Hz, the terpolymer had a dielectric constant (53) higher than that of PVDF (12), while that of the polymer blend increased with a higher terpolymer content, reaching 56 for a terpolymer/PVDF composition of 90/10 vol% (Fig. 45-a). Furthermore, the dielectric

breakdown strength of the blends was also enhanced, yielding a high energy density (19.6 J/cm^3) for blends made of 40/60 vol% (Fig. 45-b).

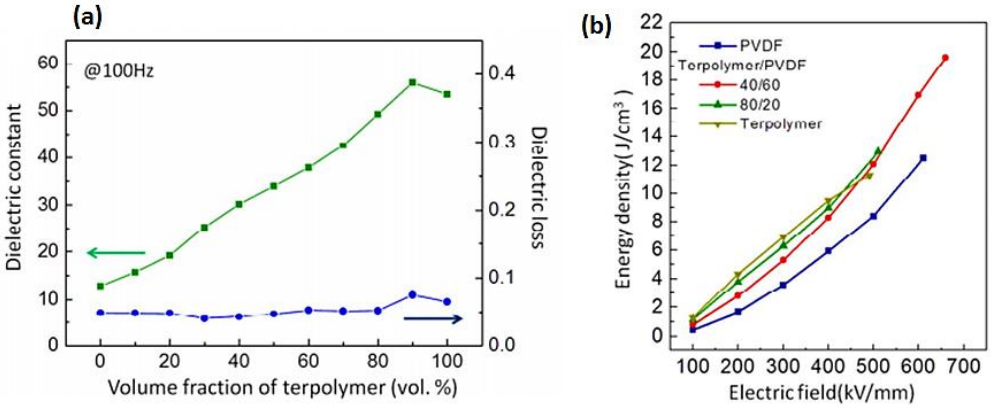

Fig. 45: (a) Variations of dielectric constant (green square) and dielectric loss (blue circle) *versus* the terpolymer volume fraction in the blends, and (b) Maximum discharged energy density of neat PVDF, poly(VDF-*ter*-TrFE-*ter*-CFE) terpolymer and blends (composition of 40/60 vol% and 80/20 vol. % for terpolymer/PVDF) vs. the electric field.[345] Copyright 2016. Reproduced with permission from the American Chemical Society.

A similar procedure was reported by Mao et al. [346] to increase the breakdown strength and enhance the energy storage properties of poly(VDF-*ter*-TrFE-*ter*-CFE) terpolymer. To overcome these limitations, these authors blended such a terpolymer with PVDF by casting at high temperature followed by quenching the film (Fig. 46). These polymer blends filled with 20 wt % of terpolymer exhibited high discharge energy density (13.63 J/cm^3) at an enhanced breakdown strength of 480 MV/cm, making them novel candidates for energy storage applications.

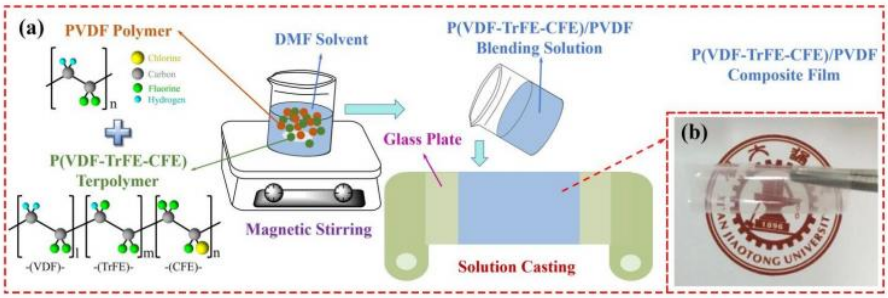

Fig. 46: Schematic illustration of (a) the fabrication process for the poly(VDF-*ter*-TrFE-*ter*-CFE) / PVDF polymer films and (b) photograph of such films blended with 20 wt % poly(VDF-*ter*-TrFE-*ter*-CFE) terpolymer [346]. Copyright 2020. Reproduced with permission from RSC.

Another series of EA poly(VDF-*ter*-TrFE-*ter*-M) terpolymers, where M stands for 3,3,3-trifluoropropene (TFP) [120], *trans*-1,3,3,3-tetrafluoropropene (1234ze) [134,340], 2,3,3,3-tetrafluoropropene (1234yf) [133], HFP [347] and MAF [119] was synthesized by radical terpolymerization and the resulting cast films exhibited ferroelectric properties. These terpolymers contained a VDF/TrFE molar ratio of 65/35 while M was introduced using different compositions, ranging from 0 to 10 mol%. Incorporated M units were mostly located in the amorphous phase of the terpolymer, hence increasing the T_g in the resulting terpolymers. Despite the differences in their microstructures, poly(VDF-*ter*-TrFP-*ter*-1234ze) terpolymers were rather homogeneous in composition in contrast to poly(VDF-*ter*-TrFE-*ter*-TFP) ones linked to the relative reactivities (low for 1234ze and high for TFP and 1234yf, Table 1) about those of VDF and TrFE. However, both these terpolymers shared identical electroactive properties (Fig. 47). For instance, both terpolymers exhibited comparably a high electric field E_c (50-60 MV under 150 MV.m^{-1}), close to the E_c of the reference ferroelectric material [*i.e.*, poly(VDF_{65}-*co*-$TrFE_{35}$) copolymer] [340].

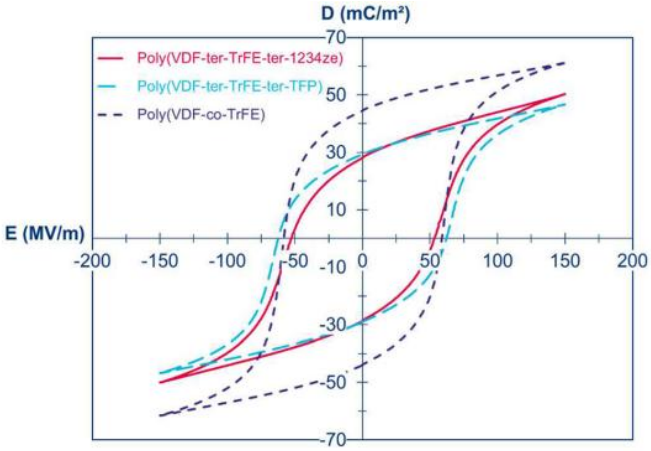

Fig. 47: Comparison of continuous bipolar D−E loops for annealed poly(VDF_{65}-co-$TrFE_{35}$) reference copolymer (purple dashed line), poly(VDF_{67}-*ter*-$TrFE_{28}$-*ter*-TFP_5) (blue dashed line), and poly(VDF_{69}-*ter*-$TrFE_{25}$-*ter*-$1234ze_6$) (red full line), all synthesized under same solution copolymerization

conditions. [134,340]. 2017. Copyright. Reproduced with permission from the American Chemical Society.

As a matter of fact, from a boran/oxygen initiator at room temperature, Chung's team [89,90] produced novel poly(VDF-*ter*-CTFE-*ter*-F_2C=CF-R-Si$(OR)_2CH_3$) terpolymers (Scheme 26) obtained in solution or in bulk at ambient temperature, in reasonable yield and the targeted alkoxy silane function was chosen to favor a strong adhesion of this material onto glass.

MAF was also chosen as functional termonomer, since thanks its carboxylic acid group, the resulting poly(VDF-*ter*-TrFE-*ter*-MAF) terpolymers containing 1 mol% MAF only, well-adhered onto gold and steel electrodes [119]. The coated electrodes were polarized at 200 $MV.m^{-1}$ up to 5 times and no delamination or loss of ferroelectric properties were noted.

Zhu's [348] and Zhang's [349] teams as well as other groups described the electroactive features and nanoconfinement of poly(VDF-*ter*-TrFE-*ter*-CTFE)-*g*-PSt (Scheme 61) and poly(VDF-*ter*-TrFE-*ter*-CTFE)-*g*-PXMA graft terpolymers (where *X* represents methyl, ethyl, etc), produced by ATRP of St or methacrylates from poly(VDF-*ter*-TrFE-*ter*-CTFE) macroinitiators, respectively. After crystallization, the polystyrene (PSt) side chains segregated to the periphery of poly(VDF-*co*-TrFE) crystals inducing a nanoscale PSt interfacial layer. The low polarizability of this confined layer produced a compensation polarization at the amorphous-crystalline interface that decreased while the local polarization field became weaker than that of pure poly(VDF-*co*-TrFE) copolymer. The PSt side chains, covalently linked to the poly(VDF-*co*-TrFE) polymer backbone behaved as an anchor in the amorphous phase hence preventing dipoles flipping along the electric field. Moreover, grafting different poly(alkyl methacrylate)s (PXMAs) onto poly(VDF-*ter*-TrFE-*ter*-CTFE) terpolymers provided very good compatibility of PXMA with the main chains and could effectively impede the crystallization of poly(VDF-*ter*-TrFE-*ter*-CTFE) backbone [349].

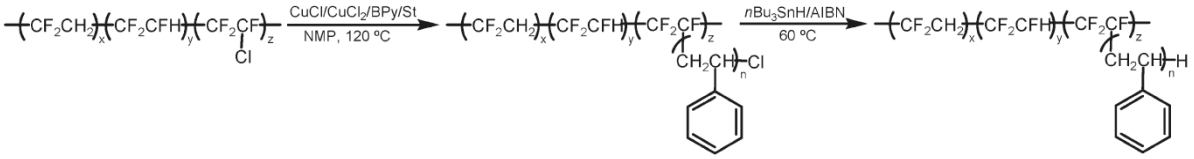

Scheme 61: synthesis of poly(VDF-*ter*-TrFE-*ter*-CTFE)-*g*-PSt graft copolymers achieved by ATRP of styrene, followed by the reduction step to avoid any thermal crosslinking during melt processing [348]. Copyright 2013. Reproduced with permission from the American Chemical Society.

The D-E hysteresis behaviors of such terpolymers clearly showed that the grafted poly(VDF-*ter*-TrFE-*ter*-CTFE)-g-PXMA tuned from ferroelectric to either anti-ferroelectric or linear dielectric by depending on the types and amount of XMA monomers onto it as shown in Fig. 48.

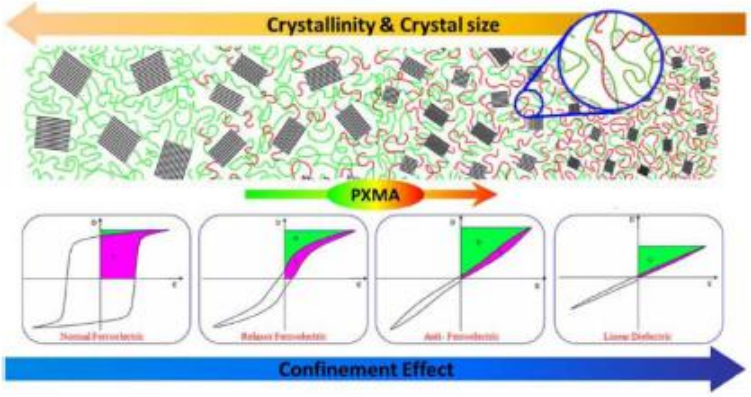

Fig. 48: Crystallization mechanism diagram structure and the dielectric polarization behavior of PVDF-based polymer (the black zones represent the crystalline PVDF, the green one means amorphous PVDF while the red ones represent PXMA). [315,349]. Copyright 2016. Reproduced with permission from RSC.

Besides, many unimorph actuators involving EAPs have been achieved. Nevertheless, the high strain change and the high elastic energy density of the terpolymer can lead to a high motion of a based terpolymer unimorph. One prototype is supplied in Fig. 49 with two layers of terpolymer (45 mm in length, 10 mm in width and 20 μm in thickness) bonded together. When the active layer is excited by an electric field, the electrostrictive layer extends in length and the free extremity of the unimorph follows a curved trajectory as noted in Fig. 49 [350].

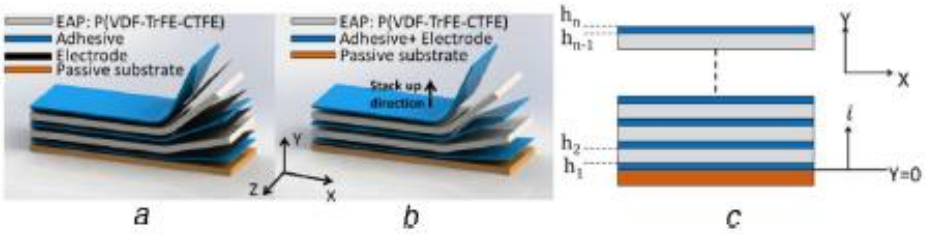

Fig. 49: Unimorph actuator consists of couple of layers of the poly(VDF-*ter*-TrFE-*ter*-CTFE) terpolymer films: a Schematic of unimorph actuator consists of a couple of layers of poly(VDF-*ter*-TrFE-*ter*-CTFE). Each EAP layer is an electrode on top and bottom using 50 nm sputtered silver so that they can act as an active layer. After electroding, two consecutive EAPs were linkeed together using scotch spray adhesive. For simplicity of the electromechanical model, electrodes and adhesive are considered as one layer since the electrode layer is very thin compared to the adhesive layer.
b Simplified schematic after considering adhesive and electrode as a single layer.
c Side view of the multi-layered unimorph actuator where h_i stands for the height; Y = 0 is the reference axis [350]. Copyright 2004. Reproduced with permission from the IOP Publishing.

As a conclusion on that sub-section, Capsal's team suggested a figure-of-merit (Fig. 50) [351] showing that plasticized terpolymers (e.g. with diethyl phthalate, DEHP) performed all of the considered materials (the constant figure-of-merit being depicted as dashed lines), including RFE ceramics, by several orders of magnitude. Indeed, with 15% DEHP, the energy density of poly(VDF-*ter*-TrFE-*ter*-CFE) terpolymer was 5,000 J.m^{-3} while it was 23 J.m^{-3} only for the pristine terpolymer.

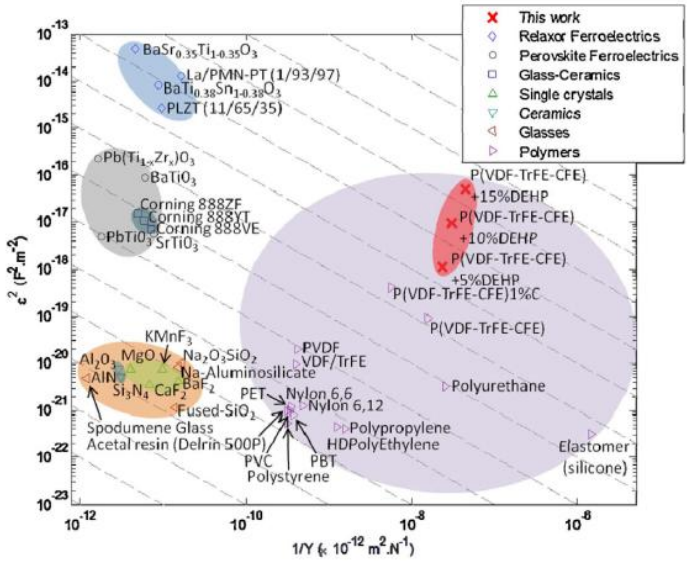

Fig. 50: Figure-of-merit of electrostrictive inorganic and organic materials [351]. Copyright 2014. Reproduced with permission from the Elsevier.

7.6.4. Dye sensitized solar cells (DSSCs)

DSSC technology is regarded as an artificial photosynthesis process.[352] DSSCs are currently comprised of nanocrystalline titanium dioxide (TiO_2) photo-anode sensitized by a dye (that acts as the photosensitizer), an electrolyte separating both electrodes and a counter electrode. Fluorinated electrospun membranes have received considerable attention as gel polymer electrolytes for tackling the liquid electrolyte drawbacks such as leakage and volatilization.[353] In this way, Bandara et al. [354] prepared electrospun poly(VDF-*co*-HFP) GPEs for application in DSSCs, and compared them to liquid electrolytes and conventional GPEs. The electrospun GPE showed an energy conversion efficiency quasi similar to that of the liquid electrolyte (5.36% vs. 6.01%) but higher than that of conventional GPE (4.70%). The order of the resistance value for charge transport and the durability (i.e., lifetime duration) was as follows: the highest one obtained for the conventional GPE, followed by the electrospun system and finally the liquid electrolyte.

In another work, Pang et al. [355] grafted 1-butylimidazolium iodide onto poly(VDF-*co*-HFP) copolymers (in different molar ratios) by electrospinning for *quasi*-solid state electrolytes in DSSC applications. A higher power conversion efficiency (ca. 9.26%) was released and the authors noted a higher long-term stability (> 1500 h) compared to those of standard liquid electrolytes.

7.6.5. Photovoltaics

There is still a huge challenge to convert light energy into electricity from active layer able to emit an electrical current under light irradiation as provided by photovoltaics (PVs). These devices are composed of a cathode, an active layer and an anode. In spite of their lower yields, organic materials to prepare them are advantageously cheaper than inorganic ones and their processing easier into flexible devices. The active organic layer of PVs can be designed from poly(3-hexylthiophene) (P3HT). It absorbs the photons and excitors (i.e. electron–hole are generated in P3HT). The dissociation of the excitons and transport of free charges generate the electrical current.

Though PVDF and VDF-based copolymers are also used as backsheet for photovoltaic panels, [10], a recent example was reported by Spampinato et al. [356] who designed original poly(VDF-*co*-TrFE)/P3HT blends, the fluorinated copolymer bringing ferroelectricity while P3HT is a semiconducting polymer. This combination proves to be a powerful tool for the non-destructive morphological reconstruction of multi-functional nano-structured thin films and probes layers of different thicknesses with respect to the film surface. By AFM, conductive force microscopy, kelvin probe force microscopy and piezoresponse force microscopy, these authors demonstrated that P3HT was located on the film surface (with a rather constant composition of 15%). Increasing the P3HT amount in the blend induced a segregation of P3HT at the upper layers of the films below a poly(VDF-*co*-TrFE) superficial layer. The depletion of P3HT from the substrate/film interface was reflected by the poor existence of conducting pathways that connect the top and bottom planes of the film.

7.6.6 Others

Besides such above applications, capacitors could be prepared form VDF copolymers. For example, Das et al. [357] blended IL, poly(VDF-*co*-HFP) copolymer and TiO_2 nanoparticles for high energy capacitors while Chung's team [358] synthesized poly(VDF-*ter*-TrFE-*ter*-CTFE) terpolymers for high pulsed capacitor with high energy density and low energy loss.

7.7. (Bio)medical applications

In addition to the exceptional properties and applications, VDF-containing copolymers exhibit biocompatibility, are bio-inert (i.e., inert to biomolecules such as cells or proteins), and thus can be suitable materials for (bio)medical devices.[5,6,359-360]. In addition, electrospun poly(VDF-*co*-TrFE) copolymers have been mainly studied in bone and neural tissue engineering.[361,362] Piezoelectric scaffolds in bone tissues, by experiencing mechanical stresses, can favor charges and promote the bone

regeneration, while in neural tissues, they can stimulate the neurite outgrowth and regeneration in response to electrical pulses.[9, 276]

Lee et al.[363] described scaffolds for neural tissue engineering elaborated from annealed electrospun poly(VDF-*co*-TrFE) copolymers. Such a thermal treatment was achieved to improve the *β*-phase content. Both scaffolds with randomly oriented and aligned fibers were investigated, and the fluorinated polymer scaffolds were demonstrated to be compatible with neuron cells. Actually, electrospun poly(VDF-*co*-TrFE) scaffolds exhibited better cell adhesion and neurite outgrowth than the pristine poly(VDF-*co*-TrFE) films. The cellular interaction with the substrate during the adhesion may induce some deformation to the scaffold while the subsequent piezoelectric effect can trigger the nerve tissue regeneration.

Augustine et al. [364] reported nanocomposites electrospun systems made of poly(VDF-*co*-TrFE)/ZnO for vascular tissue engineering (human endothelial cells) leading to higher cell viability and proliferation on the composite electrospun scaffolds, compared to control plates and pristine fluoropolymer scaffolds (without filler addition), as shown in Fig. 51. Indeed, angiogenesis was also enhanced *in vivo* after implantation in rats.

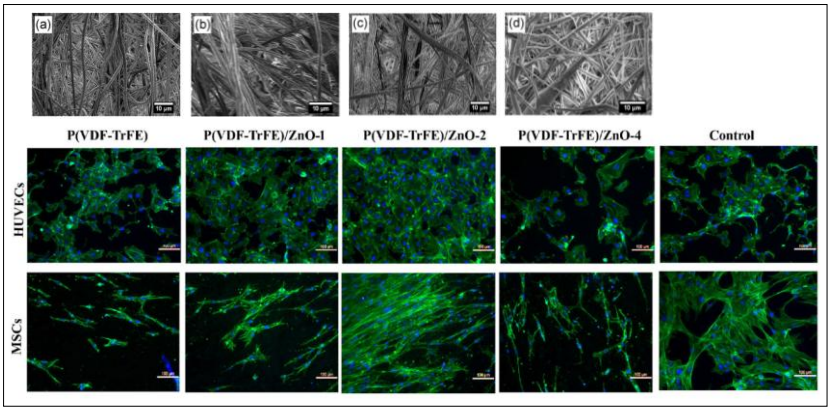

Fig. 51: SEM images of electrospun fibers of poly(VDF-*co*-TrFE) and poly(VDF-*co*-TrFE) composite containing: a. 0, b. 1, c. 2, d. 4 w/w ZnO, with their cell adhesion examined by human umbilical vein endothelial cells (HUVECs) and human mesenchymal stem cells (hMSCs).[364] Copyright 2017. Reproduced with permission from Springer.

Other potential biomedical applications of VDF co/terpolymers deal with tissue engineering [364-365], wound healing and energy storage devices (e.g., harvesting energy from breathing) [366,367], mechano-electrical transductions for tissue engineering applications and blood pressure sensors, mainly for bone, muscle and nerve regeneration (Table 7) [366]). In the first above topic, Nunes-Pereira *et al.*[369] tested PVDF, poly(VDF-*co*-HFP) and poly(VDF-*co*-TrFE) copolymers as porous membranes with two types of cells seeded onto them. Cells viability was then achieved to check suitable membranes for tissue engineering. These authors observed a higher cell proliferation on PVDF membranes of lower porosity and pore sizes, while lower proliferation was noted from poly(VDF-*co*-HFP) films (Fig. 52) [369].

Sensitive element of the pressure sensor	***Experience***	***pressure range (mmHg)***	***Sensitivity (mV/mmHg)***
P(VDF-*co*-TrFE) film	Air pressure chamber	0-300	0.099
P(VDF-*co*-TrFE) nanofibers	Air pressure chamber	0-300	0.280
P(VDF-*co*-TrFE)/PEDOT : PSS nanofibres	Air pressure chamber	0-300	4
PVDF film	Simulation	0-225	10-200[a]
P(VDF-*co*-TrFE) film	Simulation	40-200	0.237-0.373[a]
P(VDF-*co*-TrFE) film	Sensor wrapped around a Polydimethylsiloxane tube	40-120	0.35
PVDF film	Sensor wrapped around a latex tube	100-170	173
PVDF film	Sensor wrapped around the aorta of a pig (in vivo)	160-220	14

Table 7: Sensitivity of blood pressure sensors. Reproduced with permission of [327].
[a] according to sensors dimensions

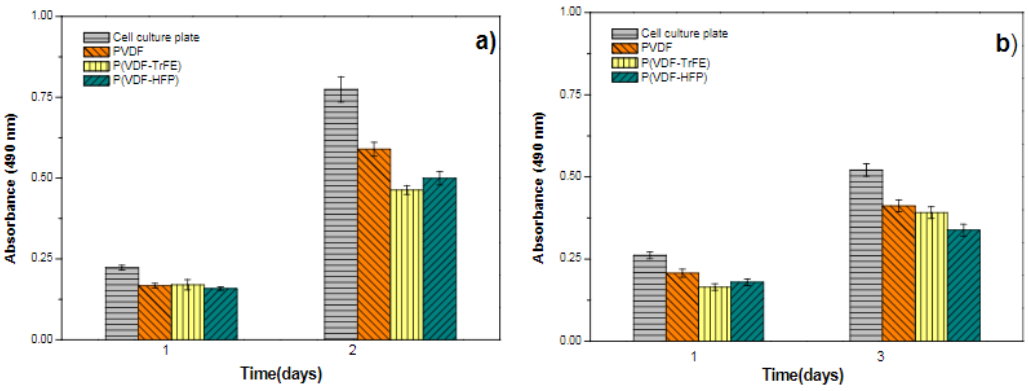

Fig. 52: Cell viability of different cells growing on porous membranes made of PVDF and VDF copolymers as measured by MTS assay (it is a colorimetric method for sensitive quantification of viable cells in cell proliferation assay): a) C2C12 (myoblast) cells up to 2 days of culture and b) MC3T3-E1 (pre-osteoblast) cells up to 3 days of culture [369]. Copyright 2015. Reproduced with permission of Elsevier.

8. Conclusions

Because of their unique outstanding properties which are critical to ensure optimal performances, VDF-containing copolymers are considered as irremplaceable materials in many applications Indeed, there are not any alternative products which are able to bear drastic aggressive conditions. Though many comonomers react with VDF, except isolated cases (functional elastomers or TPEs, and electroactive terpolymers manufactured on pilots only), the nowadays market does not provide any functional PVDF. Consequently, one of the simplest strategies to produce them is the radical copolymerization of VDF with functional comonomers. That route has already led to a wide range of functional VDF-containing copolymers. Indeed, the reactivity of the comonomers *versus* that of VDF, the choice of the medium and the nature of the initiators are key parameters to tune the desired functional copolymers for the expected application(s). The reactivity of both comonomers must be studied to find out the suitable VDF content in the copolymer and this review summarizes these trends *via* the kinetic section. Actually, VDF is known to copolymerize randomly with other monomers, and among the most known fluorinated monomers, it is atypical since has led to a few alternating copolymers without inducing any acceptor-donor copolymerization trend, in contrast to TFE and

CTFE. This behavior can be explained by the lower number of electron-withdrawing atoms compared to those in such both highly fluorinated alkenes. These alternating copolymers can be produced from comonomers which do not homopolymerize under radical initiation: $H_2C=C(CF_3)_2$ [that yields commercially available poly(VDF-*alt*-HFIB)], $F_2C=CFCO_2CH_3$ and $H_2C=C(CF_3)CO_2R$ (R=H or *tert*-Butyl). Such tendencies are difficult to explain from the usually reversed polarity of both comonomers and the structures can be triggered from the presence of bulky groups in the comonomers. Regretly, to the best of our knowledge almost no theoretical calculation or simulation has been reported in the literature to get some input in prediction of the reactivity of ~~~~~~~PVDF° macroradical toward the comonomers as well as that of any macroradical terminated by the comonomers onto VDF.

Various methods of RDRP are useful for the synthesis of well-designed fluoropolymers, and especially block copolymers: two-step ITP, stepwise RAFT polymerizations. Interestingly, the number of publications and patents has increased over the recent years. Although ITP was pioneered in the late seventies, more interest has been observed from the mid-nineties when *pseudo*-living radical controlled polymerization (RDRP) emerged. Actually, their syntheses do not require special processes (as in the case of ionic polymerizations) or using specific molecules (such as counter radicals or complex catalysts) and are tolerant to various media (even in water). This explains why many investigations have been carried out and also why Dai®el is commercially available, having reached industrial production since the 90ies. Another advantage concerns the versatility of the process, which can occur in solution, suspension, emulsion, or microemulsion. However, drawbacks arise from the cost and environmental issues of α,ω-diiodoperfluoroalkanes, regarded as PFASs and probably not in the family of polymers of low concern (PLC) because of their low molar masses. [370] Nevertheless, ITP can be adapted to hydrocarbon monomers [(meth)acrylate and styrenic] and, particularly, to fluoroalkenes, for which ITP is a mature technology industrially scaled up.

Fluoropolymers are thermally, biologically and chemically stable, non-mobile, non-bioaccumulative, non-toxic and display well-established safety profiles. They fullfill the widely

accepted polymer hazard assessment criteria to be considered PLC [96-97,370-372]. Commercially available fluoropolymers that meet such criteria are representative of approximately 96% of the global fluoropolymer market. The life-cycle stages of fluoropolymer creation (aka manufacturing) and disposal at the end of industrial or consumer use (e.g. end-of-life) are important to consider. The primary focus in these life-cycle stages is generally non-polymer PFAS from the manufacturing process or fluoropolymer degradation in end-of-life disposal [371-373]. Emissions from fluoropolymer productions are a key product life-cycle focus. Emissions of concern encompass non-polymer PFAS as unreacted monomers, fluorinated polymerization aids (PAs), oligomers, or other unintended by-products formed during the process. Indeed, significant emissions reduction has been already reached by one of the major fluoropolymer manufacturers, claiming 99% removal of fluorinated PA in wastewater treatment and 99.99% capture and destruction efficiency of gaseous emissions injected in thermal oxidizer [374].

Actually, these copolymers are essential to achieving important societal goals such as renewable energies, decarbonization, and/or competitiveness in the digital transition [371]. They are indispensable for critical applications in the chemical, healthcare, electronics, transportations and the deployment of 5G networks. Given the expected fluoropolymer market growth, ranging from approximately 5% to 8% [375-376], a proforma market table was created for 2021 using a 5% global growth rate evidencing the great benefits of such irremplaceable copolymers in our daily life.

9. Copyright Permission

10. Acknowledgments

The author thanks all coworkers cited in the references below as well as academic and industrial (especially Arkema, Pall and Tosoh Fine chemicals Companies) partners and the French National

agency (Fluopol and Premhys project grants ANR-14-CE07-0012 and 09-MAPR-0004-01, respectively). The French Fluorine Network (GIS) is also acknowledged? AS WELL AS Dr; Brinati for supplying clear Fig. 11.

10. References

[1] Puts GJ, Crouse P, Ameduri BM. Polytetrafluoroethylene: synthesis and characterization of the original extreme polymer. Chem Rev 2019;119:1763-805.

[2] Ameduri B, Fomin S. Fluoropolymers: Research, Production Issues, and New Applications. Progress in Fluorine Science. Volume 2: Fascinating Fluoropolymers and their Applications. Amsterdam: Elsevier, 2020. 474 pp.

[3] Humphrey JS, Amin-Sanayei R. Vinylidene Fluoride Polymers. In: Mark HF, editor. Encyclop Polym Sci Techn. New York: John Wiley & Sons Inc. 2004; 3rd ed. p. 510-33.

[4] Goldbach JT, Amin-Sanayei R, He W, Henry J, Kosar W, Lefebvre A, O'Brien G, Vaessen D, Wood K, Zerafati S. Commercial Synthesis and Applications of Poly(vinylidene fluoride). In: Ameduri B, Sawada H, editors. Fluorinated Polymer. Applications. Vol. 2. Oxford: Royal Society of Chemistry; 2016. p. 127-157.

[5] Cardoso V, Correia D, Ribeiro C, Fernandes M, Lanceros-Méndez S. Fluorinated polymers as smart materials for advanced biomedical applications. Polymers 2018;10:161-187.

[6] Li Y, Liao C, Tjong SC. Electrospun polyvinylidene fluoride-based fibrous scaffolds with piezoelectric characteristics for bone and neural tissue engineering. Nanomaterials. 2019;9:952-960.

[7] Cui Z, Drioli E, Lee YM. Recent progress in fluoropolymers for membranes. Prog Polym Sci 2014;39:164–198.

[8] Barbosa J, Dias J, Lanceros-Méndez S, Costa C. Recent advances in poly(vinylidene fluoride) and its copolymers for lithium-ion battery separators. Membranes 2018;8:45-80.

[9] Surya Prakash GK, Smart MC, Wang QJ, Atti A, Pleynet V, Yang B, McGrath K, Olah GA, Narayanan SR, Chun W, Valdez T, Surampudi S. High efficiency direct methanol fuel cell based on

poly(styrenesulfonic) acid (PSSA)–poly(vinylidene fluoride) (PVDF) composite membranes. J Fluorine Chem 2004;125:1217-30.

[10] Julien SE, Kempe MD, Eafanti JJ, Morse J, Wang Y, Fairbrother AW, Napoli S, Hauser AW, Ji L, O'Brien JS, Gu X, French RH, Bruckman LS, Wan KT, Boyce KP. Characterizing photovoltaic backsheet adhesion degradation using the wedge and single cantilever beam tests, Part II: Accelerated tests. Solar Energy Mat Solar Cells 2020;211:110524-34.

[11] Soulestin T, Ladmiral V, Dominguez Dos Santos F, Ameduri B. Vinylidene fluoride- and trifluoroethylene-containing fluorinated electroactive copolymers. How does chemistry impact properties? Prog Polym Sci 2017;72:16-60.

[12] Altomare A, Bozorg M, Loos K. PVDF-Based Multiferroic. In: Ameduri B, Fomin S, editors. Fluoropolymers: Research, Production Issues, and New Applications. Fascinating Fluoropolymers and Applications, Progress in Fluorine Science, vol. 2. Amsterdam: Elsevier. 2020. p. 45-81.

[13] Costa CM, Fernandes Cardoso V, Brito-Pereira R, Martins P, Correia DM, Correia V, Ribeiro C, Martins PM, Lanceros-Mendez S. Electroactive Poly(vinylidene fluoride)-based Materials: Recent Progress, Challenges, and Opportunities. In: Ameduri B, Fomin S, editors. Fluoropolymers: Research, Production Issues, and New Applications. Fascinating Fluoropolymers and Applications, Progress in Fluorine Science, vol. 2. Amsterdam: Elsevier. 2020. Chapt. 1. p. 1-43.

[14] Moore AL. Cured Systems in Fluoroelastomers. In Moore AL, editor. Fluoroelastomers Handbook: the Definitive User's Guide and Databook. Norwich, New York: William Andrew Publishing, 2006. Chapt. 5, p. 77-102.

[15] Tournut C. Copolymers of Vinylidene fluoride. In: Scheirs J, editor. Modern Fluoropolymers: High Performance Polymers for Diverse Applications, New York: Wiley & Sons. 1997; chapt. 31, p. 577-596.

[16] Ameduri B. From Vinylidene Fluoride (VDF) to the Applications of VDF-Containing Polymers and Copolymers: Recent Developments and Future Trends. Chem Rev 2009;109:6632-86.

[17] Moore AL. Fluoroelastomers Handbook: the Definitive User's Guide and Databook. Norwich, New York: William Andrew Publishing, 2012. 378 pp.

[18] Ameduri B. Synthesis of Original fluoromonomers and their copolymerization with Vinylidene fluoride. In Roesky HW, editor. Efficient Preparation of Fluorine Compounds. Hoboken: John Wiley & Sons Inc. 2012. chapter 59, p. 383-393.

[19] Smith Jr DW, Iacono ST, Iyer SS. Handbook of Fluoropolymer Science and Technology. New York: John Wiley & Sons Inc, 2014. 672 pp.

[20] Ebnesajjad S. Fluoroplastics; Melt Processable Fluoropolymers: The Define Users' Guide and Databook. Volume 2. Norwich: Plastics Design Library, 2015. 665 pp.

[21] Drobny J. Handbook of Fluoroelastomers; 2nd edition; New York: Wiley & Sons, 2016. 561 pp.

[22] Hercules DA, Parrish CA, Thrasher JS. Research and Non-Major Commercial co- and Terpolymers of Tetrafluoroethylene. In: Ameduri B, Sawada H, editors. Fluoropolymers: From Fundamentals to Applications. Vol. 2. Applications. Oxford: Royal Society Chemistry. 2016. p. 206-64.

[23] Ameduri B, Fomin S. Fluoropolymers: Research, Production Issues, and New Applications. Progress in Fluorine Science, Volume 1: Opportunities in Fluoropolymers: Synthesis, Processing and Simulations; Amsterdam: Elsevier. 2020. 359 pp.

[24] Kashio H, Horie K, Suzuki F. Epoxy group-containing vinylidene fluoride copolymer and its application to secondary battery European Patent 1996/0,751,157 (assigned to Kureha Ltd. Co.).

[25] Firetto V, Scialdone O, Silvestri G, Spinella A, Galia A, J Polym Sci Part A Polym Chem 2010;48:109-121.

[26] Miyabayashi T, Sakabe N, Zen S. Vinylidene fluoride-acrylic acid ester copolymer, process for producing the same and composition containing the same, US1990/4,925,907 (assigned to Japan Synthetic Rubber).

[27] Abusleme J, Pieri R, Barchiesi E. Vinylidene Fluoride copolymers. US2012/8,337,725 (assigned to Solvay Solexis).

[28] Sanguineti A, Mirenda M, Kapelyushko V. Thermoplastic compositions comprising a blend of one or more VDF copolymers and one or more acrylic or methacrylic ester polymers. WO2020/157238 (assigned to Solvay Specialty Polymers).

[29] Boguslavskaya LS, Panteleeva IY, Morozova TV, Kartashov AV, Chuvatkin NN. α–Fluoracrylates: synthesis, properties and uses. Russian Chem Rev, 1990;59:906-17.

[30] Chuvatkin NN, Panteleeva IT. α-Fluoroacrylates: synthesis, properties and use; Polyfluoroacrylates. In: Scheirs J, editor. Modern fluoropolymers: High Performance Polymers for Diverse Applications. New York: Wiley & Sons. 1997. chapter 9; p. 191-205.

[31] Guiot J. New functional monomers and their copolymerizations with vinylidene fluoride. PhD dissertation, University of Montpellier, 2003; 212 pp.

[32] Boschet F, Cracowski JM, Montembault V, Ameduri B. Radical Copolymerization of α,β-DifluoroAcrylic Acid with Vinylidene Fluoride. Macromolecules 2010;43:4879-88.

[33] Laflamme P, Porzio F, Ameduri B, Soldera A. Characterization of the telomerization reaction path for the vinylidene fluoride with °CCl_3 radicals. Polym Chem 2012;3:652-57.

[34] Fuchikami T, Yamanouchi A, Ojima I. An Effective and Convenient Route to 5-Trifluoromethyl-5,6-dihydrouracils and their Thio Derivatives. Synthesis 1984;9:766-68.

[35] Patil Y, Ameduri B. Advances in the (Co)polymerization of Alkyl 2-Trifluoromethacrylates and 2-(Trifluoromethyl)acrylic Acid. Prog Polym Sci 2013;38:703-39.

[36] Souzy R, Guiot J, Ameduri B, Boutevin B, Paleta O. Unexpected alternating copolymerization of vinylidene fluoride incorporating methyl trifluoroacrylate. Macromolecules 2003;36:9390-95.

[37] Minhas PS, Petrucelli F. A new high-performance fluoropolymer that can be readily melt-processed. Plast. Eng 1977;33:60-3.

[38] Ebnesajjad S. Fluoroplastics; Melt processible fluoropolymers. The Define Users' Guide and Databook. Volume 2. Norwich: Plastic design library, 2003. p. 82.

[39] Falireas PG, Wehbi M, Alaaeddine A, Ameduri B. Kinetics of radical copolymerization of vinylidene fluoride with tert-butyl 2-trifluoromethyl acrylate: a suitable pair for the synthesis of alternating fluorinated copolymers. Polym Chem 2018;9: 3754-61.

[40] Banerjee S, Ameduri B. Emerging Opportunities in (co)Polymerization of Alkyl 2-(Trifluoromethyl)acrylates and 2-(Trifluoromethyl)acrylic acid and their Applications. In: Ojima I, editor. Frontiers of Organofluorine Chemistry, Hackensack, NJ: World Scientific. 2020, Chapt. 17, p. 735–79.

[41] Banerjee S, Wehbi M, Manseri A, Mehdi A, Alaaeddine A, Hachem A, Ameduri B. Poly(vinylidene fluoride) Containing Phosphonic Acid as Anti-Corrosion Coating for Steel. ACS Appl Mat Interf 2017;9:6433−43.

[42] Wehbi M, Banerjee S, Mehdi A, Alaaeddine A, Hachem A, Ameduri B. Poly(vinylidene fluoride) with Improved Adhesion Properties via Crosslinking of Pendant Triethoxysilane Functionalities. Macromolecules 2017; 50:9329−39.

[43] Boujiouii F, Zhuge F, Damerow J, Wehbi M, Ameduri B, Gohy JF. Solid polymer electrolytes from a fluorinated copolymer bearing cyclic carbonate pendant groups. J Chem Mat A 2018;6:8514-22.

[44] Banerjee S, Tawade B, Ameduri B. Functional fluorinated polymer materials and preliminary self-healing behavior. Polym Chem 2019;10:1993–97.

[45] Wehbi M, Dolphjin G, Brassinne J, Gohy JF, Ameduri B. Synthesis of Vinylidene Fluoride-Based Copolymers Bearing Perfluorinated Ether Pendant Groups and Their Application in Gel Polymer Electrolytes, Macromolecules 201952:3056-65.

[46] Logothetis AL. Chemistry of Fluorocarbon Elastomers. Prog Polym Sci 1989;14:251-96.

[47] Ameduri B, Boutevin B, Kostov G. Fluoroelastomers: synthesis, properties and applications Prog Polym Sci 2001;26:105-87.

[48] Feiring AE, Doyle M, Roelofs MG, Farnham WB, Bekiarian PG, Blau HA. Polyvinylidene Fluoride Ionomers Containing Pendant Fluoroalkylsulfonyl Imide or Fluoroalkylsulfonyl Methide Groups. USPatent 2003/6,667,377 (assigned to DuPont).

[49] Xu K, Li K, Ewing CS, Hickner MA, Wang Q. Synthesis of proton conductive polymers with high electrochemical selectivity Macromolecules 2010;43:1692-94.

[50] Sayler TS. Preparation of perfluorinated ionomers for fuel cell applications. University of Tuscaloosa, Alabama, USA. 2012.

[51] Colpaert M, Lopez G, Zaton M, Jones D, Ameduri B. Revisiting the radical copolymerization of vinylidene fluoride with perfluoro-3,6-dioxa-4-methyl-7-octene sulfonyl fluoride for proton conducting membranes. Intern J Hydrog Energy 2018;43:16986-97.

[52] Schmiegel WW. Crosslinking of elastomeric vinylidene fluoride copolymers with nucleophiles. Angew Chem 1979;76/77:39-65.

[53] Boyer C, Ameduri B, Hung MH. Telechelic copolymers based on perfluoromethyl vinyl ether. US Patent 2013/012674 (assigned to Dupont Performance Elastomers).

[54] Guiot J, Neouze MA, Sauguet L, Ameduri B, Boutevin B. Synthesis and copolymerization of fluorinated monomers bearing a reactive lateral group. XX. Copolymerization of vinylidene fluoride with 4-bromo-1,1,2-trifluorobut-1-ene. J Polym Sci Part A Polym Chem 2005;43:917-26.

[55] Friesen CM, Ameduri B. Outstanding telechelic perfluoropolyalkylethers and applications therefrom. Progr Polym Sci 2018;81:238-80.

[56] Friesen CM, Ameduri B. Radical Copolymerization of Vinylidene fluorinated with Krytox® Perfluorovinylether to get thermoplastic Elastomers. Macromolecules 2015;48:7060-70.

[57] Burgess T, Vitale A, Manseri, A, Joly-Duhamel C, Bongiovanni R, Ono T, Friesen C, Ameduri B. Synthesis of poly[oligo(hexafluoropropylene oxide) perfluoroisopropenylether (PIPE)] graft copolymers with vinylidene fluoride (VDF) using CF_3 radicals. Polym Chem 2019;10:6651-61.

[58] Qiu J, Matyjaszewski K, Polymerization of substituted styrenes by atom transfer radical polymerization, Macromolecules 1997;30:5643-8.

[59] Hvilsted S, Borkar S, Siesler HW, Jankova K. Novel fluorinated polymer materials based on 2,3,5,6-tetrafluoro-4-methoxystyrene. In Matyjaszewski K, editor. Advances in Controlled /Living Radical Polymerization, ACS Symposium Series 854, Washington DC: Amer Chem Soc. 2003. Chapt 17, p. 236-49.

[60] Narita T. Anionic polymerization of fluorinated vinyl monomers. Prog Polym Sci 1999;24:1095-23.

[61] Walkowiak J, Martinez del Campo T, Ameduri B, Gouverneur V. Syntheses of Mono-, di-, and trifluorinated styrenic monomers. Synthesis 2010;11:1883–90.

[62] Wehbi M, Mehdi A, Allaeddine A, Negrell C, David G, Ameduri B. Fluoropolymers containing phosphorous atoms: Recent developments and Future trends. Appl Mater Interf 2020;12:38-59.

[63] Asandei A, Chen Y. Room temperature synthesis of vinylidene fluoride/vinylethoxysilane copolymers with under UV irradiation. Polym Prepr 2007;48:270–1.

[64] Wehbi M, Dolphjin G, Brassinne J, Gohy JF, Ameduri B. Solid polymer electrolytes from copolymers based on vinyl dimethyl phosphonate and vinylidene fluoride. Macromol Chem Phys 2021;222:2000389 ;| 1-8.

[65] Wehbi M, Bourgeois D, Ameduri B. Use of poly(vinylidene fluoride-*co*-vinyl dimethylphosphonate) copolymers for efficient extraction of valuable metals. Polym Chem 2019;10:4173-84.

[66] Ahmed TS, DeSimone JM, Roberts GW. Continuous copolymerization of vinylidene fluoride with hexafluoropropylene in supercritical carbon dioxide: Low hexafluoropropylene content semicrystalline copolymers. Macromolecules 2007;40:9322-33.

[67] Boschet F, Ameduri B. (Co)polymers of chlorotrifluoroethylene: synthesis, properties, and applications. Chem Rev 2014;114:927-80.

[68] Sauguet L, Ameduri B, Boutevin B. Radical copolymerization of vinylidene fluoride with 8-bromo-1H,1H,2H-perfluorooct-1-ene: microstructure, crosslinking and thermal properties. Macromol Chem Phys 2007;208:1061-72.

[69] Sauguet L, Boyer C, Ameduri B, Boutevin B. Synthesis and characterization of poly(vinylidene fluoride)-g-poly(styrene) graft polymers obtained by atom transfer radical polymerization of styrene. Macromolecules 2006;39:9087-101.

[70] Ito H, Giese B, Engelbrecht R. Radical reactivity and Q-e values of methyl alpha-(trifluoromethyl)acrylate. Macromolecules 1984;17:2204-5.

[71] McElroy KT, Purrington ST, Bumgardner CL, Burgess JP. Lack of polymerization of fluorinated acrylates. J Fluorine Chem 1999;95:117-20.

[72] Souzy R, Ameduri B, Boutevin B. Radical copolymerization of α-trifluoromethylacrylic acid with vinylidene fluoride and vinylidene fluoride / hexafluoropropene. Macromol Chem Phys 2004;205:476-85.

[73] Wadekar NM, Patil YR, Ameduri B. Superior thermostability and hydrophobicity of poly(vinylidene Fluoride-co-Fluoroalkyl 2-trifluoromethacrylate). Macromolecules 2014;47:13–25.

[74] Alaaddine A, Vergnaud J, Rolland J, Vlad A, Gohy JF, Ameduri B. Synthesis of an Original Fluorinated triethylene glycol methacrylate Monomer and its Radical Copolymerisation with Vinylidene Fluoride. Application as Polymer Electrolyte Gel for Li- Ion Batteries. Polym Chem 2015;6:6021-8.

[75] Kostov GK, Sauguet L, Ameduri B, Kaspar H, Zipples T, Hintzer K. Radical Copolymerization of Vinylidene Fluoride with 1-bromo-2,2-difluoroethylene. J Polym Sci Part A Polym Chem 2010;48:3964–76.

[76] Lannuzel T, Ameduri B. Copolymers derived from poly(vinylidene fluoride) WO2015/028,752A1 (assigned to ARKEMA and CNRS).

[77] Gadinski MR, Chanthad C, Han K, Dong L, Wang Q. Synthesis of poly(vinylidene fluoride-co-bromotrifluoroethylene) and effects of molecular defects on microstructure and dielectric properties. Polym Chem 2018;9:3754-61.

[78] Thenappan A, Rainal E, Ameduri B, Boschet F, Ajjelal N, Lopez G. Process, properties and applications of Graft Copolymers. US 2016/9,234,062 (assigned to Honeywell).

[79] Litt MH, Lando JB. The crystal structure of the alternating copolymer of hexafluoroisobutylene and vinylidene fluoride. J Polym Sc Polym Phys Ed 1982;20:535-52.

[80] Tedder JM. The importance of polarity, bond strength and steric effects in determining the site of attack and the rate of free radical substitution in aliphatic compounds. Tetrahedrom 1982;38:313-29.

[81] Souzy R, Ameduri B, Von Ahsen S, Willner H, Arguello GA. Use of bis(trifluoromethyl)peroxy dicarbonate as initiator in the radical homopolymerisation of vinylidene fluoride (VDF) and copolymerisation of VDF with hexafluoropropylene J Fluorine Chem. 2003;123:85-93.

[82] Scherer KV, Ono T. F-2,4-dimethyl-3-ethyl-3-pentyl and F-2,4-dimethyl-3-isopropyl-3-pentyl - stable tert-perfluoroalkyl radicals prepared by addition of fluorine or trifluoromethyl to a perfluoroalkene. J Amer Chem Soc 1985;107:718-9.

[83] Asandei AD, Adebolu OI, Simpson CP, Kim JS. Visible-Light Hypervalent Iodide Carboxylate Photo(trifluoro)methylations and Controlled Radical Polymerization of Fluorinated Alkenes. Angew Chem Int Ed 2013;52:10027-30.

[84] Maher K, Shireen M. Recent Trifluoromethylation Reactions. (A Mini Review). Orient J Chem 2018;34:2708-15.

[85] Xiao H, Zhang Z, Fang Y, Zhu L, Li C. Radical trifluoromethylation. Chem Soc Rev 2021;50:6308-19.

[86] Boschet F, Ono T, Ameduri B. Novel Source of trifluoromethyl Radical as Efficient Initiator for the Polymerization of Vinylidene Fluoride. Macromol Rapid Comm 2012;33:302−08.

[87] Mei H, Han J, White S, Butler G, Soloshonok VA. Perfluoro-3-ethyl-2,4-dimethyl-3-pentyl persistent radical: A new reagent for direct, metal-free radical trifluoromethylation and polymer initiation. J Fluor Chem 2019;227:109370-8.

[88] Patil Y, Alaaaeddine A, Ono T, Ameduri B. Novel Method to Assess the Molecular Weights of Fluoropolymers by Radical Copolymerization of Vinylidene Fluoride with Various Fluorinated Comonomers Initiated by a Persistent Radical. Macromolecules 2013;46:3092−106.

[89] Bonnet A, Devisme S, Ameduri B, Eid N. Method for making highly crystalline and thermally stable vinylidene fluoride-based polymers. WO2021/229081 (assigned to Arkema, CNRS and University of Montpellier).

[90] Eid N, Ameduri B, Gimello O, Bonnet A, Devisme S. Chain-End Functionality: the Key Factor toward Fluoropolymers Thermal Stability. Macromolecules 2021;54:7690–701.

[91] Zhang ZC, Wang Z, Chung TC. Synthesis of Chain End Functionalized Fluoropolymers by Functional Borane Initiators and Application in the Exfoliated Fluoropolymer/Clay Nanocomposites. Macromolecules 2007;40:5235–40.

[92] Chung TCM. Synthesis of Fluoropolymers Using Borane-Mediated Control Radical Polymerization for Energy Storage Applications. In: Smith DW, Iacono ST, Iyer SS, editors. Handbook of Fluoropolymer Science and Technology. Hoboken: Wiley & Sons. 2014. Chapt.12; p. 291-314.

[93] https://www.epa.gov/assessing-and-managing-chemicals-under-tsca/fact-sheet-20102015-pfoa-stewardship-program/; 2010 [accessed February 2022].

[94] Hintzer K, Schwertfeger W. Fluoropolymers Environmental aspects. In: Smith Jr DW, Iacano ST, Iyer SS, editors. Handbook of Fluoropolymer Science and Technology. Hoboken: Wiley & Sons. 2014. Chapter21, p. 495–520.

[95] Henry BJ, Carlin JP, Hammerschmidt JA, Buck RC, Buxton LW, Fiedler H, Seed J, Hernandez O. A Critical Review of the Application of Polymer of Low Concern and Regulatory Criteria to Fluoropolymers. Integ Environm Assess Manag 2017;14:316–34.

[96] Lohmann R, Cousins IT, DeWitt JC, Glüge J, Goldenman G, Herzke D, Lindstrom AB, Miller MF, Ng CA, Patton S, Scheringer M, Trier X, Wang Z. Are Fluoropolymers Really of Low Concern for Human and Environmental Health and Separate from Other PFAS? Environ Sci Technol 2020;54:12820–28.

[97] Ameduri B. Perfluoroalkyl substances: Synthesis, Properties, Applications and Regulations. Oxford: Royal Society of Chemistry. 2022. 652 pp.

[98] Peshoria S, Nandini D, Tanwar RK, Narang R. Short-chain and long-chain fluorosurfactants in firefighting foam: a review. Environ Chem Lett 2020;18:1277–1300.

[99] Brandl F, Beuermann S. Halbkontinuierliche Emulsions polymerisation von Vinylidenfluorid. Chem Ing Tech 2018;90:372–79.

[100] Bhattacharya BS, Chauhan R, Rathour JK, Kumar G. Method for aqueous polymerization of fluoromomnomers using perfluorobutanesulfonic acid or a salt thereof. WO2020/129083 (assigned to Gujarat Fluorochemicals Ltd).

[101] Brothers PD, Gangal SV, Khasnis DD. Aqueous polymerization of fluoromonomer using hydrocarbon surfactant. WO 2012/064841 Al (assigned to Dupont).

[102] Durali M, Hedhli L, Amin-Sanayei RA. Polymerization of fluoropolymers using non-fluorinated surfactants. US 2014/8,697,822 B2 (assigned to Arkema Inc.).

[103] Gupta B, Bhattacharya BS, Chauhan R, Rathour JK, Kumar G, Verma C. Process for producing fluoropolymers using 2-alkoxyacetate surfactants. WO2020/136679 (assigned to Gujarat Fluorochemicals Ltd).

[104] Reis da Cunha F, Davidovich I, Talmon Y, Ameduri B. Emulsion copolymerization of vinylidene fluoride (VDF) with perfluoromethyl vinyl ether (PMVE). Polym Chem 2020;11:2430-40.

[105] Banerjee S, Schmidt J, Talmon Y, Hori H, Asai T, Ameduri B. A degradable fluorinated surfactant for emulsion polymerization of vinylidene fluoride. Chem Commun 2018;54:11399-402.

[106] DeSimone JM, Maury EE, Menceloglu YZ, McClain JB, Romack TJ, Combes JR. Dispersion

Polymerizations in Supercritical Carbon Dioxide. Science 1994;265:356-9.

[107] Kennedy KA, Roberts GW, DeSimone JM. Heterogeneous Polymerization of Fluoroolefins in Supercritical Carbon Dioxide. Adv Polym Sci 2005;175:329-46.

[108] Du L, Kelly JK, Roberts GW, DeSimone JM. Fluoropolymer synthesis in supercritical carbon dioxide. J Supercr Fluids 2009;47:447-457.

[109] Baradie B, Shoichet MS. Synthesis of Fluorocarbon−Vinyl Acetate Copolymers in Supercritical Carbon Dioxide: Insight into Bulk Properties. Macromolecules 2002;35:3569-75.

[110] Siegmann R, Drache M, Beuermann S. Detailed copolymerization propagation kinetics of homogeneous phase VDF–HFP copolymerization in supercritical CO2. J Fluorine Chem 2014;159:48–56.

[111] Walkowiak-Kulikowska J, Boschet F, Kostov G, Gouverneur V, Ameduri B. On the Reactivity of α-Trifluoromethylstyrene in Radical Copolymerizations with Various Fluoroalkenes. Eur Polym J 2016;84:612–21.

[112] Souzy R, Ameduri B, Boutevin B. Synthesis of functional polymers–vinylidene fluoride based fluorinated copolymers and terpolymers bearing bromoaromatic side-group. J Polym Sci Part A Polym Chem 2004;42:5077-96.

[113] Souzy R, Ameduri B, Boutevin B, Capron P, Marsacq D, Gebel G. Proton-conducting polymer electrolyte membranes based on fluoropolymers incorporating perfluorovinyl ether sulfonic acids and fluoroalkenes: synthesis and characterization. Fuel Cell 2004;5:383-96.

[114] Hull DE, Johnson BV, Rodricks IP, Staley JB. THV Fluoroplastic. In Scheirs J, editor. Modern Fluoropolymers. New York: Wiley & Sons. 1997. Chapt. 13; p. 257-271.

[115] Ghosh A, Rajeev RS, Bhattacharya AK, Bhowmick AK, De SK. Atomic Force Microscopic Studies on Microheterogeneity of Blends of Silcone Rubber and Tetrafluoroethylene/Propylene/Vinylidene Fluoride Terpolymer. Rubber Chem Technol 2003;76:220-38.

[116] Schmiegel WW. A Review of Recent Progress in the Design and Reactions of Base-resistant Fluoroelastomers. KGK Kautschuk Gummi Kunstst 2004;57:313-19.

[117] Yamamoto K, Asakura J, Miwa T, Saito M. Unsaturated Bond Existing in Tetrafluoroethylene-propylene-vinylidene Fluoride Terpolymer. J. Fluorine Chem 2004;125:735-40.

[118] Taguet A, Ameduri B, Boutevin B. Crosslinking of vinylidene fluoride containing fluoropolymers. Adv Polym Sci 2005;184:127-211.

[119] Soulestin T, Marcellino Dos Santos Filho P, Ladmiral V, Lannuzel T, Dominguez-Santos F, Ameduri B. Ferroelectric Fluorinated Copolymers with Improved Adhesion Properties. Polym Chem 2017;8:1017-27.

[120] Soulestin T, Ladmiral V, Lannuzel T, Dominguez-Santos F, Ameduri B. Importance of microstructure control for designing new electroactive terpolymers based on vinylidene fluoride and trifluoroethylene. Macromolecules 2015;48:7861–71.

[121] Ameduri B, Alaaeddine A. Copolymers containing vinylidene fluoride and trifluoroethylene. US 2016/0,046,746 (assigned to Arkema; CNRS and University of Montpellier).

[122] Lannuzel T, Domingues Dos Santos F, Soulestin T, Ladmiral V, Ameduri B. Functionalized fluorinated copolymers. US2016/15,769,275 (assigned to Arkema and CNRS).

[123] Tillet G, Boutevin B, Ameduri B. Crosslinking and post-crosslinking of polymers. Progr Polym Sci 2011;36:191–217.

[124] Wang Y, Bai Y. The functionalization of fluoroelastomers: approaches, properties, and applications. RSC Adv 2016;6:53730-48.

[125] Sauguet L, Ameduri B, Boutevin B. Fluorinated Copolymers and Terpolymers Based on Vinylidene Fluoride and Bearing Sulfonic Acid Side-Group. J Polym Sci 2007;45:1814-34.

[126] Ameduri B, Boutevin B. Synthesis, properties and applications of fluoroalternated copolymers. In: Ameduri B, Boutevin B, editors. Well-Architectured Fluoropolymers: Synthesis, Properties and Applications. Amsterdam: Elsevier, 2004. Chapter 3; p. 187-230.

[127] Sorokin AD, Volkova EV, Naberezhnykh RA. Radiation copolymerization of fluoroolefins with ethylene Radiat Khim 1972;2:295-97.

[128] Caporiccio G, Sianesi D. Polymerization and copolymerization of vinyl fluoride. II. Radical copolymerization Chim Ind 1970;52:37-41.

[129] Ameduri B, Bauduin G. Synthesis and Polymerization of Fluorinated Monomers Bearing a Reactive Lateral Group. XIV. Radical Copolymerization of Vinylidene Fluoride with Methyl 1,1-Dihydro-4,7-dioxaperfluoro-5,8-dimethyl Non-1-enoate. J Polym Sci Part A Polym Chem 2003;41:3109-17.

[130] Yagi T, Tatemoto M. A fluorine-19 NMR study of the microstructure of vinylidene fluoride-trifluoroethylene copolymers. Polym J 1979;11:429-36.

[131] Banerjee S, Zaghloul S, Alaaeddine A, Ameduri B. Kinetics and Mechanistic Aspects of the Iodine Transfer Copolymerization of Vinylidene Fluoride with 2,3,3,3-Tetrafluoro-1-propene and Functionalization into ω-Hydroxy Fluorinated Copolymer. Polym Chem 2016;7:6099-109.

[132] Falireas PG, Ameduri B. Cobalt-Mediated Radical Copolymerization of Vinylidene Fluoride and 2,3,3,3-trifluoroprop-1-ene. Polymers 2021;13:2676-89.

[133] Soulestin T, Ladmiral V, Lannuzel T, Domingues Dos Santos F, Ameduri B. Differences in electroactive terpolymers based on VDF, TrFE and 2,3,3,3-tetrafluoropropene prepared by batch solution and semi-continuous aqueous suspension polymerizations. Polym Chem 2017;8:735-47.

[134] Soulestin T, Dos Santos Filho PM, Ladmiral V, Totee C, Silly G, Lannuzel T, Domingues Dos Santos F, Ameduri B. Influence of trans-1,3,3,3-Tetrafluoropropene on the Structure− Properties Relationship of VDF- and TrFE-Based Terpolymers Macromolecules 2017;50:503−14.

[135] Usmanov KU, Yul'chibaev AA, Mukhamadaliev N, Sarros TK. Radiation copolymerization of 2-hydropentafluoropropylene with vinylidene fluoride. Izv Vys Uch Zav Kh 1975;18:464-6.

[136] Otazaghine B, Sauguet L, Ameduri B. Synthesis and copolymerisation of fluorinated monomers bearing a reactive lateral group. Part 21. Radical copolymerisation of vinylidene fluoride with 2-

hydroperfluorooct-1-ene. J Fluorine Chem 2005;126:1009-16.

[137] Moggi G, Bonardelli P, Bart JCJ. Copolymers of 1,1-difluoroethene with tetrafluoroethene, chlorotrifluoroethene, and bromotrifluoroethene. J Polym Sci Part A Polym Chem 1984;22:357-63.

[138] Dohany JE; Humphrey JS. Vinylidene Fluoride Polymers. In Mark HF, Bikales NM, Overberger CG, Menges G, editors. Encyclopedia of Polymer Science and Engineering. New York: Wiley. 1989. Chapter 17, p. 532-48.

[139] Soulestin T. Synthesis and Characterizations of new fluorinated electroactive copolymers. PhD Dissertation. University of Montpellier. November 2016.

[140] Naberezhnykh RA, Sorokin AD, Volkova EV, Fokin AV. Radiation copolymerization of fluoroolefins. Izv Akad Nauk SSSR Ser Khim 1974;1:232–9.

[141] Moggi G, Bonardelli P, Russo S. Emulsion polymerization of the vinylidene fluoride-hexafluoropropene system. 6th Conf. Conv Ital Sci Macromol 1983;2:405-6.

[142] Bonardelli P, Moggi G, Turturro A. Glass transition temperatures of copolymer and terpolymer fluoroelastomers Polymer 1986;27:905-14.

[143] Gelin MP, Ameduri B. Radical copolymerization of vinylidene fluoride with hexafluoropropene. J Fluorine Chem 2005;126:577-84.

[144] Beginn U, Najjar R, Ellmann J, Vinokur R, Martin R, Moeller M. Copolymerization of Vinylidene Difluoride with Hexafluoropropene in Supercritical Carbon Dioxide. J Polym Sci Part A Polym Chem 2006;44:1299-1308.

[145] Tai H, Wang W, Howdle SM. Copolymerization of vinylidene fluoride and hexafluoropropylene in supercritical carbon dioxide. Macromolecules 2005;38:9135–42.

[146] Ahmed TS, DeSimone JM, Roberts GW. Continuous Copolymerization of Vinylidene Fluoride with Hexafluoropropylene in Supercritical Carbon Dioxide: High-Hexafluoropropylene-Content Amorphous Copolymers. Macromolecules 2008;41:3086-97 (and references herein: see Table 6).

[147] Otazaghine B, Sauguet L, Boucher M, Ameduri B. Radical copolymerization of vinylidene fluoride with perfluoroalkylvinyl ethers. Eur Polym J 2005;41:1747-56.

[148] Boyer C, Ameduri B, Hung MH. Telechelic Diiodopoly(VDF-*co*-PMVE) Copolymers by Iodine Transfer Copolymerization of Vinylidene Fluoride (VDF) with Perfluoromethyl Vinyl Ether (PMVE). Macromolecules 2010;43:3652-63.

[149] Guiot J, Ameduri B, Boutevin B. Synthesis and polymerization of fluorinated monomers bearing a reactive lateral group. XII. Copolymerization of vinylidene fluoride with 2,3,3-trifluoroprop-2-enol. J Polym Sci Part A Polym Chem 2002;40:3634-44.

[150] Ameduri B, Boutevin B, Bauduin G, Petrova P, Kostov G. Synthesis and Polymerization of Fluorinated Monomers Bearing a Reactive Lateral Group-Part 9-Bulk Copolymerization of Vinylidene Fluoride with 4,5,5-Trifluoro-4-ene pentyl acetate. Macromolecules 1999;32:4544-53.

[151] Ameduri B, Boutevin B, Petrova P, Kostov G. Synthesis and Polymerization of Fluorinated Monomers Bearing a Reactive Lateral Group-Part 10-Copolymerization of Vinylidene fluoride (VDF) with 5-Thioacetoxy-1,1,2-trifluoropentene for the Preparation of Novel PVDF Containing Mercaptan side Functions. Des Monomers Polym 1999;2:267-75.

[152] Khodzhaev SG, Yusupbekova FZ, Yul'Chibaev AA. Synthesis of derivatives of perfluoromethacrylic acid and some polymers made of them. Sb Nauchn Tr-Tashk Gos 1981;667:34-41 (Chem. Abstr. 1981, 97, 163545).

[153] Guiot J, Ameduri B, Boutevin B. Synthesis and polymerization of fluorinated monomers bearing a reactive lateral group 13. Copolymerization of vinylidene fluoride with 2-benzoyloxy pentafluoropropene. Eur Polym J 2003;39:887-95.

[154] Maeda K, Yamauchi T, Tsutsumi K. Microstructural studies of vinylidene fluoride hexafluoroacetone copolymer. Polym J 1990;22:681-87.

[155] Kostov G, Boschet F, Brandstadter S, Ameduri B. Random and Sequential Radical Cotelomerizations of 3,3,3-Trifluoropropene (H2C=CHCF3) with Vinylidene Fluoride (F2C=CH2). J Polym Sci Part A Polym Chem 2009;47:3964-81.

[156] Barner Kowollik C. Handbook of RAFT Polymerization, 2008; Wiley-VCH: Weinheim, pp. 556.

[157] Gigmes D. Nitroxide Mediated Polymerization: From Fundamentals to Applications in Materials Science. Oxford: RSC. 2008. 512 pp.

[158] Matyjaszewski K, Gao H, Sumerlin BS, Tsarevskyy NV. Reversible Deactivation Radical Polymerization: Mechanisms and Synthetic Methodologies. Vol. 1284. Washington: ACS Symposium Series. 2018. 402 pp.

[159] Matyjaszewski K, Gnanou Y, Hadjichristidis N, Muthukumar M. Macromolecular Engineering: From Precise Synthesis to Macroscopic Materials and Applications. Second Edition. Weinheim: Wiley-VCH GmbH, 2022. 3264 pp.

[160] Gregory A, Stenzel MH. Complex polymer architectures via RAFT polymerization: From fundamental process to extending the scope using click chemistry and nature's building blocks. Progr Polym Sci 2012;37:38-105.

[161] Keddie DJ. A guide to the synthesis of block copolymers using reversible-addition fragmentation chain transfer (RAFT) polymerization. Chem Soc Rev 2014;43:496-505.

[162] Anastasaki A, Nikolaou V, Nurumbetov G, Wilson P, Kempe K, Quinn JF, Davis TP, Whittaker MR, Haddleton DM. Cu(0)-Mediated Living Radical Polymerization: A Versatile Tool for Materials Synthesis. Chem Rev 2016:116:835−77.

[163] Pan X, Tasdelen MA, Junkers T, Yagci Y, Matyjaszewski K. Photomediated controlled radical polymerization. Progr Polym Sci 2016;62:73–125.

[164] Destarac M. Industrial development of reversible-deactivation radical polymerization: is the induction period over? Polym Chem 2018;9:4947-67.

[165] Moad G. A Critical Survey of Dithiocarbamate Reversible Addition- Fragmentation Chain

Transfer (RAFT) Agents in Radical Polymerization. J Polym Sci Part A Polym Chem 2019;57:216-27.

[166] Demarteau J, Debuigne A, Detrembleur C. Organocobalt Complexes as Sources of Carbon-Centered Radicals for Organic and Polymer Chemistries. Chem Rev 2019;119:6906-55.

[167] Corrigana N, Jung K, Moad G, Hawker CJ, Matyjaszewski K, Boyer C. Reversible-deactivation radical polymerization (Controlled/living radical polymerization): From discovery to materials design and applications. Progr Polym Sci 2020;111:101311-36.

[168] Ameduri B. Controlled Radical (Co)polymerization of Fluoromonomers. Macromolecules 2010;43:10163-84.

[169] Voet VSD, ten Brinke G, Loos K. Well-defined copolymers based on poly(vinylidene fluoride): From preparation and phase separation to application. J Polym Sci Part A Polym Chem 2014;52:2861-77.

[170] Asandei AD. Photomediated Controlled Radical Polymerization and Block Copolymerization of Vinylidene Fluoride. Chem Rev 2016;116:2244-74.

[171] Zapsas G, Patil Y, Gnanou Y, Ameduri B, Hadjichristidis N. Poly(vinylidene fluoride)-based Complex Macromolecular Architectures: From Synthesis to Properties and Applications. Prog Polym Sci 2020;104:101231| 1-21.

[172] Mohammad SA, Shingdilwar S, Banerjee S, Ameduri B. Macromolecular Engineering Approach for the Preparation of Fluorinated Olefins based Architectures, and Applications. Progr Polym Sci 2020;106:101255| 1-61.

[173] Gong HH, Zhang Y, Cheng YP, Lei MX, Zhang ZC. The application of Controlled/living radical polymerization in modification of PVDF-based Fluoropolymer. Chinese J Polym Sci 2021;39:1110-26.

[174]Tatemoto M. The first Regular Meeting of Soviet-Japanese Fluorine Chemists. Tokyo, Japan. September, 1979.

[175] Tatemoto M, Nakagawa T. Segmented polymers. US1979/4,158,678 (assigned to Daikin Kogyo Co Ltd).

[176] Oka M, Tatemoto M. Vinylidene fluoride-hexafluoropropylene copolymer having terminal iodines. In: Bailey WJ, Tsuruta T, editors. Contemporary Topics in Polymer Science. New-York: Plenun Press. 1984. p. 763-81.

[177] Tatemoto M. Iodine transfer polymerization. In: Salamone JC, editor. Polymeric Materials Encyclopedia. Vol. 5. Boca Raton: CRC. 1996. Chapter 5, p. 3847-62.

[178] David G, Boyer C, Tonnar J, Ameduri B, Lacroix-Desmazes P, Boutevin B. Use of iodocompounds in radical polymerization. Chem Rev 2006;106:3936-62.

[179] Hansen NML, Jankova K, Hvilsted S. Fluoropolymer materials and architectures prepared by controlled radical polymerizations. Eur Polym J 2007;43:255-93.

[180] Ogura Y, Takenaka M, Sawamoto M, Terashima T. Fluorous gradient copolymers via in-Situ Transesterification of a Perfluoromethacrylate in Tandem Living Radical Polymerization: Precision Synthesis and Physical Properties. Macromolecules 2018;51:864-71.

[181] Banerjee S, Chakrabartyb A, Singha NK, Ameduri B. Recent Advances in the Controlled Radical (co)Polymerization of Fluorinated Alkenes/Acrylates/Methacrylates/Styrenes. In Singha NK, Mays JW, editors. Functional Polymers by Controlled Radical Polymerization: Concepts, Strategies and Applications, Shawbury: Smithers RAPRA. 2017. chapt 6, p. 215-68.

[182] Apostolo M, Arcella V, Storti G, Morbidelli M. Free Radical Controlled Polymerization of Fluorinated Copolymers Produced in Microemulsion. Macromolecules 2002;35:6154-66.

[183] Boyer C, Ameduri B. Iodine Transfer Copolymerization of Vinylidene Fluoride and α-Trifluoromethacrylic Acid in Emulsion Process without any Surfactants. J Polym Sci Part A Polym Chem 2009;47:4710-22.

[184] Brandl F, Drache M, Beuermann S. Kinetic Monte Carlo Simulation Based Detailed Understanding of the Transfer Processes in Semi-Batch Iodine Transfer Emulsion Polymerizations of Vinylidene Fluoride. Polymers 2018;10:1008-15.

[185] Lee JH, Lee B, Won JW, Kim CH. Synthesis of novel telechelic fluoropolyols based on

vinylidene fluoride/hexafluoropropylene copolymers by iodine transfer polymerization. Macromol Res 2017;25:1028-34.

[186] Banerjee S, Patil Y, Ono T, Ameduri B. Synthesis of ω-Iodo and Telechelic Diiodo Vinylidene Fluoride-Based (Co)polymers by Iodine Transfer Polymerization Initiated by an Innovative Persistent Radical. Macromolecules 2017;50:203-14.

[187] Boyer C, Ameduri B, Boutevin B, Dolbier WR, Winter R, Gard G. Radical Terpolymerization of 1,1,2-Trifluoro-2-pentafluorosulfanylethylene and Pentafluorosulfanylethylene in the Presence of Vinylidene Fluoride and Hexafluoropropylene by Iodine Transfer Polymerization,Macromolecules 2008;41:1254-63.

[188] Asandei AD, Adebolu OI, Simpson CP. Mild-Temperature $Mn_2(CO)_{10}$-Photomediated Controlled Radical Polymerization of Vinylidene Fluoride and Synthesis of Well-Defined Poly(vinylidene fluoride) Block Copolymers. J Am Chem Soc 2012;134:6080-3.

[189] Tatemoto M, Shimizu T. Fluorinated Thermoplastic Elastomers In: Scheirs J, editor. Modern Fluoropolymers. New-York: Wiley & Sons. 1997. Chapter 25, p. 565-76.

[190] Brandl F, Schwaderer J, Drache M, Beuermann S. Iodine transfer emulsion polymerization of vinylidene fluoride. In Ameduri B, Fomin S, editors. Opportunities for Fluoropolymers: Synthesis, Characterization, Processing, Simulations and Recycling. Oxford: Elsevier. 2020. chapter 2, p. 49-68.

[191] Ameduri B, Boutevin B. Update on fluoroelastomers: from perfluoroelastomers to fluorosilicones and fluorophosphazenes. J Fluorine Chem 2005;126:221-29.

[192] Brinati G, Arcella V. Branching and pseudo-living technology in the synthesis of high performance fluoroelastomers. Rubber World 2001;224:27-32.

[193] Carella S, Mazzola M, Brinati G, Oriani V, Di Nicolo E. US Appl. 2022/0025087 (assigned to Solvay Specialty Polymers Italy S.p.A.).

[194] Hung MH, Ameduri B, Kostov G. Fluoropolymer having diacrylate ends. US2011/0,015,358 (assigned to DuPont Performance Elastomers and CNRS), 2011.

[195] Kostov G, Holan M, Ameduri B, Hung MH. Synthesis and Characterizations of Photo-Cross-Linkable Telechelic Diacrylate Poly(vinylidene fluoride-*co*-perfluoromethyl vinyl ether) Copolymers. Macromolecules 2012;45:7375-87.

[196] Soules A, Ameduri B, Boutevin B, Calleja G. Original Fluorinated Copolymers Achieved by Both Azide/Alkyne "Click" Reaction and Hay Coupling from Tetrafluoroethylene Telomers. Macromolecules. 2010;43:4489-99.

[197] Hung M-H, Ameduri B. Process for preparation of fluorosilicon polymer. US 2012/8,138,274B2 (assigned to Dupont Performance Elastomers and CNRS).

[198] Rizzardo E, Chiefari J, Mayadunne RTA, Moad G, Thang SH. Synthesis of Defined Polymers by Reversible Addition Fragmentation Chain Transfer: The RAFT Process. ACS Symp Ser 2000;768:278-96.

[199] Hill MR, Carmean RN, Sumerlin BS. Expanding the scope of RAFT polymerization: recent advances and new horizons. Macromolecules 2015;48:5459-69.

[200] Perrier S. 50th Anniversary Perspective: RAFT Polymerization-A User Guide. Macromolecules 2017;50:7433-47.

[201] Kostov G, Boschet F, Buller J, Badache L, Brandsadter S, Ameduri B. First Amphiphilic Poly(vinylidene fluoride-co-3,3,3-trifluoropropene)-b-oligo(vinyl alcohol) Block Copolymers as Potential Nonpersistent Fluorosurfactants from Radical Polymerization Controlled by Xanthate. Macromolecules 2011;44:1841-55.

[202] Ameduri B, Patil Y. Controlled radical copolymerization of fluorinated monomers via xanthate or trithiocarbonate. US2015/9,184,461 B2 (assigned to Arkema and CNRS).

[203] Patil Y, Ameduri B. First RAFT/MADIX radical copolymerization of *tert*-butyl 2-trifluoromethacrylate with vinylidene fluoride controlled by xanthate. Polym Chem 2013;4:2783-99.

[204] Banerjee S, Patil Y, Gimello O, Ameduri B. Well-defined multiblock poly(vinylidene fluoride) and block copolymers thereof: a missing piece of the architecture puzzle. Chem Commun

2017;53:10910-3.

[205] Ameduri B, Gerard JF, Bounor Legare V, Seck S, Buvat P, Bigarre J. Process for Preparing an Ion-Exchange Composite Material Comprising a Polymer Matrix and a Filler Consisting of Ion-Exchange Particles. US2016/0156052A1 (assigned to CEA, INSA, ENSCM, CNRS).

[206] Seck S, Magana S, Prebe A, Buvat P, Bigarre J, Chauveau J, Ameduri B, Bounor Legare V. New fluorinated polymer-nanocomposites based via combination of sol-gel chemistry and reactive extrusion for polymer electrolyte membranes fuel cells (PEMFC). Mater Chem Phys 2020,252:123004-12.

[207] Ameduri B, Alaaeddine A. Controlled free-radical copolymerization of trifluoroethylene. US 2015/0119523 A1 (assigned to Arkema and CNRS).

[208] Girard E, Marty JD, Ameduri B, Destarac M. Direct synthesis of vinylidene fluoride-based amphiphilic diblock copolymers by RAFT/MADIX polymerization. ACS Macro Lett 2012;1:270-4.

[209] Fuentes-Exposito M, Norsic S, Fevrier T, Dugas PY, Boutti S, Devisme S, Bonnet A, D'Agosto F, Lansalot M. Surfactant-free emulsion polymerization of vinylidene fluoride mediated by RAFT/MADIX reactive poly(ethylene glycol) polymer chains. Polym Chem 2021;12:5640-49.

[210] Banerjee S, Ladmiral V, Debuigne A, Detrembleur C, Poli R, Ameduri B. Organometallic Mediated Radical Polymerization of Vinylidene Fluoride. Angew Chem Intern Ed 2018;57:2934–7.

[211] Falireas P, Ladmiral V, Debuigne A, Detrembleur C, Poli R, Ameduri B. Straightforward Synthesis of Well-Defined Poly(vinylidene fluoride) and Its Block Copolymers by Cobalt-Mediated Radical Polymerization. Macromolecules 2019;52:1266-76.

[212] Rice DE, Sandberg CL. Carboxy- and ester-terminated copolymers of vinylidene fluoride and hexafluoropropene. US Patent 1965/3,438,953 (assigned to 3M).

[213] Rice DE. Bis(α-substituted perfluoroacyl) peroxides. US Patent 1969/3,461,155 (assigned to 3M).

[214] Rice DE. Process for preparing carboxy-terminated copolymers, US Patent 1969/3,457,245 (assigned to 3M).

[215] Novikov VA, Sass VP, Ivanova LS, Sokolov LF, Sokolov SV. Kinetics of thermal decomposition of perfluorodiacyl peroxides. Polymer Sciences USSR Serie A 1975;9:1414-7.

[216] Oka M, Morita S, Fluorine-containing diacyl peroxides and use thereof. Eur Pat. 1985/0,186,215 (assigned to Daikin).

[217] Saint-Loup R, Manseri A, Ameduri B, Lebret B Vignane P. Synthesis and properties of novel fluorotelechelic macrodiols containing vinylidene fluoride, hexafluoropropylene and chlorotrifluoroethylene. Macromolecules 2002;35:1524-36.

[218] Eid N, Ameduri B, Gimello O, Bonnet A, Devisme S. Vinylidene fluoride polymerization by metal-free selective activation of hydrogen peroxide: microstructure determination and mechanistic study. Polym Chem 2021;12:926-38.

[219] Chan ML, Reed Jr R, Gollmar HG, Gotzmer C, Gill RC, Plastic bonded explosives using fluorocarbon binders, US Patent 1991/5,049,213 (assigned to US Navy).

[220] Guiot J, Ameduri B, Boutevin B, Lannuzel T. Original crosslinking of poly(vinylidene fluoride) via trialkoxysilane-containing cure-site monomers. J Polym Sci Part A Polym Chem 2006;44:3896-910.

[221] Chen J, Tan S, Gao G, Li H, Zhang Z. Synthesis and characterization of thermally self-curable fluoropolymer triggered by TEMPO in one pot for high performance rubber applications. Polym Chem 2014;5:2130–41.

[222] Choi SS, Kim YK. Analysis of pyrolysis products of poly(vinylidene fluoride-co-hexafluoropropylene) by pyrolysis-gas chromatography/mass spectrometry. J Fluorine Chem 2014;165: 33-8.

[223] Beyer EC. Gap Junctions. In: Friedlander M, Mueckler M, editors. Molecular Biology of Receptors and Transporters: Pumps, Transporters and Channels, San Diego: Academic Press Inc., 1993. p. 2-24.

[224] Walmor C De Mello, Modulation of Junctional Permeability. In: Walmor C. Mello, editor. Cell-to-Cell Communication, New-York: Springer. 1987. p. 29-64.

[225] Alberts B, Bray D, Lewis J, Raff M, Roberts K, Watson JD. Molecular Biology of the Cell, 3rd Ed., New-York: Garland Science, , 1994. 1352 pp.

[226] Simon CM, Kaminsky W. Chemical recycling of polytetrafluoroethylene by pyrolysis. Polym Degrad Stab 1998;62;1-7.

[227] Schlipf M, Schwalm T. Closing the Recycling Loop. Kunststoffe Int 2014;6:58−60.

[228] https://www.agc.com/en/news/detail/20040318e.html/; [assessed on April 2022].

[229] Recycling of fluoropolymers. Fluoropolymergroup. Kunststoff. May, 2018 https://www.pro-kunststoff.de/fachwissen/recycling-of-fluoropolymers.html]; 2018 [assessed on February 2022].

[230] Dams R, Hintzer K. Industrial Aspects of Fluorinated Oligomers and Polymers. In: Ameduri B, Sawada H. Fluorinated Polymers: Volume 2: Applications. Oxford: RSC. 2016. Chapter 1. p. 1-31.

[231] Honma R, Hori H. Decomposition of fluoropolymers by their mineralization in subcritical water. In: Ameduri B, Fomin S, editors. Opportunities for Fluoropolymers synthesis, characterization, processing, simulations and recycling. Oxford: Elsevier. 2020. Chapt. 11. p. 303-31.

[232] Honma R, Hori H, Reis da Cunha F, Horiike N, Steinbach L, Ameduri B. Permanganate-Induced Efficient Mineralization of PVDF and VDF Based Copolymers in Low Temperature Subcritical Water. Ind Eng Chem Res 2019;58:13030−40.

[233] Hori H, Tanaka H, Tsuge T, Honma R, Banerjee S, Ameduri B. Decomposition of fluoroelastomer: poly(vinylidene fluoride-*ter*-hexafluoropropylene-*ter*-tetrafluoroethylene) terpolymer in subcritical water. Eur Polym J 2017;94:322−31.

[234] Hori H, Honma R, Igarashi K, Manseri A, Ameduri B. Oxidative Mineralization of Poly[vinylidene fluoride-co-2-(trifluoromethyl)acrylic acid] Copolymers in Superheated Water. Indus Engin Chem Research 2022;61:1386-97.

[235] Drobny JG. Technology of Fluoropolymers. New-York: Springer Science and Business Media LLC. 2008. 225 pp.

[236] Teng H. Overview of the development of the fluoropolymer industry. Appl Sci 2012;2:496-512.

[237] Gardiner J. Fluoropolymers: Origin, Production, and Industrial and Commercial Applications. Aust J Chem 2015;68:13−22.

[238] Drobny JG. Compounds for Automotive Fuel Systems. In: Drobny JG, editor. Fluoroelastomers Handbook, Oxford: Elsevier. 2016. p. 471–82.

[239] Drobny JG. Compounds for Automotive Power Train Systems. In: Drobny JG, editor. Fluoroelastomers Handbook, Oxford: Elsevier. 2016. p. 483–90.

[240] Ameduri B. The Promising Future of Fluoropolymers. Macromol Chem Phys 2020;221:1900573| 1-14.

[241] Bouharras F, Lopez G, M. Raihane M, Ameduri B. Fluoropolymers for Automotive and Aerospace industries. In: Matyjaszewski K, Gnanou Y, Hadjichristidis N, Muthukumar M, editors. Macromolecular Engineering: From Precise Synthesis to Macroscopic Materials and Applications. Weinheim: Wiley-VCH Verlag GmbH. Second Edition. 2022. Chapter 26, p. 1371-402.

[242] Ait-Haddou H, Belmont J, Ameduri B, Lopez G. Porous membrane having a fluorinated copolymer as surface treatment. US Patent 2021/11,040,312 (assigned to Pall and CNRS).

[243] Worm AT, Grootaert W. Fluorocarbon Elastomers. In: Kirk RE, Othmer D. editors. Encyclopedia of Polymer Science & Technology, New York: Wiley & Sons. 2002;2:577-90.

[244] Tarascon JM, Gozdz AS, Schmutz CN, Shokoohi F, Warren PC. Performance of Bellcore's plastic rechargeable Li-ion batteries. Solid State Ionics 1995;49:86-95.

[245] Wang S, Legare JM. Perfluoroelastomers and fluoroelastomer seals for semiconductor wafer processing equipment. J Fluorine Chem 2003;122:113–19.

[246] Allcock HR. Structural Diversity in Fluorinated Polyphosphazenes: Exploring the Change from Crystalline Thermoplastics to High-performance Elastomers and Other New Materials. In: Ameduri B,

Sawada H, editors. Fluoropolymers: From Fundamentals to Applications. Vol 2. Applications. Oxford: Royal Society Chemistry. 2016. p.54-79.

[247] Twum EB, McCord EF, Lyons DF, Fox P, Rinaldi PL. Characterization of End Groups and Branching Structures in Copolymers of Vinylidene Fluoride with Hexafluoropropylene using Multidimensional NMR Spectroscopy. Eur Polym J 2014;53:136-50.

[248] Twum EB, McCord EF, Lyons DF, Rinaldi PL. Multidimensional ^{19}F NMR Analyses of Terpolymers from Vinylidene Fluoride (VDF)−Hexafluoropropylene (HFP)−Tetrafluoroethylene (TFE) Macromolecules 2015;48:3563−76.

[249] Ameduri B, Boutevin B. Synthesis, Properties and Applications of Fluorinated Diblock, Triblock and Multiblock Copolymers. In: Ameduri B, Boutevin B, editors. Well-Architectured Fluoropolymers: Synthesis, Properties and Applications. Amsterdam: Elsevier, 2004. Chapter 4; p. 231-346.

[250] Yagi T, Tsuda N, Noguchi T, Sakaguchi K, Tanaka Y, Tatemoto M. Fluorine containing block copolymers and artificial lens comprising the same. Eur. Patent Appl. 1990/0,422,644 A2 (assigned to Daikin).

[251] Kawashima C, Ishihara A, Kawamura K, Minegishi S. Elastic fluorohydrocarbon resin and method of producing same. US patent 1997/5,696,215 (assigned to Central Glass Co. Ltd).

[252] Heidarian J, Hassan A. Microstructural and Thermal Properties of Fluoroelastomer/carbon Nanotube Composites. Composites Part B 2014;58:166-74.

[253] Heidarian J, Hassan A. Microstructural and Thermal Properties of Fluoroelastomer/acidic Surface Modified Carbon Nanotube Nanocomposites. Polym Comp 2016;37:3341-53.

[254] Heidarian J, Hassan A. Improving Heat Aging and Mechanical Properties of Fluoroelastomer Using Carbon Nanotubes. Polym J Chem Tech 2016;19:132-42.

[255] Shamsuri AA, Daik R, Jamil SNAM. A Succinct Review on the PVDF/Imidazolium-Based Ionic Liquid Blends and Composites: Preparations, Properties, and Applications. Processes 2021;9:761-77.

[256] Dias JC, Correia DM, Costa CM, Botelho G, Vilas-Vilela JL, Lanceros-Mendez S. Thermal degradation behavior of ionic liquid/ fluorinated polymer composites: Effect of polymer type and ionic liquid anion and cation. Polymer 2021;229:123995| 1-9.

[257] Dias JC, Lopes AC, Magalhães B, Botelho G, Silva MM, Esperança JMSS, Lanceros-Mendez S. High Performance Electromechanical Actuators Based on Ionic Liquid/Poly(Vinylidene Fluoride). Polym Test 2015;48:199–205.

[258] Yang J, Pruvost S, Livi S, Duchet-Rumeau J. The Role of Fluorinated IL as an Interfacial Agent in P(VDF-CTFE)/Graphene Composite Films, Nanomaterials 2019;9:1181-206.

[259] Geise GM, Lee HS, Miller DJ, Freeman BD, McGrath J. Water purification by membranes: The role of polymer science. J Polym Sc Part B Polym Phys 2010;48:1686-718.

[260] Wei B, Pan J, Feng J, Chen C, Liao S, Yu S, Li X. Highly conductive and permselective anion exchange membranes for electrodialysis desalination with series-connected dications appending flexible hydrophobic tails, Desalination 2020, 474:114184–94.

[261] Mark A. Science and technology for water purification in the coming decades. Nature 2008;452:20–9.

[262] Elimelech M, Phillip WA. The future of seawater desalination: energy, technology, and the environment. Science 2011;333:712–17.

[263] Fang S, Tu W, Mu L, Sun Z, Hu Q, Yang Y. Saline alkali water desalination project in Southern Xinjiang of China: a review of desalination planning, desalination schemes and economic analysis. Renew Sust Energ Rev 2019;113:109268–87.

[264] Rajput A, Sharma J, Raj SK, Kulshrestha V. Dehydrofluorinated poly(vinylidene fluoride-*co*-hexafluoropropylene) based crosslinked cation exchange membrane for brackish water desalination via electrodialysis. Coll Surf A Physicochem Engin Aspects 2021;630:127576-83.

[265] Yadav A, Kumar Labhasetwar K, Kumar Shahi V. Fabrication and optimization of tunable pore size poly(ethylene glycol) modified poly(vinylidene-co-hexafluoropropylene) membranes in vacuum membrane distillation for desalination. Separa Purif Techno 2021, 271, 118840-52.

[266] Yadav A, Singh K, KumarShahi V. Side-chain grafted functional groups poly(vinylidene fluoride-hexafluoropropylene) anti-fouling fluorinated polymer membrane with tuneable hydrophobicity for distillation. Desalination 2022;525:115501| 1-12.

[267] Kianfar P, Bongiovanni R, Ameduri B, Vitale A. Electrospinning of Fluorinated Polymers: Current State-of-the-art on Processes and Applications, Polym Rev 2022 (in press).

[268] Lalia BS, Guillen-Burrieza E, Arafat HA, Hashaikeh R. Fabrication and Characterization of Polyvinylidenefluoride-Co-Hexafluoropropylene (PVDF-HFP) Electrospun Membranes for Direct Contact Membrane Distillation. J Memb Sci 2013;428:104–15.

[269] Lalia BS, Guillen E, Arafat HA, Hashaikeh R. Nanocrystalline Cellulose Reinforced PVDF-HFP Membranes for Membrane Distillation Application. Desalination 2014;332:134–41.

[270] Tijing LD, Woo YC, Shim WG, He T, Choi JS, Kim SH, Shon HK. Superhydrophobic Nanofiber Membrane Containing Carbon Nanotubes for High-Performance Direct Contact Membrane Distillation. J Memb Sci 2016;502:158–70.

[271] Zhang H, Shen PK. Recent Development of polymer electrolyte membranes for fuel cells. Chem Rev 2012;112:2780−832.

[272] Couture G, Alleadine A, Boschet F, Ameduri B. Polymeric Materials for Anion-Exchange Membranes for Alkaline Fuel Cells. Progr Polym Sci 2011;36:1521–57.

[273] Sommer EM, Martins LS, Vargas JVC, Gardolinski JEFC, Ordonez JC, Marino CEB. Alkaline membrane fuel cell (AMFC) modelling and experimental validation. J Power Sources 2012;213:16–30.

[274] Tanaka Y. Development of the Mirai Fuel Cell Vehicle. In: Sasaki K, Li HW, Hayashi A, Yamabe J, Ogura T, Lyth SM, editors. Hydrogen Energy Engineering, a Japanese Perspective. Tokyo: Springer. 2016, chapter 34, p. 461-76.

[275] Bekiarian PG, Doyle M, Farnham WB, Feiring AE, Morken PA, Roelofs MG, Marshall WJ. New substantially fluorinated ionomers for electrochemical applications. J Fluorine Chem 2004;125:1187-204.

[276] Feiring AE, Doyle M, Roelofs MG, Farnham WB, Bekiarian PG, Blau HA. Polyvinylidene Fluoride Ionomers Containing Pendant Fluoroalkylsulfonyl Imide or Fluoroalkylsulfonyl Methide Groups. US Patent 2003/6,667,377 (assigned to DuPont).

[277] Sauguet L, Ameduri B, Boutevin B. Fluorinated, crosslinkable terpolymers based on vinylidene fluoride and bearing sulfonic acid side groups for fuel-cell membranes. J Polym Sci Part A Polym Chem 2006;44:4566-78.

[278] Xu K, Li K, Ewing CS, Hickner MA, Wang Q. Synthesis of proton conductive polymers with high electrochemical selectivity. Macromolecules 2010;43:1692-94.

[279] Sayler TS. Preparation of perfluorinated ionomers for fuel cell applications. PhD Dissertation. University of Tuscaloosa, Alabama, USA, 2012.

[280] Colpaert M, Lopez G, Zaton M, Jones D, Ameduri B. Revisiting the radical copolymerization of vinylidene fluoride with perfluoro-3,6-dioxa-4-methyl-7-octene sulfonyl fluoride for proton conducting membranes. Intern J Hydrog Energy 2018;43:16986-97.

[281] Ma W, Zhao C, Yang J, Ni J, Wang S, Zhang N, Lin H, Wang J, Zhang G, Li Q, Na H. Cross-linked aromatic cationic polymer electrolytes with enhanced stability for high temperature fuel cell applications. Energy Environ Sci 2012;5:7617-25.

[282] Arena F, Mitzel J, Hempelmann R. Permeability and Diffusivity Measurements on Polymer Electrolyte Membranes. Fuel Cells 2013;13:58-64.

[283] Subianto S, Pica M, Casciola M, Cojocaru P, Merlo L, Hards G, Jones DJ. Physical and chemical modification routes leading to improved mechanical properties of perfluorosulfonic acid membranes for PEM fuel cells. J Power Sources 2013;233:216-30.

[284] Sel O, Soules A, Ameduri B, Boutevin B, Laberty-Robert C, Gebel G, Sanchez C. Original Fuel-Cell Membranes from Crosslinked Terpolymers via a ‘‘Sol–gel’’ Strategy. Adv Funct Mater 2010;20:1090-98.

[285] Colpaert M, Zaton M, Ladmiral V, Jones D, Ameduri B. Crosslinked terpolymers Based on Vinylidene fluoride, perfluoro- 3,6-dioxa-4-methyl-7-octene sulfonyl fluoride, and cure site monomers for membranes in PEMFC applications. Polym Chem 2019;10:2176-89.

[286] Yandrasits M, Hamrock S, Grootaert W, Guerra M, Jing N. Polymer electrolyte membranes crosslinked by nitrile trimerization, US 2005/0107489 A1 (assigned to 3M innovative).

[287] Nasef MM, Güven O. Radiation-grafted copolymers for separation and purification purposes: Status, challenges and future directions. Progr Polym Sci 2012;37:1597-656.

[288] Souzy R, Ameduri B, Boutevin B. Synthesis and Characterizations of Novel Proton-Conducting Polymer Electrolyte Membranes Based on Fluoropolymers Grafted by Aryl sulfonic acids. Macromolecules 2012;45:3145−60.

[289] Wandelt K. Encyclopedia of Interfacial Chemistry, Surface Science and Electrochemistry. Amsterdam: Elsevier, 2018. 572 pp.

[290] Peng G, Zhu C, Liao J, Gao X, Hao L, Sotto A, Shen J. A two-step strategy for the preparation of anion-exchange membranes based on poly(vinylidenefluoride-*co*-hexafluoropropylene) for electrodialysis desalination. Polymer 2021;218:123508-15.

[291] McHugh PJ, Das AK, Wallace AG, Kulshrestha V, Shahi VK, Symes MD. An Investigation of a (Vinylbenzyl) Trimethylammonium and N-Vinylimidazole-Substituted Poly(Vinylidene Fluoride-Co-Hexafluoropropylene) Copolymer as an Anion-Exchange Membrane in a Lignin-Oxidising Electrolyser. Membranes 2021;11:425-40.

[292] Caravaca A, Garcia-Lorefice WE, Gil S, De Lucas-Consuegra A, Vernoux P. Towards a sustainable technology for H_2 production: Direct lignin electrolysis in a continuous-flow Polymer Electrolyte Membrane reactor. Electrochem Commun 2019;100:43–7.

[293] Das AK, Manohar M. Acid resistant sulphonated poly(vinylidene fluoride-*co*-hexafluoropropylene)/graphene oxide composite cation exchange for water splitting by iodine-sulfur bunsen process for hydrogen production. J Membr Sci 2018;552:377-86.

[294] Costa CM, Lizundia E, Lanceros-Méndez S. Polymers for advanced lithium-ion batteries: State of the art and future needs on polymers for the different battery components. Prog Energy Combust Sci 2020;79:100846.

[295] Liu B, Zhang J-G, Xu W. Advancing Lithium Metal Batteries. Joule 2018;2:833–45.

[296] Albertus P, Babinec S, Litzelman S, Newman A. Status and Challenges in Enabling the Lithium Metal Electrode for High-Energy and Low-Cost Rechargeable Batteries. Nat Energy 2018;3:16–21.

[297] Li T, Zhang X-Q, Shi P, Zhang Q. Fluorinated Solid-Electrolyte Interphase in High-Voltage Lithium Metal Batteries. Joule 2019;3:2647–61.

[298] Dias JC, Correia DM, Costa CM, Botelho G, Vilas-Vilela JL, LancerosMendez S. Thermal degradation behavior of ionic liquid/ fluorinated polymer composites: Effect of polymer type and ionic liquid anion and cation. Polymer 2021;229:123995 |1-12.

[299] Correia DM, Sabater Serra R, Gómez Tejedor JA, de Zea Bermudez V, Andrio Balado A, Meseguer-Dueñas JM, Gomez Ribelles JL, Lanceros-Méndez S, Costa CM. Ionic and Conformational Mobility in Poly (Vinylidene Fluoride)/Ionic Liquid Blends: Dielectric and Electrical Conductivity Behavior. Polymer 2018;143:164–72.

[300] Singh SVK, Singh RK. Development of ion conducting polymer gel electrolyte membranes based on polymer PVdF-HFP, BMIMTFSI ionic liquid and the Li-salt with improved electrical, thermal and structural properties. J Mater Chem C 2015;3:7305-18.

[301] Suleman M, Kumar Y, Hashmi SA. Structural and Electrochemical Properties of Succinonitrile-Based Gel Polymer Electrolytes: Role of Ionic Liquid Addition. J Phys Chem B 2013;117:7436–43.

[302] Chanthad C, Masser KA, Xu K, Runt J, Wang Q. Synthesis of triblock copolymers composed of poly(vinylidene fluoride-co-hexafluoropropylene) and ionic liquid segments. J Mater Chem 2012;22:341-4.

[303] Le AV, Wang M, Noelle DJ, Shi Y, Meng SY, Wu D. Using high-HFP-content cathode binder for mitigation of heat generation of lithium-ion battery. Int J Energy Res 2017;41:2430–8.

[304] Huang F, Xu Y, Peng B, Su Y, Jiang F, Hsieh Y, Wei Q. Coaxial Electrospun Cellulose-Core Fluoropolymer-Shell Fibrous Membrane from Recycled Cigarette Filter as Separator for High Performance Lithium-Ion Battery. ACS Sustain Chem Eng 2015;3:932–40.

[305] Lee H, Yanilmaz M, Toprakci O, Fu K, Zhang X. A Review of Recent Developments in Membrane Separators for Rechargeable Lithium-Ion Batteries. Energy Environ. Sci 2014;7:3857–86.

[306] Wang L, Wang Z, Sun Y; Liang X; Xiang H. Sb2O3 Modified PVDF-CTFE Electrospun Fibrous Membrane as a Safe Lithium-Ion Battery Separator. J Memb Sci 2019;572:512–19.

[307] Nguyen TKL, Lopez G, Iojoiu C, Bouchet R, Ameduri B. Novel single-ion PVDF-based polymer electrolytes for Lithium metal batteries. J Power Sources 2021;498:229920 | 1-10.

[308] Leones R, Costa CM, Machado AV, Esperanza JMSS, Silva MM, Lanceros-Mendez S. Effect of Ionic Liquid Anion Type in the Performance of Solid Polymer Electrolytes Based on poly(Vinylidene fluoride-trifluoroethylene). Electroanalysis 2015;27:457-64.

[309] Nunes-Pereira J, Costa CM, Leones R, Silva MM, Lanceros-Méndez S. Li-Ion Battery Separator Membranes Based on Poly(Vinylidene Fluoride-Trifluoroethylene)/Carbon Nanotube Composites. Solid State Ionics 2013;249–250:63–71.

[310] Chuxin B, Liang Z, Neese R, Linqing M, Wang L, Bauer F, Zhang Q. A Dielectric Polymer with High Electric Energy Density and Fast Discharge Speed. Science 2006;313:334-36.

[311] Meng N, Ren X, Santagiuliana G, Ventura L, Zhang H, Wu J, Yan H, Reece MJ, Bilotti E. Ultrahigh β-phase content poly(vinylidene fluoride) with relaxor-like ferroelectricity for high energy density capacitors. Nat Commun 2019;10:1-9.

[312] Lee C, Tarbutton JA. Polyvinylidene fluoride (PVDF) direct printing for sensors and actuators. Int J Adv Manuf Technol 2019;104:3155-62.

[313] Li Q, Wang Q. Ferroelectric Polymers and Their Energy-Related Applications. Macromol Chem Phys 2016;217:1228−44.

[314] Alluri NR, Chanderashkear A, Kim SJ. Hybrid Structures for Piezoelectric Nanogenerators: Fabrication Methods, Energy Generation, and Self-Powered Applications. In Manyala R, editor. Energy Harvesting, New York: InTechOpen Book Series, 2018, p. 5-20.

[315] Xia W, Zhang Z. PVDF-based dielectric polymers and their applications in electronic materials. IET Nanodielectr 2018;1:17-31.

[316] Stadlober B, Zirkl M, Irimia-Vladu M. Route towards sustainable smart sensors: Ferroelectric polyvinylidene fluoride-based materials and their integration in flexible electronics. Chem Soc Rev 2019;48:1787-825.

[317] Ciofani G, Menciassi A. Piezoelectric Nanomaterials for Biomedical Applications. Berlin, Heidelberg: Springer, 2012. 246 pp.

[318] Niu X, Tian B, Zhu Q, Dkhil B, Duan C. Ferroelectric polymers for neuromorphic computing. Applied Physics Reviews 2022;9,021309| 1-8.

[319] Chen X, Han X, Shen QD. PVDF-Based Ferroelectric Polymers in Modern Flexible Electronics. Adv Electron Mater 2017;3:1600460 |1-9.

[320] Rahul MT, Kalarikkal N, Thomas S, Ameduri B, Rouxel D, Balakrishnan R. Engineered Polymer Nanocomposites for Energy Harvesting Applications. Oxford: Elsevier, 2022. 362 pp.

[321] Wang X, Sun F, Yin G, Wang Y, Liu B, Dong M. Tactile-Sensing Based on Flexible PVDF Nanofibers via Electrospinning: A Review. Sensors 2018;18:16-28.

[322] Martins P, Lopes AC, Lanceros-Mendez S. Electroactive phases of poly(vinylidene fluoride): determination, processing and applications. Prog Polym Sci 2014;39:683-706.

[323] Prateek T, Thakur VK, Gupta RK. Recent Progress on Ferroelectric Polymer-Based

Nanocomposites for High Energy Density Capacitors: Synthesis, Dielectric Properties, and Future Aspects. Chem Rev 2016;116:4260–317.

[324] Nguyen VS, Rouxel D, Meier M, Vincent B, Dahoun A, Thomas S. Effect of ultrasonication and other processing conditions on the morphology, thermomechanical, and piezoelectric properties of poly(vinylidene difluoride-trifluoroethylene) copolymer films. Polym Eng Sci 2014;54:1280–8.

[325] Huang Y, Rui G, Allahyarov E, Li R, Fukuto M, Zhong GJ, Xu JZ, Li ZM, Taylor, P, Zhu L. Enhanced piezoelectricity from highly polarizable oriented amorphous fractions in biaxially oriented poly(vinylidene fluoride) with pure ß crystals. Nat Commun 2021;12:675-1-8.

[326] Hadji R, Nguyen VS, Vincent B, Rouxel D, Bauer F. Preparation and characterization of P(VDF-TrFE)/Al2O3 nanocomposite. IEEE Transactions Ultrasonics Ferroelectr Freq Control 2012;59:163–7.

[327] Thevenot C, Rouxel D, Sukumaran S, Rouabah S, Vincent B, Chatbouri S, Ben Zineb T. Plasticized P(VDF-TrFE): A new flexible piezoelectric material with an easier polarization process, promising for biomedical applications. J Appl Polym Sci 2021;138:50420-31.

[328] Lou Z, Chen S, Wang L, Jiang K, Shen G. An Ultra-Sensitive and Rapid Response Speed Graphene Pressure Sensors for Electronic Skin and Health Monitoring. Nano Energy 2016;23:7–14.

[329] Terzic I, Meereboer NL, Acuautla M, Portale G, Loos K. Electroactive materials with tunable response based on block copolymer self-assembly. Nat Commun 2019;10:601-9.

[330] Dias JC, Correia DM, Costa CM, Ribeiro C, Maceiras A, Vilas JL, Botelho G, de Zea Bermudez V, Lanceros-Mendez S. Improved Response of Ionic Liquid-Based Bending Actuators by Tailored Interaction with the Polar Fluorinated Polymer Matrix. Electrochim Acta 2019;296:598–607.

[331] Ghosh A, Louis L, Asandei AD, Nakhmanson S. First-principles studies of spontaneous polarization in mixed poly(vinylidene fluoride)/ 2,3,3,3-tetrafluoropropene polymer crystals. Soft Matter 2018;14:2484-91.

[332] Capsal JF, Dantras E, Lacabanne C. Molecular mobility interpretation of the dielectric relaxor behavior in fluorinated copolymers and terpolymers. J Non-Cryst Solids 2013;363:20-25.

[333] Gadinski MR, Li Q, Zhang G, Zhang X, Wang Q. Understanding of Relaxor Ferroelectric Behavior of Poly(vinylidene fluoride–trifluoroethylene–chlorotrifluoroethylene) Terpolymers. Macromolecules 2015;48:2731-39.

[334] Zhang Q, Xia W, Zhu, Z, Zhang Z. Crystal phase of poly(vinylidene fluoride-*co*-trifluoroethylene) synthesized via hydrogenation of poly(vinylidene fluoride-*co*-chlorotrifluoroethylene). J Appl Polym Sci 2013;127:3002-8.

[335] Xia WM, Xu Z, Zhang ZC. Dielectric, piezoelectric and ferroelectric properties of a poly(vinylidene fluoride-co-trifluoroethylene) synthesized via a hydrogenation process. Polymer 2014;54:440–46.

[336] Bargain F, Thuau D, Panine P, Hadziioannou G, Tencé-Girault S, Dominguez Dos Santos F. Thermal behavior of poly(VDF-ter-TrFE-ter-CTFE) copolymers: Influence of CTFE termonomer on the crystal-crystal transitions. Polymer 2019;161:64-77.

[337] Bargain F, Thuau D, Panine P, Hadziioannou G, Tencé-Girault S, Dominguez Dos Santos F. Phase diagram of poly(VDF-*ter*-TrFE-*ter*-CTFE) copolymers: Relationship between crystalline structure and material properties. Polymer 2021;213:12303-12.

[338] Yang L, Tyburski BA, Domingues Dos Santos F, Endoh MK, Koga T, Huang D, Wang Y, Zhu L. Relaxor ferroelectric behavior from strong physical pinning in a poly(vinylidene fluoride-co-trifluoroethylene-co-chlorotrifluoroethylene) random terpolymer. Macromolecules 2014;47:8119–25.

[339] Liu Q, Richard C, Capsal JF. Control of crystal morphology and its effect on electromechanical performances of electrostrictive P(VDF-TrFE-CTFE) terpolymer. Eur Polym J 2017;91:46–60.

[340] Bargain F, Soulestin T, Domingues Dos Santos F, Ladmiral V, Ameduri B, Tencé-Girault S. Semicrystalline organization of VDF- and TrFE-based electroactive terpolymers: impact of the trans-1,3,3,3-tetrafluoropropene termonomer. Macromolecules 2017;50:3313–22.

[341] Della Schiava N, Le MQ, Galineau J, Domingues dos Santos F, Cottinet PJ, Capsal JF. Influence of Plasticizers on the Electromechanical Behavior of a P(VDF-TrFE-CTFE) Terpolymer: Toward a High Performance of Electrostrictive Blends. J Polym Sci Part B Polym Phys 2017;55:355–69.

[342] Della Schiava N, Pedroli F, Thetpraphi K, Flocchini A, Le MQ, Lermusiaux P, Capsal JF, Cottinet PJ. Effect of beta-based sterilization on P(VDF-TrFE-CFE) terpolymer for medical applications. Sci Rep 2020;10:8805-12.

[343] Li Q, Zhang G, Liu F, Han K, Gadinski MR, Xiong C, Wang Q. Solution-processed ferroelectric terpolymer nanocomposites with high breakdown strength and energy density utilizing boron nitride nanosheets. Energy Environ Sci 2015;8:922–31.

[344] Cheng Z-Y, Li H, Xia F, Xu H, Olson D, Huang C, Zhang QM, Kavarnos GJ. Electromechanical Properties and Molecular Conformation in P(VDF-TrFE)-Based Terpolymer. In: Bar-Cohen Y, editor. Smart Struct Mater; Electroact Polym Actuators Devices. Bellingham: SPIE. 2002. vol. 4695; p. 167–75.

[345] Zhang X, Shen Y, Shen Z, Jiang J, Chen L, Nan CW. Achieving High Energy Density in PVDF-Based Polymer Blends: Suppression of Early Polarization Saturation and Enhancement of Breakdown Strength. ACS Appl Mater Interfaces 2016;8:27236–42.

[346] Mao P, Wang J, Zhang L, Sun Q, Liu X, He L. Tunable dielectric polarization and breakdown behavior for high energy storage capability in P(VDF–TrFE–CFE)/PVDF polymer blended composite films. Phys Chem Chem Phys 2020;22:13143–53.

[347] Li Y, Soulestin T, Ladmiral V, Ameduri B, Lannuzel T, Santos-Dominguez F, Zhong G, Li ZM, Zhu L. Stretching-Induced Relaxor Ferroelectric Behavior In a Poly(vinylidene fluoride-*co*-trifluoroethylene-*co*-hexafluoropropylene) Random Terpolymer. Macromolecules 2017;50:7646–56.

[348] Yang L, Allahyarov E, Guan F, Zhu L. Crystal orientation and temperature effects on double hysteresis loop behavior in a poly(vinylidene fluoride-*co*-trifluoroethylene-*co*-chlorotrifluoroethylene)-*graft*-polystyrene graft copolymer. Macromolecules 2013;46:9698-711.

[349] Miao B, Liu J, Zhang X, Lu J, Tan S, Zhang Z. Ferroelectric relaxation dependence of poly(vinylidene fluoride-co-trifluoroethylene) on frequency and temperature after grafting with poly(methyl methacrylate). RSC Adv 2016;6:84426–38.

[350] Frecker MI, Aguilera WM. Analytical modeling of a segmented unimorph actuator using electrostrictive P(VDF-TrFE) copolymer. Smart Mater Struct 2004;13:82–91.

[351] Capsal JF, Galineau J, Lallart M, Cottinet PJ, Guyomar D. Plasticized relaxor ferroelectric terpolymer: toward giant electrostriction, high mechanical energy and low electric field actuators. Sens Actuators A Phys 2014;207:25–31.

[352] Dong Z, Kennedy SJ, Wu Y. Electrospinning Materials for Energy-Related Applications and Devices. J Power Sourc 2011;196:4886–4904.

[353] Shi X, Zhou W, Ma D, Ma Q, Bridges D, Ma Y, Hu A. Electrospinning of Nanofibers and Their Applications for Energy Devices. J Nanomater 2015;2015:1-20.

[354] Bandara TMWJ, Weerasinghe AMJS, Dissanayake MAKL, Senadeera GKR, Furlani M, Albinsson I, Mellander BE. Characterization of Poly (Vinylidene Fluoride-Co-Hexafluoropropylene) (PVdF-HFP) Nanofiber Membrane Based Quasi Solid Electrolytes and Their Application in a Dye Sensitized Solar Cell. Electrochim Acta 2018;266:276–83.

[355] Pang HW, Yu H-F, Huang Y-J, Li C-T, Ho K-C. Electrospun Membranes of Imidazole-Grafted PVDF-HFP Polymeric Ionic Liquids for Highly Efficient Quasi-Solid-State Dye-Sensitized Solar Cells. J Mater Chem A 2018;6:14215–23.

[356] Spampinato N, Pecastaings G, Maglione M, Pavlopoulou E, Hadziioannou G. Non-destructive depth-dependent morphological characterization of ferroelectric:semiconducting polymer blend films. Colloid Polym Sci 2021;299:551-60.

[357] Das S, Ghosh A. Solid Polymer Electrolyte Based on PVDF-HFP and Ionic Liquid Embedded with TiO2 Nanoparticle for Electric Double Layer Capacitor (EDLC) Application. J Electrochem Soc 2017;164:1348–53.

[358] Zhang ZC, Chung TCM. Study of VDF/TrFE/CTFE terpolymers for high pulsed capacitor with high energy density and low energy loss, Macromolecules 2007;40:783–785.

[359] Lv J, Cheng Y. Fluoropolymers in Biomedical Applications: State-of-the-Art and Future Perspectives. Chem Soc Rev 2021;50:5435-5467.

[360] Koguchi R; Jankova K, Tanaka M. Fluorine-Containing Bio-Inert Polymers: Roles of Intermediate Water. Acta Biomater 2022;138:34-56.

[361] Damaraju SM, Wu S, Jaffe M, Arinzeh TL. Structural Changes in PVDF Fibers Due to Electrospinning and Its Effect on Biological Function. Biomed Mater 2013;8:045007 |1-8.

[362] Abazari MF, Hosseini Z, Karizi S, Norouzi S, Faskhoudi M, Saburi E, Enderami SE Ardeshirylajimi A, Mohajerani H. Different Osteogenic Differentiation Potential of Mesenchymal Stem Cells on Three Different Polymeric Substrates. Gene 2020;740:144534-45.

[363] Lee YS, Collins G, Arinzeh TL. Neurite Extension of Primary Neurons on Electrospun Piezoelectric Scaffolds. Acta Biomater 2011;7:3877–86.

[364] Augustine R, Dan P, Sosnik A, Kalarikkal N, Tran N, Vincent B, Thomas S, Menu P, Rouxel D. Electrospun Poly(Vinylidene Fluoride-Trifluoroethylene)/Zinc Oxide Nanocomposite Tissue Engineering Scaffolds with Enhanced Cell Adhesion and Blood Vessel Formation. Nano Res 2017;10:3358–76.

[365] Weber N, Lee YS, Shanmugasundaram S, Jaffe M, Arinzeh TL. Characterization and in Vitro Cytocompatibility of Piezoelectric Electrospun Scaffolds. Acta Biomater 2010;6:3550–6.

[366] Ribeiro C, Sencadas V, Correia DM, Lanceros-Méndez S. Piezoelectric polymers as biomaterials for tissue engineering applications. Colloids Surfaces B Biointerfaces 2015;136:46–55.

[367] Granstrom J, Feenstra J, Sodano HA, Farinholt K. Energy harvesting from a backpack instrumented with piezoelectric shoulder straps. Smart Mater Struct 2007;16:1810-18.

[368] Sun C, Shi J, Bayerl DJ, Wang X. PVDF microbelts for harvesting energy from respiration. Energy Environ Sci 2011;4:4508–12.

[369] Nunes-Pereira J, Ribeiro S, Ribeiro C, Gombek CJ, Gama FM, Gomes AC, Patterson DA, Lanceros-Méndez S, Poly(vinylidene fluoride) and copolymers as porous membranes for tissue engineering applications. Polym Test 2015;44:234–41.

[370] Korzeniowski SH, Buck RC, Newkold RM, El Kassmi A, Laganis E, Matsuoka Y, Dinelli B, Beauchet S, Adamsky F, Weilandt K, Soni VK, Kapoor D, Gunasekar P, Malvasi M, Brinati G, Musio S. A Critical Review of the Application of Polymer of Low Concern Regulatory Criteria to Fluoropolymers II: Fluoroplastics and Fluoroelastomers. Integ. Envron. Assessm. Manag. 2022 (in press).

[3I] Fluoropolymer Products Group of Plastics Europe, Risk Management Options https://fluoropolymers.plasticseurope.org/index.php/fluoropolymers/irreplaceable-uses-1/reports-policy-documents/rmoa/; 2021 [accessed April 2022].

[372] Guelfo JL, Korzeniowski S, Mills MA, Anderson J, Anderson RH, Arblaster JA, Conder JM, Cousins IT, Dasu K, Henry BJ, Lee LS, Liu J, McKenzie ER, Willey J. Environ Sources, Chemistry, Fate and Transport of Per- and Polyfluoroalkyl Substances: State of the Science, Key Knowledge Gaps, and Recommendations. Presented at the August 2019 SETAC Focus Topic Meeting. Environ Toxic Chem 2021;40: 3234-60.

[373] ECHA. The national authorities of Germany, the Netherlands, Norway, Sweden and Denmark invite interested parties to send in evidence and information on the use of per- andpolyfluoroalkyl substances (PFAS), https://echa.europa.eu/-/five-european-states-call-for-evidence-on-broad-pfas-restriction/; 2020 [accessed April 2022].

[374] https://www.chemours.com/en/-/media/files/corporate/fayetteville-works/2020-0320-thermal-oxidizer-efficiency-results announced.pdf?rev=87dbfd0ebb9c45aeaa475fddd2a899b4&hash=05916EC2AC2B5A3C41135773A3FCDED0/; 2020 [accessed April 2022].

[375] Future Market Insights 2022. Fluoropolymer Market Overview.https://www.futuremarketinsights.com/reports/fluoropolymers-market/; 2022 [accessed April 2022].

[376] Allied Market Research 2022. Fluoropolymers Market by Product Type. https://www.alliedmarketresearch.com/fluoropolymers-market/; 2022 [accessed April 2022].